Pedro Freire de Sousa Martins

Licenciado em Biologia

Biological Evaluation of Chlorogold Complexes as Potential Anti-Tumoural Compounds: Unraveling Mechanisms of Action

Dissertação para obtenção do Grau de Mestre em
Genética Molecular e Biomedicina

Orientadora: Maria Alexandra Núncio de Carvalho Ramos Fernandes, Professora Doutora, FCT/UNL

Presidente: Professora Doutora Ilda Santos Sanches
Arguente: Professora Doutora Luísa M.D.R.S. Martins
Vogal: Professora Doutora Maria Alexandra Núncio de Carvalho Ramos Fernandes

FACULDADE DE CIÊNCIAS E TECNOLOGIA
UNIVERSIDADE NOVA DE LISBOA

Setembro 2014

UNIVERSIDADE NOVA DE LISBOA

FACULDADE DE CIÊNCIAS E TECNOLOGIA

DEPARTAMENTO DE CIÊNCIAS DA VIDA

Pedro Freire de Sousa Martins

Biological Evaluation of Chlorogold Complexes as Potential Anti-tumoural Compounds: Unraveling Mechanisms of Action

Dissertação apresentada para a obtenção do Grau de Mestre em Genética Molecular e Biomedicina, pela Universidade Nova de Lisboa, Faculdade de Ciências e Tecnologia

Orientadora:

Professora Doutora Alexandra Fernandes (FCT/UNL)

LISBOA

2014

My master studies have resulted in the following publications:

Martins, P., Rosa, D., Fernandes, A.R., Baptista, P. V 2014b. Nanoparticle Drug Delivery Systems : Recent Patents and Applications in Nanomedicine. Recent Patents on Nanomedicine 3: 1–14.

Martins, P., Marques, M., Coito, L., Pombeiro, A.J.L., Viana Baptista, P., R. Fernandes, A. 2014a. Organometallic Compounds in Cancer Therapy_ Past Lessons and Future Directions. Anticancer Agents Med Chem. 14: 1199–1212.

Biological Evaluation of Chlorogold Complexes as Potential Anti-tumoural Compounds: Unraveling mechanisms of action

Acknowledgements

Probably the best way to describe the last few months of my live is as being a bumpy ride, with some good “ups” but definitely with some “downs” as well. Nonetheless the path I took could not have been accomplished without the help of some important people.

First and foremost I would like thank my supervisor Prof. Alexandra Fernandes for accepting me in her laboratory. The influence, the constant support and the challenges thrown at me were undoubtedly paramount for the fulfillment of this thesis as well as for my upbringing from an academic point of view. I am deeply grateful for the opportunity.

From the CIGMH, the research group next door, first would like to thank Prof. Pedro V. Baptista for the good sense of humor as well as for all the valuable inputs in my research, and secondly to all the remaining members that were helpful enough to share their insights, and expertise.

Also, a big thanks to Dr. Guadalupe Cabral and to all CEDOC personnel for the collaboration and availability which allowed for the accomplishment of flow cytometry assays, and to the Centro de Química Estrutural do Instituto Superior Técnico, for providing the tested compounds.

For all the advice, orientation and support in the lab I would like to express my appreciation to Joana Silva. Her expertise and experience in the field as well as her willingness to teach others are of great value to this laboratory, playing an important role in my current knowledge. Every cell culture in the future will certainly remind me of her. Not only gifted by her intellect, she is a fun and amusing person to a hang around contributing to an enjoyable environment in the lab and in that sense she is a true cornerstone in the research group. For all the precious help and fun moments thank you!

To Lidia and Soraia, fantastic members of this lab, I would like to thank the companionship, the laughs and all the support given when needed. The countless shared coffees in the patio, and good moments surely won’t be forgotten!!

Even though I consider her as having a rather complicated temperament, Mara is probably one of the persons that most surprised me in a good way. I also would like to thank her for the good company and shared knowledge.

Also would like to express my gratitude to all the other members of the lab, Catarina Rodrigues, Luis Raposo, Ana Tomaltcheva, Ana Carina, João Jesus and Daniela for the patience and help given when needed, and the good moments offered.

Some good old friends could not have been more important as well. For the company, the laughs, the nights out, the countless coffees and the patience throughout this moment of my life I also would like to thank to João Carneiro, Raimundo Diz, Rodolfo Marques, David Lopes, Sónia Castro, Bruna Pereira to Diana Bordalo and to Nádia Albuquerque.

To my entire family I would like to express my gratitude for the concern and support during the elaboration of this thesis. However there aren't enough words to describe how grateful I am to my grandfather. His incredible joy and interest in my career inspired me and gave me strength to complete my thesis and even though he is not around anymore I am sure he would be proud of my accomplishments.

Finally, for all the unconditional love and continuous support my next thank you notes are unquestionably directed towards my mom and dad. For being "there" through thick and thin situations, for the way they raised me to be a better person, and for the way they always presented themselves available for any problem I had, THANK YOU for being who you are!

For all of those who supported me and shared this experience with me, thank you!

Resumo

A quimioterapia citotóxica encontra-se actualmente definida como sendo característica tradicional do tratamento oncológico; no entanto efeitos secundários adversos e a aquisição de ressistência a medicamentos quimioterapeuticos permanecem grandes desafios a ultrapassar. Nos últimos anos tem sido desenvolvido um grande esforço no sentido de encontrar novos compostos quimioterapeuticos com propriedades farmacodinâmicas e farmacocinéticas de forma a atingir maior especificidade tumoral e efeitos secundários reduzidos. Este trabalho teve como objectivo caracterizar o efeito anti-tumoral de compostos de cloro-ouro e explorar os mecanismos pels quais estes exercem a sua actividade antiproliferativa, como parte deste esforço. Ensaios de citotoxicidade *in vitro* envolvendo os compostos cloro(trimetilfosfina)ouro(I) e cloro(trifenilfosfina)ouro(I) na linha A549 revelaram valores de IC_{50} de 44.4 e 30.0 μM respectivamente, e 3.3 e 5.4 μM na linha H1975 respectivamente. A citoselectividade dos mesmos compostos para linhas não tumorais, avaliada na cultura normal de fibroblastos revelou valores de IC_{50} de 7.7 e 19.1 μM respectivamente. Características morfológicas de apoptose foram igualmente confirmadas. Marcação por Hoechst 33258 nas linhas A549 e H1975 quando expostas aos compostos ao seu valor de IC_{50} revelaram indícios de fragmentação nuclear e condensação da cromatina. Estes resultados foram ainda comprovados por citometria de fluxo. A dupla marcação com Anexina V-FITC e IP das células A549 após exposição ao composto B, demonstrou a capacidade de indução de mecanismos de morte celular por apoptose de uma forma dependente de dose. O composto cloro(trimetilfosfina)ouro(I) demonstrou ainda capacidade de induzir atrasos no ciclo celular sendo este efeito mais evidente na fase S. Interação dos compostos com a molécula de DNA revelou ser relativamente fraca ou inexistente revelada através da incapacidade dos compostos de comprometerem a conformação de DNA plasmidíco. Os estudos proteómicos apesar de pouco conclusivos quanto ao mecanismo de acção dos compostos, permitiram identificar potenciais novos biomarcadores para o prógnostico de adenocarcinoma pulmonar.

Palavras Chave: Cancro, Complexos de Cloro-ouro, Citotoxicidade, Apoptose, Ciclo Celular, Proteómica.

Abstract

Cytotoxic chemotherapy at the present state is set as the traditional hallmark of oncological treatment; however host toxicity and drug resistance acquisition remain as main challenges to overcome. Over the past few years there has been a great effort towards finding new chemotherapeutic compounds with improved pharmacodynamic and pharmacokinetic properties in order to achieve higher cancer specificity and reduced undesirable side effects. The present work intended to characterize and elucidate the anti-tumoural effect of chlorogold complexes bearing phosphine or N,O-donor ligands, and explore the mechanisms by which they exert their antiproliferative properties as a part of this effort. Chloro(trimethylphosphine)gold(I) and Chloro(triphenylphosphine)gold(I) *in vitro* cell viability assays in A549 tumour cell line exhibited IC_{50} values of 44.4 and 30.0 μM respectively, plus 3.3 and, 5.4 μM in H1975 respectively. Predisposition of the chlorogold complexes to target non-tumoural cells, evaluated in fibroblasts normal cell line, revealed an IC_{50} value of 7.7 and 19.1 μM respectively. Apoptosis morphological features were also confirmed. A549 and H1975 cell line exposure to both chlorogold complexes at their respective IC_{50} values, revealed nuclear fragmentation and chromatin condensation, observed by Hoechst 33258 staining. These results were further proven for by flow cytometry analysis. Double staining with Annexin V-FITC and Propidium Iodide in A549 after compound exposure revealed the ability to induce mechanisms of cell death by apoptosis in a dose-dependent fashion. Chloro(triphenylphosphine)gold(I) was further proven to be able to induce cell cycle delay, this effect being especially evident for S-phase. Moreover compound interaction with the DNA molecule was proven to be either weak or inexistent through electrophoretic mobility assay revealed by the compounds' inability to compromise plasmid DNA conformation. Proteomic studies even though not conclusive regarding chlorogold compounds' mechanism of action, allowed the identification of new potential biomarkers for prediction of prognosis in non-small-cell lung carcinoma.

Key-Words: Cancer, Chlorogold complexes, Cytotoxicity, Apoptosis, Cell Cycle, Proteomics.

General Contents

Figure Index

Table Index

Abbreviation List

Abs	Absorbance
Abs260/Abs230	Ratio between 260 nm and 230 nm absorbance
Abs260/Abs280	Ratio between 260 nm and 280 nm absorbance
Apaf-1	Apoptosis protease activating factor-1
APS	Ammonium Persulfate
ATP	Adenosine-5'-triphosphate
BAX	Encoding gene for pro-apoptotic protein Bax, of the protein family Bcl-2
Bax	Bcl-2-associated X protein
BCL-2	Encoding gene for pro-apoptotic protein Bcl-2, of the protein family Bcl-2
Bcl-2	B-cell lymphoma protein 2
Bid	BH3 interacting domain death agonist
Bis	N,N'-Methylenebisacrylamide
BRCA1	Breast cancer 1 susceptibility gene
BRCA2	Breast cancer 2 susceptibility gene
CASP3	Encoding gene for Cysteine-aspartic protease 3
Caspase	Cysteine-aspartic protease
Cdk	Cyclin-dependent kinases
cDNA	Complementar DNA
CHAPS	(3-[(3-Cholamidopropyl)dimethylammonio]-1 propanesulfonate)
CT-DNA	Calf Thymus-DNA
DISC	Death inducing signaling complex
DMEM	Dulbecco's Modified Eagle Medium
DMSO	Dimethyl Sulfoxide
Dnase	Desoxirribonuclease
DOX	Doxorrubicin
DTT	Dithiothreitol
E2F	E2 transcription factor
EGF	Epidermal growth factor
EMSA	Electrophoretic Mobility Shift Assay
FADD	Fas-associated death domain
FasL	Fatty acid synthetase ligand
FBS	Fetal Bovine Serum
FITC	Fluorescein Isothiocyanate
HCT116	Colorectal carcinoma cell line
HepG2	Hepatocellular carcinoma cell line
HER	Human epidermal growth factor receptor-2
HER2	Codifying gene for membrane receptor HER
IAP	Inhibitory of apoptosis proteins

IC50	50 % growth inhibition concentration
IFNγ	Interferon gamma
IKKβ	Serine/threonine protein kinase that phosphorylates the I-kappa-B protein
JNK1	Protein kinase of the MAPK family
Kb	Affinity binding constant
MTS	3-(4,5-dimetiltiazol-2-il)-5-(3-carboximetoxifenil)-2-(4-sulfofenil)-2H-tetrazólio
PBS	Phosphate Buffered Saline
PI	Propidium Iodide
PMS	Phenazine Methosulphate
PMSF	Phenylmethylsulfonyl fluride
pUC18	Plasmid DNA
Rb	Retinoblastoma tumour suppressor protein
RIPK	Receptor interacting protein kinases
ROS	Reactive Oxygen Species
RPMI-1640	Rosswell Park memorial institute medium 1640
SDS	Sodium dodecyl sulfate
SDS-PAGE	Sodium dodecyl sulfate - Polyacrylamide gel electrophoresis
SGTA	Small glutamine-rich tetratricopeptide repeat-containing protein alpha
SMAC/DIABLO	Second mitochondria-derived activator of caspase/Direct IAP-binding protein with low pI
TAE	Tris base, acetic acid and EDTA buffer
TEMED	Tetramethylethylenediamine
TNF	Tumour necrosis factor
TNFR1	Tumour necrosis factor receptor 1
TOPO II	Topoisomerase II
TP53	p53 protein encoding gene
TRADD	TNF receptor-associated death domain
TrxR	Thioredoxin reductase
Tris-HCl	Tris-Hidroclorite
WHO	World Health Organization

Units List

% (w/v)	Weight/volume percentage
% (v/v)	Volume/volume percentage
A; mA	Amperes; miliamperes
AU	Absorbance units
bp	Base pairs
°C	Celsius degrees
H; min; s	Hours; minutes; seconds
kDa; Da	KiloDalton; Dalton (10^{-3}kg)
Kg; g; mg; µg; ng	Quilogramas; grama (10^{-3}kg); miligrama (10^{-6} kg); microgama (10^{-9} kg); ng – nanograma (10^{-12} kg)
L; mL; µL	Liter; mililiter(10^{-3} L); µL – microliter (10^{-6} L)
m; cm; mm; nm	Meter; centimeter (10^{-2} m); milimeter (10^{-3} m); nanometer (10^{-9} m)
M; mM; µM	Molar (mol/L); milimolar (10^{-3} M); micromolar (10^{-6} M)
mol; pmol	Mole; picomole
rpm	Rotations per minute
U	Unit; mU – miliunit
V	Volts
W	Watts

Symbol List

[Complex]	Complex concentration
[DNA]	DNA concentration
Σ	Summation
ε	Molar extinction coefficient
ε_a	Apparent molar extinction coefficient
ε_b	Molar extinction coefficient when bound to DNA
ε_f	Molar extinction coefficient when unbound
λ	Wavelength
ℓ	Optical path

1. Introduction

1.1. Cancer Etiology

At any given moment an adult human is composed of approximately 10^{15} cells endowed with grand versatility and plasticity, paramount for different morphogenesis mechanisms and maintenance of adult tissues through cell turnover processes (Bertram, 2001). These numerous processes are usually tightly regulated by a network of overlapping molecular mechanisms which govern, among other factors, both cell proliferation and programmed cell death in a perfect balance. At the same time the genomic sequences' susceptibility to corruption, either by intrinsic or extrinsic factors may tip this intricate homeostatic balance, leading to changes that are incompatible with an organismic structure. In other words cells that undergo this process, typically become unresponsive to normal cell signaling factors, and "behave" in a organismic-independent fashion, often leading to altered cell proliferation programs and consequently to large populations of renegade cells that ultimately lead to cancer formation (Bertram, 2001; Weinberg, 2013).

An important concept to grasp when considering cancer is that it is generally accepted as a genetic disease or as a group of genetic diseases, although not always heritable. Even though hereditary cancer predisposition syndromes have become more and more easily identified and studied, only 5 to 10 % of all cancer cases can actually be attributed to such genetic defects (Garber and Offit, 2005; Anand *et al.*, 2008). In fact since the review by Doll and Peto in 1981 (Doll and Peto, 1981) it was concluded that the main causes of cancer are mainly related to environmental and lifestyle factors, accounting for the remaining 90 to 95 % of incidence cases (Anand *et al.*, 2008).

1.1.1. From Carcinogens and Lifestyle Habits to Genetic Influence

Among other causes mutations can arise from exposure to a series of environmental mutagens, such as cigarette smoke, alcohol, radiation, infectious agents, diet related and many others described extensively elsewhere (Baan *et al.*, 2009; Bouvard *et al.*, 2009; El Ghissassi *et al.*, 2009; Grosse *et al.*, 2009; Jemal *et al.*, 2010; Secretan *et al.*, 2009; Straif *et al.*, 2009). The link between environmental mutagens and the incidence and mortality cancer rates across the world are particular evident by observing trends and habits over the last century (Anand *et al.*, 2008; *World Cancer Report*, 2008). In fact while the incidence and mortality rates are actually decreasing for the majority of western countries, these are on the rise for several less developed and economically transitioning countries due to the adoption unhealthy lifestyles, typical of western countries, such as smoking, physical inactivity, and the consumption of high calorie foods (Jemal *et al.*, 2010). Lifestyle-cancer associations have been extensively studied. For instance increases in intakes of fat, red meat or processed meat and alcohol, alongside with obesity and lack of physical exercise, have shown through a series of cohort

and meta-analysis studies, to increase to variable extent, the risk of contracting colorectal, breast and/ or prostate cancer (*World Cancer Report*, 2008). Furthermore the relationship between diet and cancer becomes more obvious when observing incidence rates among populations in migratory studies (McCracken *et al.*, 2007). For instance Asians have been shown to have 25 times lower incidence of prostate cancer and 10 times lower incidence of breast cancer (Anand *et al.*, 2008) however the rates of these types of cancer tend to increase in migrating Asian-American populations indicating that they have been subjected to a more Western lifestyle, becoming simultaneously more prone to the same risk factors associated for these specific cancers (McCracken *et al.*, 2007). Smoking and related mutagens on the other hand, can almost be considered as particular class due to its importance and influence on the tinkering of specific molecular networks and mechanisms and consequently on the emergence of cancer. In particular cigarette smoke is known to contain approximately 60 mutagens (Takahashi *et al.*, 2011) ranging from polycyclic aromatic hydrocarbons to specific nitrosamines. Exposure to such mutagens to airway epithelial cells through continuous smoking leads to severe molecular lesions and diminished repair capability, being accountable as the major cause of cancer in humans, and correlated to 13 different types such as lung, oral cavity, nasal cavity and nasal sinuses, pharynx, larynx, oesophagus, stomach, pancreas, liver, urinary bladder, kidney, uterine cervix and myeloid leukaemia (*World Cancer Report*, 2008). Benzopyrenediol epoxide is one example of a cigarette smoke metabolite that as actually been etiologically linked to lung cancer, which is known to form adducts on guanine residues with a particular incidence on the tumour suppressor gene *TP53* (Lemjabbar *et al.*, 2003). Similarly DNA adduction and mutagenesis were also reported for aromatic amines derived from cigarette smoking (Besaratinia and Tommasi, 2013). Recent studies have also connected the capacity of tobacco smoke to trigger chronic inflammation, through IKKβ and JNK1 pathway activation (Takahashi *et al.*, 2011), which has been extensively demonstrated to play decisive roles at different stages of tumour development (Grivennikov *et al.*, 2010).

Even though these lifestyle habits and associated mutagens further emphasize the effect and burden that the surrounding environment has over the organismic structure of the human body and its genetic constitution it is known that these factors alone do not entirely justify the onset and emergence of cancer. For example it is clear that intrinsic factors resulting from by-products of endogenous processes trigger important molecular alterations at the genetic and epigenetic level, fundamental for promoting the emergence of cancer. Reactive oxygen species (ROS) for instance, such as superoxide radical, hydrogen peroxide, singlet oxygen or hydroxyl radical have reportedly demonstrated to have a significant role in genomic instability (Kanvah *et al.*, 2010). Particularly genomic instability caused by ROS seems to involve mainly guanine modifications causing G→T transversions (Kanvah *et al.*, 2010). Mutations range from oxidized purines and pyrimidines to single strand breaks and instability formed directly or by DNA repair processes (Waris and Ahsan, 2006).

On the other hand DNA replication itself can be considered as a source of mutational events. DNA replication enzymes inherent mutation rate is as little as 1 in 10^9 (Loeb *et al.*, 1974) however error prone phenotypes in DNA replication enzymes or in translesion DNA inherently increase this error rate, leading to genomic instability and to cancer susceptibility (Suzuki and Takahashi, 2013). Genetic disturbances can range from chromosome alterations to point mutations which ultimately can disable tumour suppressor genes or activate proto-oncogenes that respectively can alter cell proliferation and survival pathways (Suzuki and Takahashi, 2013).

1.2. Incidence and Mortality Rates

Cancer burden worldwide is known to be increasing over the years, in part as a reflection of westernized habits, but also as consequence of the continuous growth and aging of the world's population (Jemal *et al.*, 2011). Accordingly to the most recent data from the World Health Organization (WHO), in 2012 alone it was estimated 14.1 million new cancer cases, alongside with 8.2 million related deaths, turning cancer into a major leading cause of death worldwide ("World cancer factsheet," 2014). Of particular importance 44 % of all cancer cases and 53 % of related deaths occurred in low or medium developing countries (Rise, 2013). Globally, the most commonly diagnosed cancers were those of the lung (1.8 million, 13.0 % of the total), breast (1.7 million, 11.9 %), and colorectal (1.4 million, 9.7 %) whereas the most common causes of cancer death were cancers of the lung (1.6 million, 19.4 % of the total), liver (0.8 million, 9.1 %), and stomach (0.7 million, 8.8 %) (Figure 1.1) ("GLOBOCAN," 2012).

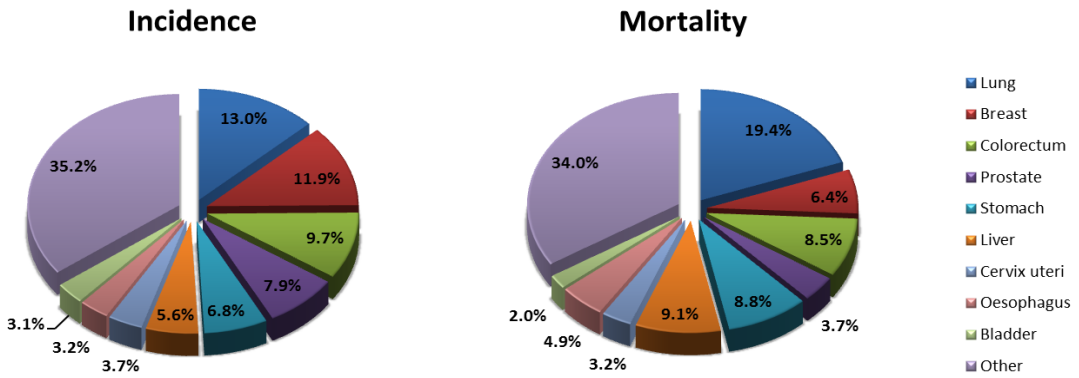

Figure 1.1 – Incidence and mortality rates worldwide for most common cancers (Adapted from "GLOBOCAN," 2012).

The close relationship evidenced between incidence and mortality rates for some types of cancer such as lung, colorectal and stomach, allows not only to infer about social and cultural habits, as well as draws attention to a more pressing issue that is the inefficiency of current therapeutic strategies applied for these same cancers. In the end with current trends it is predicted that globally, cancer burden will increase significantly, up to 19.3 million new cancer cases per year by 2025 ("GLOBOCAN," 2012; "World cancer factsheet," 2014) stressing out ever more the importance of a complete understanding over the underlying molecular mechanisms that lead to the onset of cancer,

and of the establishment of priorities and control strategies to fray down the overwhelming spread of cancer globally.

1.2.1. Lung Cancer Incidence

In 2012 1.8 million new cases of lung cancer were estimated ("GLOBOCAN," 2012), compared with 1.6 million in 2008 and is considered the most common cause of death in developing and developed countries (Jemal *et al.*, 2011). Notably in Europe and in Eastern Asia the incidence rates for men surpasses the 50 cases per 100000 persons while in women these rates are slightly lower due to historic variants. The highest estimate rates for women are evidenced for North America and Northern Europe with values of 32.8 and 23.7 cases per 100000 persons respectively. In contrast low developing countries in the Western and Middle Africa area report the lowest incidence rates in an order of magnitude of 0.8 to 1.1 cases per 100000 persons ("GLOBOCAN," 2012).

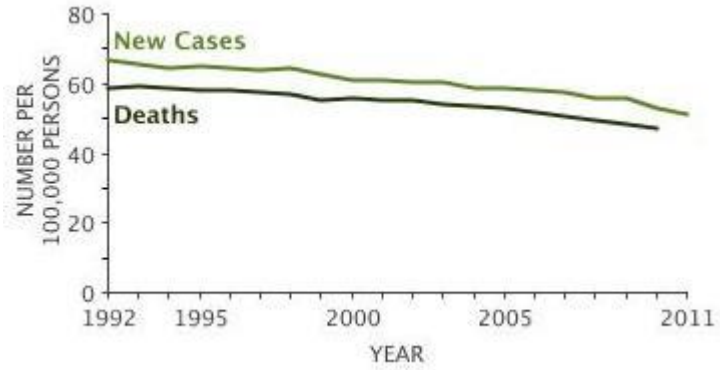

Figure 1.2 – Lung and bronchus cancer incidence and mortality rates in the United States ("Cancer of the Lung and Bronchus - SEER Stat Fact Sheets," 2010).

Despite these statistical numbers the fact is that the incidence and mortality rates for lung cancer is actually decreasing for the majority of western countries including many European countries (Jemal *et al.*, 2010). This trend is particularly evident when observing the decrease of lung and bronchus cancer incidence and mortality rates in the United States (US) over the years (Figure 1.2), in particular since it peaked in middle of the last century. Tobacco control interventions, increased cigarette prices, restriction of tobacco advertising and an awareness rising against the dangers of smoking, among other antismoking strategies are between some of the control measures taken by developed countries that actually justify this specific decline in incidence and mortality rates. To put in perspective recent studies demonstrate that tobacco control implementations in the US, during the period 1975–2000, have averted 32 % of lung cancer deaths due to changes in smoking behaviours (Moolgavkar *et al.*, 2012). Nevertheless the high overall ratio of mortality to incidence (around 0.87) forces a pattern where mortality rates closely follows those of incidence ("Cancer of the Lung and Bronchus - SEER

Stat Fact Sheets," 2010), emphasizing the continuous need for better control programs and particularly treatment strategies.

1.3. Cancer Biology: Cellular and Molecular Basis

1.3.1. Genomic instability and other Contributing Factors for Neoplasic Transformation

The occurrence of aberrational events within the genome, either of temporary or permanent nature, commonly referred to as genomic instability in the literature, are often associated and characteristic of most cancers (Negrini *et al.*, 2010). Both numerical aberrations and structural rearrangements of chromosomes or even the accelerated rate of chromosomal alterations, which result in gains or losses of whole chromosomes as well as inversions, deletions, duplications and translocations of large chromosomal segments, are the most frequent form of genomic instability. Although expansion and contraction of the number of oligonucleotides repeats in microsatellite sequences have also been described (Negrini *et al.*, 2010; Gordon *et al.*, 2012).

Even though the genomic instability in hereditary cancers is well understood, and strongly linked to mutations in DNA repair genes such as those involved in the nucleotide and base excision repair processes (*BRAC1*, *BRAC2*, *MSH2*, *MYH*), the molecular basis is not so clear for sporadic cancers. Recent reports have however shed some light over this subject mentioning that mutations in caretaker genes (like DNA repair genes) are infrequent in early cancer development (69 to 97 % of cancers did not present mutations in caretaker genes) and propose oncogene-induced DNA replication stress as the most likely responsible for the processes involved in genomic instability for these cancers (Negrini *et al.*, 2010). With increased genomic instability, spontaneous DNA damage events are more likely to occur as a result of DNA replication stress (compromised fidelity of replication enzymes). Events such as depurination due to N-glycosidic breakage, or deamination of cytidine to uridine, and deamination of methylcytosine to thymidine greatly increase the mutagenic susceptibility (Bertram, 2001), selectively promoting specific mutations as those occurring in *TP53*, resulting in cells evading death and senescence (Figure 1.3) (Negrini *et al.*, 2010; Farnebo *et al.*, 2010).

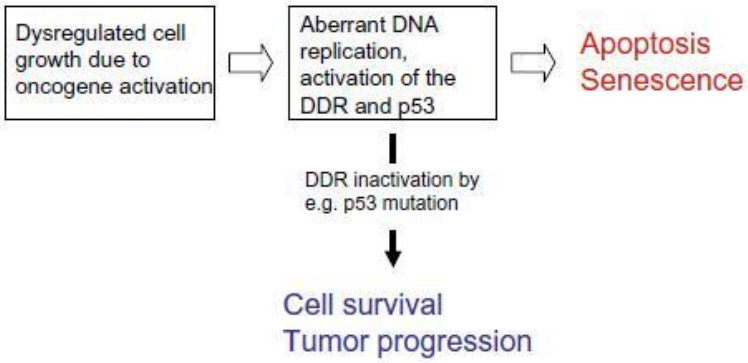

Figure 1.3 – p53 as a barrier against tumour development. Oncogene activation or deregulated cell cycle progression leads to stalled DNA replication forks and activation of the DNA damage response (DDR) (Adapted from Farnebo, *et al.*, 2010)

In addition a recent cohort study involving 3281 tumours across 12 tumour types as part of the Cancer Genome Atlas effort, has demonstrated that *TP53* is in fact the most frequently mutated gene (Kandoth *et al.*, 2013). Other reports have actually linked *TP53* mutations to over 50 % of all human cancers including lung carcinoma where it represents an extremely common event (Vincenzi *et al.*, 2006; Farnebo *et al.*, 2010; Wong, 2011). Furthermore *PIK3CA* was found to be second most frequently mutated gene representing a frequency of over 10 % of most cancer types (Kandoth *et al.*, 2013), and the remaining frequently deregulated genes mainly encoded classical oncoproteins like epidermal growth factor receptor (EGFR), KRAS and NRAS family, phosphatase and tensin homologue (PTEN) (Negrini *et al.*, 2010; Kandoth *et al.*, 2013).

Apart from the genetic mechanisms described above, epigenetic studies are gaining increasing relevance as more and more evidences point out a more significant role for DNA alterations and associated chromatin changes in gene expression and in tumourigenesis (Waldmann and Schneider, 2013). Hallmarks of epigenetic changes like DNA methylation and post-translational modifications of histones may contribute to oncogenesis through transcriptional silencing of tumour suppressor genes (Waldmann and Schneider, 2013). Global hypomethylation, possibly the first epigenetic modification to actually be linked with tumourigenesis is commonly observed in malignant cells being associated with chromosomal instability in colorectal cancer (Berman *et al.*, 2012). However methylation changes occurring at CpG islands equally play an important role in modelling transcriptional responses. Hypermethylation frequency of such regions was found to be often high. In fact typically unmethylated CpG islands in promoter genes, around 5 to 10 %, have actually been confirmed to be methylated in various cancer genomes (Dawson and Kouzarides, 2012; Waldmann and Schneider, 2013; Esteller *et al.*, 2001), but the relevance of this alterations is still to be deciphered.

Regarding the interplay between histone modifications and cancer, a few mutations have been found through genome sequencing of tumours. Specific point mutations in histones H1.5, H3.1, H3.3 have been reported and are known to change chromatin conformation, and in particular H3 mutations seem

to be linked to some specific cancers such as gliomas. Nevertheless all in all, the consequences of such mutations remain to be unravelled and further studied (Waldmann and Schneider, 2013).

Additionally specific mutations in numerous epigenetic gene regulators have also been found in several cancers which in part might explain differences in methylation patterns during oncogenesis. For example histone-lysineN-methyltransferase gene, *MLL2*, has been recurrently found mutated in several cancers (Kandoth *et al.*, 2013), but in particular high incidence in follicular lymphoma. Plus *UTX*, a histone demethylase has been found to be mutated in up to 12 histological distinct cancers (Dawson and Kouzarides, 2012). Mutations were still found in other chromatin remodelling genes such as *MLL3, MLL4* for bladder, lung and endometrial cancers, and demethylase gene *KDM5C* in kidney carcinoma (Kandoth *et al.*, 2013). By understanding the mechanisms involved in epigenetic control and their associated mutations, the foundations are laid for the production of new drugs and treatments to override such alterations that may cause cancer and many other diseases.

Other factors such as proteotoxic, metabolic and oxidative stress have reportedly influence the process of neoplasic transformation and tumourigenesis. In regards to metabolic stress, for instance, it is known that tumoural cells produce ATP through glycolysis which in turn grants tumoural cells an adaption to hypoxia conditions, and allows for the acidification of the surrounding environment. In turn it facilitates tumour invasion and immune suppression. More detailed information is presented elsewhere (Luo *et al.*, 2010).

1.3.1.1 p53 Tumour Suppressor

Despite the fact that each cancer is characterized by a specific set of mutations, as already mentioned above, the high frequency of *TP53* mutations in a broad spectrum of cancers, draws much attention to it and its particular biological functions (Olivier *et al.*, 2010), hence it will be further analyzed here. The p53 tumour suppressor has been established as a nucleophosprotein that plays an important role in cellular homeostasis (Steele and Lane, 2005; Alarcon-Vargas and Ronai, 2002). Its importance comes not only from the fact that is often mutated in over 50 % of all cancers, but also due to the increasing number of biological processes that it has been implicated in, such as cell cycle arrest, senescence, apoptosis, autophagy, angiogenesis, metabolism, and aging (Sullivan *et al.*, 2012; Farnebo *et al.*, 2010; Vousden and Prives, 2009). There are also increasing evidences that, even though p53 is best described as transcription factor, some of the biological processes in which it has been involved are cytosolic and transcription independent (Figure 1.4) (Green and Kroemer, 2009; Vousden and Prives, 2009). Particularly p53 biological activity is triggered when accumulated in response to several cellular stress inputs, including DNA damage by exogenous carcinogens, oncogene activation, telomere erosion, hypoxia, loss of cell adhesion, compromised microtubule scaffolding, transcription blockage and others (Farnebo *et al.*, 2010; Green and Kroemer, 2009).

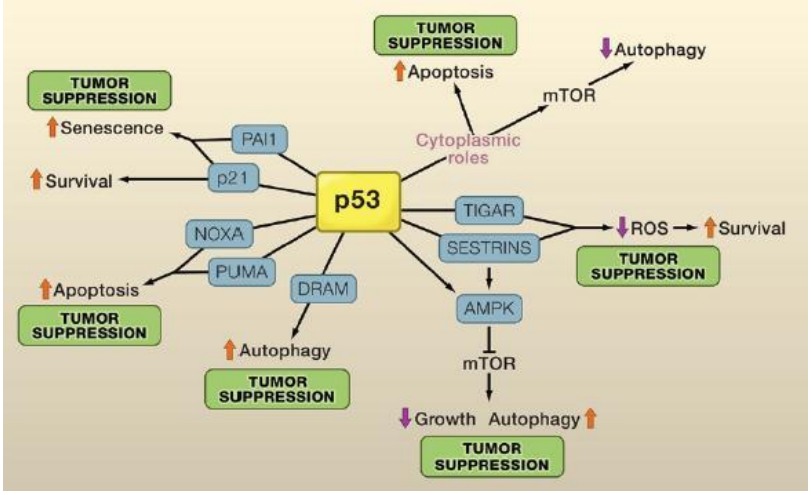

Figure 1.4 – p53 intricate circuit board of biological processes and their respective regulation, with discriminated transcriptional and cytoplasmic roles (Adapted from Vousden and Prives, 2009).

In turn it is the "impairment" of the auto-regulatory loop between Mdm2 and p53 (which regulates the overall stability and activity of p53 through post-translational modifications) through these cellular stress inputs that lead to the accumulation of p53 (Alarcon-Vargas and Ronai, 2002). This then triggers the activation of p53 target genes, such as p21, GADD45, Bax, Puma, Noxa, DR5, p53AIP, PIDD, and others, triggering apoptosis, autophagy, cell cycle arrest or senescence (Farnebo *et al.*, 2010; Alarcon-Vargas and Ronai, 2002). It is then easy to understand that activation of such pathways by p53, in normal conditions, leads to tumour suppression (Figure 1.4).

For instance cell cycle arrest can be achieved through p53 mediated activation of the cyclin-dependent kinase inhibitor p21, alongside with target genes such as 14-3-3 sigma and *GADD45* (Vousden and Prives, 2009). Particularly p21 inhibits cell cycle progression mainly through the inhibition of CDK2 and CDK1, which are involved in a myriad of phosphorylation cascades (such as the phosphorylation of RB; key for cell cycle entry), leading to a temporary growth arrest in G1/S stage of the cell cycle. Plus p21 binding to proliferating cell nuclear antigen hinders DNA polymerase activity, inhibiting replication and allowing for the activation of DDR processes (Manuscript, 2010). Together these processes concede time for DNA repair.

In turn apoptosis induction by p53 is not so clearly understood, however extensive literature report two major mechanisms; transcription dependent and transcription independent or cytoplasmatic (Bertram, 2001; Green and Kroemer, 2009). Generally in the nucleus p53 is responsible for dictating the expression levels of numerous pro-apoptotic molecules, such as BAX, PUMA, NOXA, BID that will ultimately lead to mitochondrial outer membrane permeabilisation (MOMP). In the cytoplasm the fate of the cell greatly depends on the extrinsic stress factor, and in the counterbalance between pro-apoptotic versus anti-apoptotic proteins. Hence the interactions between p53 and proteins of the Bcl-2

or Bcl-xL family can either lead the promotion or inactivation of pro-apoptotic Bcl-2 multi-domain proteins and consequently to cell death or cell survival (Chipuk and Green, 2006).

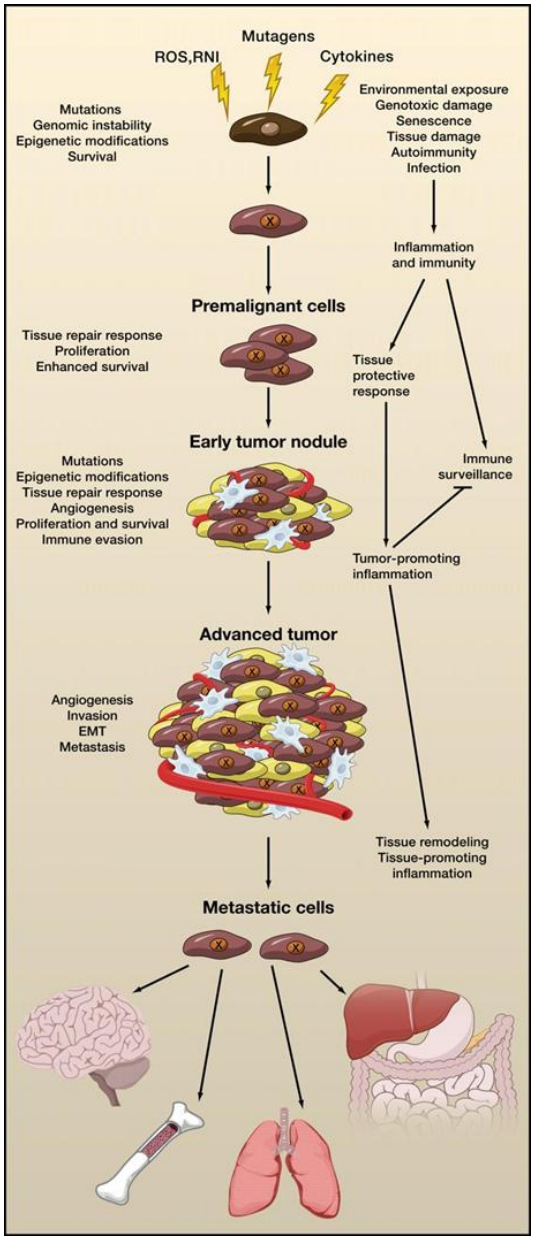

Figure 1.5 – Schematics illustrating the multistage facet of carcinogenesis. Premalignant cells are the result of an initiating event such as a compromised tissue repair response, conferring an enhanced survival. Sequentially early tumour nodules would be the result of the accumulation of successive mutational events, like immune evasion or epigenetic modifications. In the end angiogenesis factors and loss of cell adherence would lead to metastasis and to the formation of an advanced tumour (Adapted from (Grivennikov et al., 2010).

In short p53 specific DNA binding and transcriptional regulation of target genes can be hindered by a myriad of mutations which in turn compromise the ability of a controlled response to tumour suppression, and the wide number of other biological processes in which it is involved. Plus contrary to general believe, recent reports state that some of the p53 mutations, besides abrogating tumour suppression and general transcriptional regulation circuit board, actually endow the protein a set of characteristics that have been found to be fundamental for oncogenesis (Oren and Rotter, 2010).

1.3.2. Mechanisms of Carcinogenesis: A Multi-step Process

As it can be seen cancer is not the result of a single gene defect, but rather a complex multigenic disease. In other words cancer is the end result of a series of alterations that have taken part over a long period of time, nonetheless the vast number of epi- and genetic alterations found across different cancers, not all contribute and have an active role to the onset of cancer. Carcinogenesis is rather likely to be driven only by a select few mutations (gain of an oncogene or the loss of a tumour suppressor), and the remaining alterations may or may not potentiate the overall process, often being called "passenger" mutations as opposed to driver mutations (Ashkenazi *et al.*, 2008; Tomasetti *et al.*, 2013; Luo *et al.*, 2010). As already mentioned above these mutations compromise homeostatic cellular processes and tend to tip the delicate balance between cell proliferation and cell death, often leading to an abnormal and uncontrolled cell growth, giving rise to what it is clinically referred to as neoplasic growth (Bertram, 2001).

Typically the process by which mutations occur is complex and sequential. At least 4 to 7 independent events must take place in order for a cell to be considered as tumourigenic (Ashkenazi *et al.*, 2008; Bertram, 2001). The complexity that carcinogenesis represents, led to the creation of models that try to explain the progression of mutations that are known to take part during this process (Ashkenazi *et al.*, 2008; Tomasetti *et al.*, 2013). The most renowned, probably for its simplicity, models carcinogenesis as multistep process of mutation acquisition, considering a homogenous cell population, in what is known as the "initiation, promotion and progression" model (Figure1.5) (Ashkenazi *et al.*, 2008; Jakóbisiak *et al.*, 2003). In this model a tumour is initiated by a driver mutation in a gene typically involved in the control of cell proliferation, evasion of apoptosis and/or genomic integrity (oncogenic pathways), endowing the cell with superior proliferation characteristics, or any other survival advantage over the remaining cell population. With each successive clonal expansion of such cells, these become susceptible to additional mutational events that are accumulated over time and further contribute for an enhanced survival. Eventually a third event would promote an irreversible process by which the malignant potential of the cells would be enhanced, leading to tissue invasion and metastasis. Events such as increased genomic instability (which is a characteristic of all developed cancers), cytokine and chemokine modulation of tumour cells as result of inflammation, angiogenesis induction, and protease production to promote loss of cell adherence and cell detachment, all contribute for the development of a malignant tumour (Jakóbisiak *et al.*, 2003; Tomasetti *et al.*, 2013; Grivennikov *et al.*, 2010).

Overall, independently of the manifold mutational combinations acquired during the multistep development of carcinogenesis, these will ultimately result in a common set of characteristics or hallmarks that dictates and characterizes the malignant phenotype (Pietras and Ostman, 2010; Hanahan and Weinberg, 2011). These include sustained proliferative signalling, insensitivity to anti-growth signals, evading apoptosis, limitless replicative potential, sustained angiogenesis and tissue invasion and metastasis (Figure 1.6)(Pietras and Ostman, 2010; Hanahan and Weinberg, 2011).

Pivotal for a sustained proliferative growth, cancer cells must be able to be self-sufficient in growth signals in order to outgrow normal tissue cells, and to establish the three dimensional scaffolding necessary for tumour microenvironment interactions, and ultimately tumour promotion and progression.

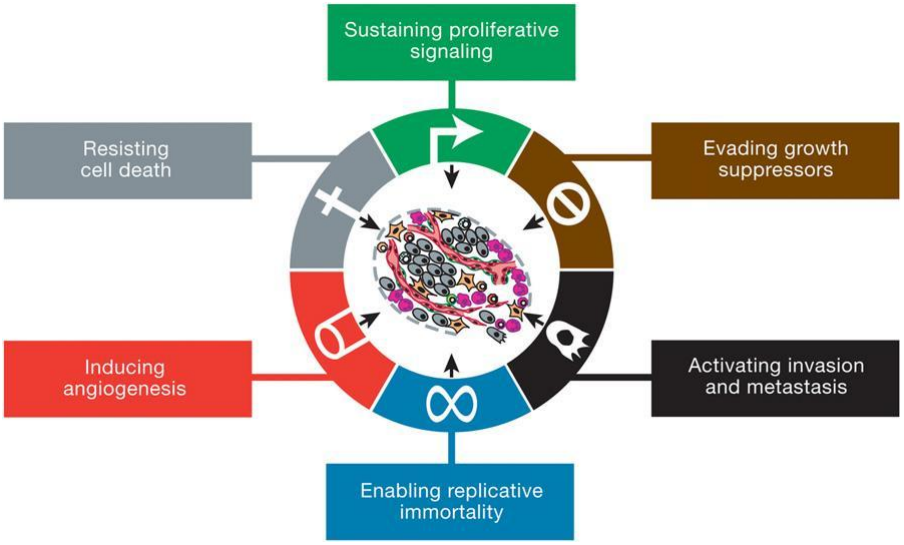

Figure 1.6 – Illustration of the six hallmarks that characterize and influence the process of carcinogenesis (Adapted from Hanahan and Weinberg, 2011).

A variety of possible mechanisms allow for such event to occur, ranging from an overexpression of receptor proteins, to autocrine proliferative stimulation and even constitutive activation of downstream components involved in cell proliferation pathways (*H-RAS* oncogene) (Hanahan and Weinberg, 2011). Secondly the evasion of growth suppressors, very much resembles as "taking away the brakes" that are meant to prevent continuous proliferation. In other words cancer cells are able to abrogate many of these powerful control programs that are often many times related with the biological function of tumour suppressor genes such as those already mentioned here, like *TP53* or the retinoblastoma gene (*RB*) involved in the control of cell cycle progression (Hanahan and Weinberg, 2011). Additionally during tumour progression to the malignant state, tumoural cells must "employ" a variety of strategies to circumvent the complex apoptotic machinery programs that act as barriers to cancer in normal tissues. *TP53* loss of function is the most frequent cause that leads to a compromised activation of the apoptotic machinery programs, however other alterations can also allow tumour cells to bypass apoptosis-triggering mechanisms, such as constitutive expression of anti-apoptotic factors (Bcl-2, Bcl-xL) or the promotion of survival regulators and pathways, to name a few (Hanahan and Weinberg, 2011). Due to the "faulty" nature of DNA replication itself, tumoural cells must also acquire a limitless replicative potential otherwise the sustained proliferative growth would eventually progressively shorten the telomeres (tandem hexanucleotide repeats at the end of chromosomes) leading to the inability to protect the ends of chromosomal DNA, threatening cell viability. In fact telomerase activity is virtually absent in normal cells, while it is expressed in significant levels in the vast majority of cancers, hence circumventing telomere shortening and chromosome instability while simultaneously acquiring replicative immortality (Hanahan and Weinberg, 2011). Additionally tumours are known to be able to induce new blood vessel growth as form to obtain an unlimited supply of nutrients and oxygen as well as a form to create their own waste management pipeline to remove sub metabolic products such as carbon dioxide. Angiogenesis is known to be orchestrated by

several regulators, positive and negative ones, such as vascular endothelial growth factor (VEGF) or platelet-derived growth factor (PDGF) to name a few. For instance VEGF expression can be upregulated by stimulating factors such as hypoxia or oncogene activation (Hanahan and Weinberg, 2011; Bergers and Benjamin, 2003). Also worth mentioning is that the rapid genesis of new blood vessels associated with chronic exposure to angiogenic activators leads to an abnormal overall vasculature different from their normal counterparts sharing different characteristics of several types of blood vessels (Bergers and Benjamin, 2003). Finally all cancers will ultimately engage in tissue invasion and the formation of metastasis. Namely loss of cell adhesion between the cells of the tumour mass allows their disaggregation contributing to an enhanced malignant phenotype, characterized by massive tissue invasion and multiple metastasis formation. Abrogation of cadherin/catenin expression levels, in particular E-cadherin has been highly associated with malignant phenotypes and micro-metastases. Additionally these cells also typically present enhanced cell motility, further assisting the invasion phenotype, through the expression of adhesion molecules like N-chaderin associated with cell migration processes. Also tumour cells are known to produce a vast range of proteases, such as cathepsins that allow the detachment from broad range of extracellular matrix/basement membrane components, including proteoglycans and collagens (Brooks *et al.*, 2010; Hanahan and Weinberg, 2011).

Other emerging hallmarks include the deregulation of cellular energetics, as already mentioned above were cancer cells redirect their energy production to glycolysis, and the evasion from the hosts' cellular and molecular immune mechanisms that are set to destroy cancerous cells such as natural killer cells (Hanahan and Weinberg, 2011).

1.3.3. Mechanisms of Cell Death: Apoptosis, Autophagy & Necrosis

Ever since the pioneering work in *Caenorhabditis elegans* revealed the genetic programme of apoptosis, cell death in the broader sense of this term, has been seen as a fundamental process often governed by an intricate array of regulators and signalling pathways, with an active role in overall development and in the maintenance of cellular homeostasis (Elmore, 2007; Vanden Berghe *et al.*, 2014). Until recently apoptosis and necrosis were considered to be the only forms of cell death, with apoptosis being seen as the fundamentally orchestrated cellular process in physiological and pathological conditions (Wong, 2011), and necrosis as the result of physicochemical abuse leading to an uncontrolled swelling, organelle dysfunction and cell lysis (Vanden Berghe *et al.*, 2014; Ouyang *et al.*, 2012). Both of these cell death modes have already been extensively described and are relatively well understood (Elmore, 2007; Patel *et al.*, 2010; Taylor *et al.*, 2008; Vanden Berghe *et al.*, 2014). Recent understandings however have led to conceptual advances regarding other forms of cell death. Autophagy is a particular example which has been shown to be important in several regulatory pathways under certain physiological conditions. It is considered as catabolic process involving the

formation of double-membrane vesicles called autophagosomes, responsible for the turnover of large portions of cytoplasm including several organelles and other specific macromolecules (Mariño *et al.*, 2014; Ouyang *et al.*, 2012). Plus it is considered as general protective response system that it is triggered under certain environmental stress such nutrient shortages (Mariño *et al.*, 2014). Over the years attempts in discovering the underlying mechanisms related to these forms of cell death have simultaneously led to the uncovering of many other, such as necroptosis, parthanatos, oxytosis, ferroptosis, ETosis, NETosis, pyronecrosis or pyroptosis (Galluzzi *et al.*, 2012; Vanden Berghe *et al.*, 2014). Were some opinions diverge, others attempt to unify perspectives over cell death and recently some authors have proposed that these several forms of cell death are merely different forms of regulated necrosis (Vanden Berghe *et al.*, 2014). Even though necrosis has been generally considered an uncontrolled process resultant from physical damage of some sort, the discovery of key regulators of necrotic death, such as receptor interacting protein kinases (RIPK1 and/or RIPK3) led to the establishment of necrosis as a possible genetically controlled cell death mode (Ouyang *et al.*, 2012; Vanden Berghe *et al.*, 2014). This regulated necrosis is known to be independent of caspase activation, and to lead to a set of biological processes such as, mitochondrial dysfunction, increased cell volume (oncosis), production of ROS, and ultimately lysis. The immunogenic nature of necrosis resultant from the extravasation of their inner components (pro-inflammatory molecules) to the extracellular environment further lead to inflammatory responses that contribute for tumourigenesis (Grivennikov *et al.*, 2010).

Understanding the underlying mechanisms of these modes of cell death is crucial as it will lay the groundwork and study platforms for different chemotherapy strategies, while simultaneously allowing for a better knowledge of the consequences of such strategies.

1.3.3.1. Apoptosis

The process of programmed cell death by apoptosis is best described as series of molecular and architectural cellular alterations controlled by an intricate system of energy-dependent biochemical mechanisms and regulators (Taylor *et al.*, 2008; Elmore, 2007). The positive induction of such mechanisms leads to distinct morphological alterations, such as cell shrinkage and convolution, detachment from the extracellular matrix, chromatin condensation, mitochondrial; Golgi; endoplasmic reticulum (ER) fragmentation, nuclear fragmentation and blebbing of the plasma membrane while maintaining its integrity (Elmore, 2007; Orrenius *et al.*, 2011). Each bleb eventually culminates into an individual vesicle, termed apoptotic body, which contain the remaining cytoplasmic components resultant from the controlled “demolition” of the overall cellular architecture. In the end these apoptotic bodies are rapidly consumed by specific cellular counterparts like macrophages that recognize particular molecular surface markers, thus avoiding an unwanted immunogenic response,

since there isn't an extravasation of the intracellular content to the surrounding tissues (Taylor *et al.*, 2008; Orrenius *et al.*, 2011).

The entire process that comprises apoptosis is vast and complex; hence the major biochemical pathways and regulators will only be discussed here briefly. The extensive research upon apoptosis has led to the identification of three major apoptotic pathways: the extrinsic or death receptor pathway, the intrinsic or mitochondrial pathway and the perforin-granzyme-dependent pathway (Figure 1.7) (Elmore, 2007; Taylor *et al.*, 2008). The perforin-granzyme-dependent pathway that will be addressed in less detail is best described as to involve the cytotoxicity of T-cells which induce apoptosis either by granzyme B or granzyme A.

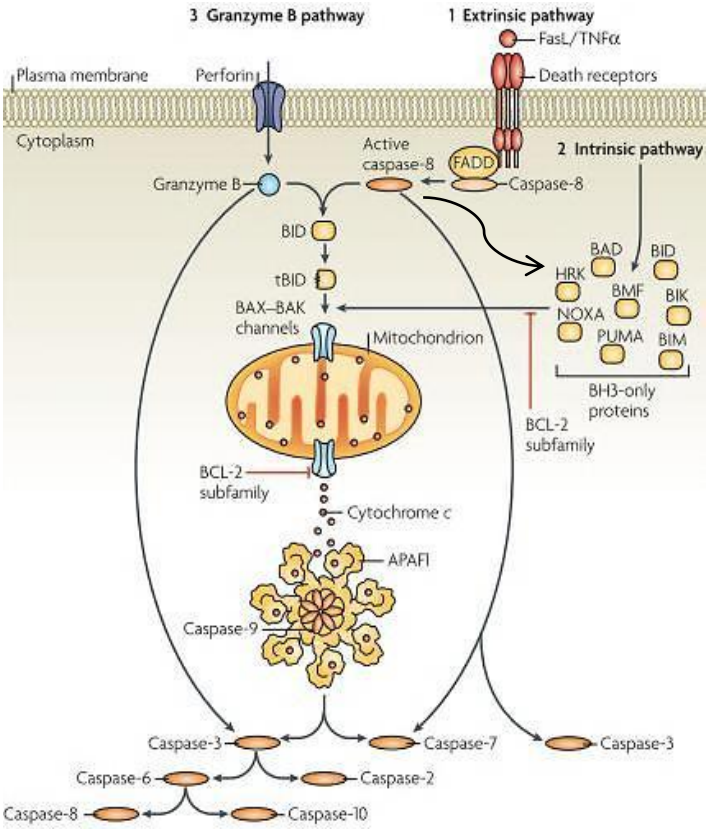

Figure 1.7 – Illustration of the different activation pathways of apoptosis. Extrinsic pathway (1) as well as intrinsic (2) and granzime B pathway (3) are depicted alongside with their main intervenients. Irrespective of the actual route to caspase activation, all pathways lead to the activation of the major effector caspases, caspase-3, caspase-6 and caspase-7, and these carry out much of the proteolysis that is seen during apoptosis (Adapted from Taylor *et al.*, 2008).

Independently of the activation pathway triggered all of these seem to converge into the same biochemical pattern, which is the activation of caspases (Orrenius *et al.*, 2011; Elmore, 2007). Caspases are present in all cells in a form of precursor enzymes or zymogens, and once activated are responsible for most if not all the biochemical changes that occur as apoptosis progresses towards its end (Taylor *et al.*, 2008). Their proteolytic activity cleaves proteins at their aspartic residues leading to protein cross-linking, DNA fragmentation (down to 200 bp fragments) and eventually to the

morphological alterations already mentioned above (Elmore, 2007). A noteworthy concept to keep in mind is that once activated, cells seemingly become committed to a programmed cell death. At the risk of being over simplistic the extrinsic pathway, as the name suggests, is activated by the binding of extracellular death ligands, such as FasL (*fatty acid synthetase ligand*) or tumour necrosis factor-α (TNFα), to their respective transmembrane death receptors (Wong, 2011). The family of transmembrane death receptors is vast including more than 20 proteins with a broad range of biological functions (Ouyang *et al.*, 2012; Schulze-bergkamen and Krammer, 2004), however the best described and more extensively studied are type 1 TNF receptor (TNFR1) and a related protein Fas (CD95- FasL receptor) (Schulze-bergkamen and Krammer, 2004; Wong, 2011). Upon ligation to their cognate ligands, receptor trimerization occurs as well as clustering of death domains and the recruitment of adaptor proteins such as Fas-associated death domain (FADD) or TNFR1-associated death domain (TRADD) which in turn form a protein complex known as the death-inducing signalling complex (DISC) (Fulda and Debatin, 2006; Wong, 2011). Once formed this protein complex is responsible for the oligomerisation of pro-caspase-8 leading to its activation through self-cleavage. In turn caspase-8 can proteolytically activate downstream caspase effectors such as caspase-3 and caspase-7, or in other situations it can promote the activation of BH3-only protein BID (BH3-interacting domain death agonist) through crosstalk with the intrinsic pathway. After proteolytic activation by caspase-8, the truncated BID induces mitochondrial outer membrane permeabilisation (MOMP) by the formation of transmembrane BAX-BAK channels (BAX-Bcl-2-associated X protein), consequently causing the release of cytochrome c and assembly of the apoptosome (Figure 1.7). The last one is multi-protein complex, comprised by 7 molecules of apoptotic protease-activating factor-1 (Apaf-1), caspase-9 and cytochrome c that binds to the C-terminal region of Apaf-1. Together this complex is responsible for further amplifying the apoptotic signal in the intrinsic pathway (Taylor *et al.*, 2008; Fulda and Debatin, 2006).

The intrinsic pathway on the other hand is marked by the diverse stimuli that trigger it. Internal stimuli like hypoxia, irreparable DNA damage, high concentrations of Ca^{2+}, oxidative stress by ROS, temperature and osmolality changes, nutrient shortages and others, may induce changes in the inner mitochondrial membrane that result in the loss of transmembrane potential leading to the release of pro-apoptotic molecules into the cytosol (Wong, 2011; Portt *et al.*, 2011). More specifically these stimuli lead to p53 mediated activation of members of the BH3-only protein family (e.g., PUMA, NOXA, BID), which when above a crucial threshold in the cytosol surpasses the inhibitory effect of the anti-apoptotic B-cell lymphoma-2 (BCL-2) family members (Taylor *et al.*, 2008). It is in fact the balance between the pro- (e.g. Bax, Bak, Bad, Bcl-Xs, Bid, Bik, Bim and Hrk) and anti-apoptotic (e.g. Bcl-2, Bcl-XL,Bcl-W,Bfl-1 and Mcl-1) proteins within the cytosol that defines whether apoptosis is carried out or not (Wong, 2011). BH3-only proteins promote the assembly of BAX-BAK channels in the mitochondria causing MOMP the consequent release of intermembrane proteins such as

cytochrome c, second mitochondria-derived activator of caspase/directed IAP (inhibitory of apoptosis proteins) binding protein with low pI (Smac/ DIABLO), and apoptosis-inducing factor (AIF). Among these cytochrome c plays perhaps the most important part, as it is a key intervenient in the assembly of the oligomerization protein platform that is the apoptosome, which is responsible, as mentioned above, for the autoproteolytic activation of caspase-9. The other released proteins have a variety of roles ranging from sequestering caspase inhibitors to the induction of morphological alterations to the nuclear envelope (Du *et al.*, 2000; Schulze-bergkamen and Krammer, 2004).

During the execution of the apoptosis process the activation of caspase effectors, like caspase-3 -6 and -7, regardless of the activation pathway, leads to the fracture of key architectural cellular structures and biochemical pathways. Namely the cytoskeleton scaffolding that ensures the 3-dimensional structure of the cell is one of the first key structures to be targeted during the execution phase of apoptosis. Molecules such as actin itself, and actin-associated proteins, like myosin, spectrins, α-actinin, gelsolin and filamin are proteolytically destroyed causing the typical morphological hallmarks of apoptosis, like the acquisition of a round shape, loss of cell adherence and membrane blebbing. Plus, chromatin condensation is thought to be the result of nuclear lamin targeting by caspases (Schulze-bergkamen and Krammer, 2004; Taylor *et al.*, 2008; Wyllie, 2010). In short the connections established between the myriad of regulators and pathways are the mere strings of the puppeteer that is the programmed cell death by apoptosis and the considerable biochemical changes that occur within the apoptotic cell.

1.3.4. Cell Division and Carcinogenesis Interplay

The highly regulated process that cell division represents is crucial for cell turnover and tissue homeostasis. Cell division, or cell proliferation is separated into three sequential processes know as interphase, mitosis and cytokinesis. Interphase is the longest phase during cell division. It is characterized by very long chromatin fibbers however these tend to shorten and become thicker as interphase progresses. Plus it is also characterized by an increase in the overall cell size and the accumulation of specific macromolecules crucial for the execution and progression of the cell cycle that ensures the formation of two daughter cells. The accumulation of these macromolecules involves among others, the duplication of the genetic material, plus accumulation of RNA levels, ribosomes and other proteins (Weinberg, 2013). Mitosis is then preceded by the duplication of the genetic material, and encompasses four distinct phases: prophase, metaphase, anaphase, and telophase. In short mitosis is responsible for nuclear division where spindle fibbers pull the chromatids apart from the condensed chromosomes to each opposite pole that will result in the formation of the two daughter cells, that is then proceeded by segregation of the cytoplasm by cytokinesis.

As any other highly regulated cellular process, cell division and the overall regulation (see below) is prone to potential alterations and aberrant phenomena as a result of mutations. Misregulation of cell cycle events and the control of the commitment to cell division have been widely shown in the literature to play an important role in cancer onset. Compromised cell cycle regulation processes, as those involving the core components of the cell cycle clock, namely cyclins and cyclin dependent kinases (CDK), affect the proper distribution of chromosomes at the metaphase to anaphase transition by the spindle-assembly checkpoint leading to overall genetic instability, aneuploidies and unscheduled proliferation (Malumbres and Barbacid, 2001; Malumbres and Barbacid, 2009).

1.3.4.1. Cell Cycle Regulation and Deregulation in Cancer

The cell cycle is comprised of 4 distinct phases (G1, G2, S, and M) all of which are controlled by numerous mechanisms to ensure a correct cell division (Figure 1.8). More specifically the cell cycle is responsible for faithfully replicate DNA during S phase, and to ensure the equal segregation of all cellular components to the daughter cells including the identical chromosomal copies during the M phase. The remaining two phases, namely G1 and G2 are intermediate periods mainly responsible for an high synthesis of macromolecules and other regulators essential for cell cycle progression through S and M phases respectively (Malumbres and Barbacid, 2001; Sherr, 1996; Lapenna and Giordano, 2009).

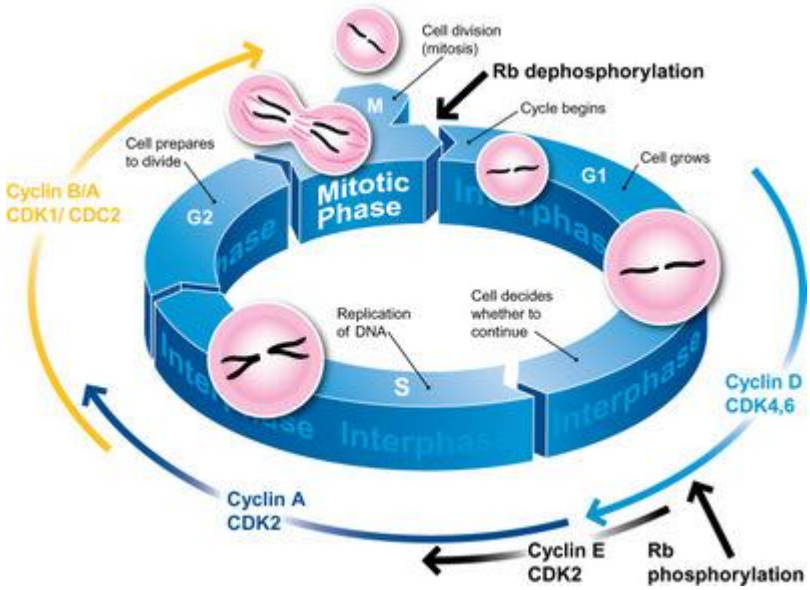

Figure 1.8 – Illustration of the regulation of the mammalian cell cycle. Key CDK/cyclin complexes role in the distinct phases of the cell cycle is also displayed. Cdk4/cyclin D complexes phosphorylate Rb in mid G1, while Cdk2/cyclin A and Cdk2/cyclin E phosphorylate Rb at the G1 to S transition. Dephosphorylation of Rb allows binding to E2F family of transcription factors, forming a silencing complex restricting the progression of cell cycle, by transcription prevention of cell cycle control genes. Cdk2/cyclin A and Cdk1/cyclin B/A complexes and their kinase activity is essential for progression through S phase and entry in M phase (Adapted from "Propidium iodide staining of cells to assess DNA cell cycle," 2014).

Apart from the already mentioned phases there is another critical moment in the cell cycle known as G0, a quiescent state where most of the non-proliferating cells stand at. Furthermore progression through the cell cycle only occurs upon a G0—G1 transition in response to stimuli such as mitogen exposure and nutrient abundance (Lea *et al.*, 2003; Schwartz and Shah, 2005). This transition is highly regulated and it is thought to be one of the several developed checkpoints that prevent an awry cell progression (Malumbres and Barbacid, 2001). In fact the transition between cell cycle phases is regulated by several different proteins, nonetheless the key regulatory proteins are cyclin-dependent kinases (CDK), the activity of which is modulated by fluctuating levels of cyclins throughout the progression of the cell cycle (Vermeulen *et al.*, 2003; Schwartz and Shah, 2005). Mitogenic signalling leads to activation of CDK/cyclins complexes, through phosphorylation cascades such as MAPK/ERK pathway (Schwartz and Shah, 2005). In particular G0—G1 transition is characterized by phosphorylation of the retinoblastoma protein (RB1), mediated by active complexes of D-type cyclins with CDK4/6. Furthermore towards the end of G1 phase RB1 is phosphorylated in additional sites by CDK2/Cyclin E complex, breaking the tight bond with E2F transcription factor family (that constituted a gene silencing complex), promoting an expedite expression of S phase related genes (Lapenna and Giordano, 2009; Vermeulen *et al.*, 2003; Sandal, 2002). In what is known as the restriction point, this event represents the point of no return in G1 in which progression through the cell cycle is "automated" and independent of external stimuli (Lapenna and Giordano, 2009). Mutations in CDK–cyclin complexes, or their regulation, as well as the conformational structure of RB like proteins are often associated with frequent tumour phenotypes leading to uncontrolled proliferation and genomic instability (Malumbres and Barbacid, 2009). For instance in same cases of lung cancer RB alterations are found in high percentage approaching incidences of 88 % to 100 % (Vincenzi *et al.*, 2006). Beyond the restriction point new intervenients come into play, namely the sequential formation of CDK2/cyclin A complex by complexation of both regulators, allows the progression through S phase into G2 phase, during which CDK2/cyclin A complex is responsible for the production of enzymes involved in DNA synthesis. DNA polymerases, histones and proliferating cell nuclear antigen (PCNA) are among the main intervenients (Lapenna and Giordano, 2009; Malumbres and Barbacid, 2009). Particularly in lung cancer PCNA is thought to have a specific role in cancer onset as it has been found to be frequently mutated (95-100%; Vincenzi *et al.*, 2006). Towards the end of the interphase, during G2 phase, levels of CDK1/cyclin A experience a substantial increase which is thought to mediate chromosome condensation and the overall microtubule scaffolding dynamics responsible for spindle fibber assembly. Entry in mitosis is determined by the degradation of cyclin A and the formation CDK1/cyclin B which is promptly relocated into the nucleus. The final process occurs when CDK1 degradation by anaphase-promoting complex (APC) leads to the complete division into daughter cells (Lapenna and Giordano, 2009; Schwartz and Shah, 2005).

The activity of many cell cycle CDK and cyclins is often deregulated in many different types of cancer as a result from genetic and epigenetic alterations in their genes or regulators, making them a tempting target when it comes to cancer therapy. For instance CDK4 overexpression has been found in several cancer types including melanoma, sarcoma and gliomas, while cyclin D1 gene translocation is often associated with B-cell malignancies (Vermeulen *et al.*, 2003). The recognition that the use of cell cycle intervenients as cancer targets, in particular CDKs by CDK inhibitors, could induce apoptosis, introduced new hope and a new possible fronts for battling cancer.

1.4. Principles of Cancer Therapy

The vast cancer therapeutic procedures mainly envision to eliminate the total cancer mass, or when unfeasible, efforts are turned towards palliation procedures to prolong and ameliorate cancer patients quality of life (*World Cancer Report*, 2008). One key aspect to keep in mind is that treatment procedures greatly depend on a variety of individual factors, resulting from the individual nature of each cancer itself to the nature and condition of the patient and even from the socioeconomical setting. Conditions such as specific pathological and molecular cancer characteristics, the development stage and health conditions of the patient are but examples of the multitude of factors that might condition treatment programs (Luqmani, 2005). As so, anti-cancer therapy must be assessed for each situation, considering all the integrating variables at hand (Luqmani, 2005). A noteworthy realization is that improvements in pathology analysis, as well as in morphological, imaging and molecular characterization tools (e.g. magnetic resonance imaging; positron emission tomography scanners; mutation mapping) have over the past decade or so, provided the means and the platforms which allow for the refined evaluation of such interacting variables, thus providing in that sense an avenue to correctly assess the most suitable treatment options (*World Cancer Report*, 2008). The classical treatment strategies mainly include surgical excision, radiotherapy, immunotherapy, endocrine therapy and chemotherapy, which normally are used in combination in order to eradicate the total tumour mass and/or diminish the possibility of invasion and metastasis. As for any other treatment program surgical removal as its own specific set of advantages and disadvantages and it must follow certain rules. Typically it is mostly applied in early detected non-invasive tumours and it involves the removal of the tumour as a hole plus the removal of the surrounding tissue as a precautionary measure (Baba and Câtoi, 2007). Similarly radiotherapy is often used in localized cancers and in conjunction with surgical procedures. It is based on the fact that tumoural cells are particularly more vulnerable to ionizing radiation than compared with healthy cells. The rationality behind it is that the use of gamma rays or x-rays will eventually damage important molecular regulators and pathways, directly or indirectly inducing DNA damage and consequently cell cycle arrest or death (*World Cancer Report*, 2008; Baba and Câtoi, 2007). Immunotherapy on the other hand is particularly interesting as it makes use of the hosts defence mechanisms as an anti-cancer strategy. Perhaps the most recognised is the specific passive immunotherapy which involves antibodies (e.g. Cetuximab/Herceptin) against specific

proteins that are overexpressed in cancer cells (Doody *et al.*, 2007; Alley *et al.*, 2010). Endocrine treatment in turn deals with cancer prevention by using counteracting hormone stimulated tumours with antagonizing agents (Luqmani, 2005). With exception for chemotherapy, which will be addressed latter, these treatment programs are beyond the scope of this project and won't be further addressed, although extensive literature reports present more detailed information on the subject (Baba and Câtoi, 2007; *World Cancer Report*, 2008).

Beyond the classical treatment strategies, there have been emerging new cancer therapies worth mentioning. These new strategies aim towards tackling classical treatment strategies' disadvantages, such as lack of selectivity or efficacy that often translates to off-target effects leading to broad cytotoxicity and myriad of other side effects. Examples of such strategies include genetic/epigenetic therapy (Cross and Burmester, 2006), siRNA based approaches (Devi, 2006), nanocarriers as vehicles for drug delivery (Peer *et al.*, 2007; Díaz and Vivas-Mejia, 2013), immunotherapy through microbial approaches (Forbes, 2010) and photodynamic therapy (Hu, 2014). Gene therapy for instance presents itself in a vast number of possibilities and approaches that offer multiple opportunities for battling cancer. In particular it can make use of genetically modified viral particles that replicate within cancer cells causing its oncolytic death, or perhaps in a more traditional perspective it can use gene transfer to introduce new genetic information into a tumoural cell or the surrounding environment to condition their biological aspect, and eventually corrupt tumour growth (Cross and Burmester, 2006; McCormick, 2001). In the most direct application tumour suppressor genes like *TP53* or *PTEN* are transfected into cancer cells in which these genes are deficient (McCormick, 2001). In another perspective nanotechnology has over the years shown the potential to revolutionize the way cancer therapy is performed (R. Fernandes and Viana Baptista, 2013; Martins *et al.*, 2014b). With the advent of nanotechnology, the formulation of nanocarriers as versatile vectorization platforms for drug delivery has been made possible (Wright, 2014). Furthermore the rational design of these nanocarriers coupled with a deep understanding of tumour biology and its several biochemical pathways offers multiple advantages over classical treatment strategies. From targeted delivery, to enhanced pharmacokinetic/pharmacodynamic properties and many others, the nanotechnology toolbox allows for a virtually endless number of possibilities to interact with cancer cells at the molecular and cellular level and ultimately to improve cancer therapeutics (Ferrari, 2005; Baptista, 2009). Prime examples of the application of nanoparticles include the conjugation of nanocarriers containing chemotherapeutic drugs with antibodies able to recognize overexpressed antigens at the surface of cancer cells, and the use of nanocarriers containing the same biological targeting abilities for imaging and diagnosis purposes (Peer *et al.*, 2007). Despite the number of opportunities offered by nanotechnology, only a few nanocarriers have actually been approved for clinical use, due in part for the lack of knowledge regarding *in vivo* interactions and toxicological issues (Fadeel and Garcia-Bennett, 2010).

All in all the stated benefits and the overall features of such alternative therapies' programs, yet to be fully understood and characterized, must still be weighed in in comparison with the classical treatment strategies of surgery, radiotherapy and chemotherapy. In this sense chemotherapy, in spite of all the recent advances, is still considered as the gold standard when it comes to clinically employed cancer therapy (Weinberg, 2013; Chabner and Jr, 2005).

1.4.1. Chemotherapy: Metal Based and other Anti-Tumoural Compounds

Chemotherapy's principle is generally based on the use of chemical substances that target tumour cells in rapid proliferation, or any other hallmark of tumour cells (Martins *et al.*, 2014a; R. Fernandes and Viana Baptista, 2013; Baba and Câtoi, 2007). The hyperactive growth signalling pathways that endows cancer cells with superior proliferative advantage over their healthy counterparts equally makes them more vulnerable to a wide range of drugs clinically employed, which target growth signalling molecules and biosynthesis processes, such as DNA replication, translation, metabolism, formation of mitotic spindles and others (Table 1.1) (Luqmani, 2005). A particular class of chemotherapeutic drugs is those based on metal compounds. The development and approval of cisplatin for clinical use for its anti-cancer properties in 1978 opened the world's eyes for the potential of metal compounds as anti-cancer drugs (Chabner and Jr, 2005). After the success of cisplatin a boom of new metal compounds were screened for their anti-proliferative properties with a new spectrum of designs and activities. Nonetheless some questions still remain on how these compounds mechanistically "work" under physiological conditions. While the mechanism of action is well established for some metal compounds such as cisplatin (DNA cross-linking), for others, it still remains an uncertain issue since their activity highly depends on their rational structural design (Gianferrara *et al.*, 2009). The chosen metal, oxidation state, their ligands and eventually the physiological setting, all have a significant influence on how these compounds develop their therapeutic activity. Cisplatin owes its success to its high anti-cancer effectiveness, displayed in several solid tumours, as direct result of its own mechanism of action (Siddik, 2003). Its cytotoxicity occurs after crossing the cell membrane where its interaction with nucleophilic N7-sites of purine bases leads to the formation of intra-strand and inter-strand DNA crosslinks. Accounting for over 85 % of all lesions 1,2-intrastrand ApG and GpG crosslinks are considered as the major forms of DNA adducts (Hannon, 2007; Siddik, 2003). These eventually alter and compromise the biosynthetic machinery leading to the activation of DNA damage response processes, culminating in the induction of programmed cell death (Siddik, 2003). Conversely regarding other metal-based compounds other than platinum, iron, cobalt and gold compounds are prime examples currently under preclinical investigation since these have attracted much attention based on their modes of action different from that of cisplatin (Ott and Gust, 2007). Ranging from oxidative stress to wide spectrum enzymatic inhibition (e.g. cyclooxygenases, thioredoxin) these compounds have shown great promise in this field (Ott and Gust, 2007).

Table 1.1 – Main groups of chemotherapeutic compounds discriminating their main representatives and modes of action (Adapted from Baba and Câtoi, 2007).

Substance group	Representatives	Mode of action
Alkylating agents	Cyclophosphamide Ifosfamide Meclorethamine	Crosslinking of DNA chains
Antitumour antibiotics	Doxorubicin Actinomycin D Mitoxantrone	Inhibition of topoisomerase II Intercalation
Antimetabolites **Vinca alkaloids**	5-Fluorouracil Methotrexate Vincristine	Inhibition of enzymes Introduction of false substances in DNA Inhibition of the division spindle
Enzymes	L-Asparaginase	Enzymatic cleavage of asparagine
Unclassified chemotherapeutics	Platinum bonds Hydroxyurea Taxol	Crosslinking of DNA chains (similarly to alkylating agents) Destruction of enzymes

Regardless of the chemotherapeutic agent in question, either metal based or non-metal based, the potential of these substances not to act merely locally on the primary tumour but to spread systemically across the organism can in a sense cure an early diagnosed metastatic cancer but, at the same time what can be considered here as an advantage is often a major setback in clinically applied chemotherapeutic agents (Baba and Câtoi, 2007; Luqmani, 2005). The intrinsic broad spectrum activity of these compounds, as a result of a lack of specificity, frequently translates to off-target effects and a generalized systemic toxicity, leading to typical side effects such as loss of hair (alopecia), fatigue, compromised immune system, nauseas, etc (Luqmani, 2005). Furthermore as mentioned earlier chemotherapy's response varies significantly, from individual to individual. Critical for its importance and for its part in the variability of drug responses between individuals are pharmacokinetic properties. Absorption, distribution, metabolism and excretion parameters vary substantially and influence toxicity and efficacy of medications (Garattini, 2007; Nishiyama and Eguchi, 2009). Plus cancers' continuously evolving nature endows it with multiple possibilities of "transformation", meaning a parallel continuous evolution for the vast array of genetic and epigenetic abnormalities intrinsically characteristic of each cancer (Weinstein and Joe, 2006). The recognition that these alterations/abnormalities frequently vary between cancers and as well as between same types of cancer (Zack *et al.*, 2013) greatly hinders the therapeutic action of existing chemotherapeutic regimens (Nishiyama and Eguchi, 2009), as a result of cancer's biological heterogeneity.

In view of these facts, the use of systemic chemotherapeutic drugs, in what has been the therapeutic paradigm for the past half-century, has a limiting therapeutic index, unspecific biodistribution and greatly increases cancer's probability to develop multidrug resistance patterns (Crawford, 2013; Pinto *et al.*, 2010). As such these fail to achieve high level consistency rates and ultimately do not to meet

the current desired requirements demanded for a robust and efficient chemotherapeutic drug. Interestingly recent efforts to change the current norm have led to fundamental advances in the understanding of tumour's mechanisms, through system biology studies, computer modelling tools and network theories, thus opening new "avenues", not only to improve current drugs and regimens but also to the development of more suitable drugs and drug delivery platforms (Nishiyama and Eguchi, 2009). Fundamentally the paradigm shift seems to move towards combined chemotherapy strategies, employing new generation drugs, and newly targeted therapies. As our knowledge over molecular cancer biology widens and new biochemical grids are unravelled, new generation drugs mainly envision and aim at targeting pathways that control cellular proliferation and death (Klein *et al.*, 2005). For instance the rationale behind targeting the cell cycle is based on the fact that inhibition of its several regulators manages to halt unrestricted tumour growth and could eventually lead to apoptosis. Flavopiridol in particular, an experimental drug is best described as a CDK inhibitor and has in fact shown to be able to bind to CDK1, CDK2, CDK4 and CDK6, compromising their activity. Plus by arresting cell cycle in G1 through inhibition of CDK2/CDK4, and in G2 through inhibition CDK1, flavopiridol has a double action function proving to be highly efficient. Other approaches for targeting cell cycle arrest, in order to halt tumour growth, include the use of several other compounds which follow the same action principle as flavopiridol (Schwartz and Shah, 2005). Compounds such as bryostatins or staurosporine analogs (e.g. UCN-01), are typically involved in the induction of p21 and subsequent inactivation of CDK2 causing cell cycle arrest. Other secondary mechanisms of action are also reported (Schwartz and Shah, 2005; Klein *et al.*, 2005). Similarly induction of programmed cell death can be achieved through targeting of several molecular regulators of the respective cell death pathways (Ricci and Zong, 2006). Interesting strategies to induce apoptosis range from activation of BH3-only proteins to antagonize antiapoptotic Bcl-2 family members to the abrogation of IAP binding to caspases by Smac/DIABLO analogs, and even stimulation of death receptor proteins such as TRAIL (Klein *et al.*, 2005; Ricci and Zong, 2006). As an noteworthy example recombinant TRAIL developed by Genentech/Amgen, targeting DR5 and DR4 death receptors has shown that it's administration not only supresses TRAIL sensitive tumours, as it doesn't present signs of systemic toxicity. The relevance of such scheme comes from the fact that the induction of apoptosis through this extrinsic pathway, means it circumvents the absence of functional p53, and thus adding value to the overall therapeutic index, as the majority of cancers exhibit some sort of modification in *TP53* (Takeda *et al.*, 2007).

Other common strategies are usually related with cancer's nutrient supply and often include the use of monoclonal antibodies (mAb) in an attempt to "starve" the tumour by blocking key intermediates of the related pathways (Gerber, 2008). The most frequently targeted pathways include those related with epidermal growth factor (EGFR), vascular endothelial growth factor (VEGF - fundamental for its role in angiogenesis processes), and Human Epidermal growth factor Receptor 2 (HER2), which can be

respectively inhibited by blockbuster mAb drugs such as cetuximab (Erbitux), bevacizumab (Avastin) and trastuzumab (Herceptin) (Iyer and Kadambi, 2011).

1.4.4.1. Gold(I) and Gold(III) Based Chemotherapeutic Compounds

Even though the application of gold compounds dates far back in history, it was not only until the finding of auranofin's potential to inhibit the growth of cultured tumour cells *in vitro,* that gold compounds were seen under a different light regarding their pharmacological properties as potential chemotherapeutic tools (Berners-Price and Filipovska, 2011; Lima and Rodriguez, 2011). Among the vast array of screened gold compounds, gold(I) and gold(III) complexes have recently attracted much attention owing to their substantial antiproliferative potential and to their specific modes of action different from that of platinum compounds (Iii, 1999; Berners-Price and Filipovska, 2011). Furthermore the rational design of such complexes which endow them with a large variety of ligands and consequently of structural geometries, virtually create an endless number of possible drug-target interactions reducing the probability of a unique mode of action for such complexes (Ott, 2009).

One of the most consensual drug-target interactions is the one established between Thioredoxin reductase (TrxR) and the vast majority of gold(I) and gold(III) complexes alike. TrxR is a large homodimeric selenzoenzime, frequently overexpressed in many tumour cells and responsible for controlling the thioredoxin system as well as the overall redox state of the cell that is often prone to inhibition by some gold complexes. Recent studies have in fact shown that both complexes, exhibit a strong inhibitory effect over thioredoxin reductase with IC_{50} values ranging from 0.020 to 1.42 μM (Bindoli *et al.*, 2009). The process by which TrxR is inhibited is thought to be related with the binding of gold compounds to the selenenylsulfide/selenolthiol redox active centre of the enzyme (Berners-Price and Filipovska, 2011; Bindoli *et al.*, 2009).

The increased activity of the overall system has been correlated with tumour growth, resistance to chemotherapy and evasion of apoptosis. In similarly studies evidences seem to point out a relationship between thioredoxin reductase inhibition and the activation of apoptosis pathways in cancer cells, emphasizing the potential for the future development of cancer agents (Liu *et al.*, 2011).

Despite the increasing interest in gold complexes as potential anticancer agents few have had a direct application in clinical practice. Still overshadowed by poor chemical stability and concerns about metal and systemic toxicity (Nobili *et al.*, 2009), extensive pharmacokinetic/pharmacodynamic and mechanistic studies still appear to be fundamental before effective translation into the clinics can be made possible.

1.4.4.2. Doxorubicin

Being at the forefront in what regards current clinical tools for cancer treatment, doxorubicin is part of a larger group of antineoplastic drugs called anthracycline antibiotics, in which epirubicin, and daunorubicin are also included (Cortés-Funes and Coronado, 2007). Since its development, doxorubicin has shown great anti-proliferative potential, being in fact proven to be fundamental for the treatment of several types of cancer and haematological malignancies, including non-Hodgkin's and Hodgkin's lymphoma, multiple myeloma, as well as lung, ovarian, gastric, thyroid, breast, sarcoma, and paediatric cancers (Gewirtz, 1999; Cortés-Funes and Coronado, 2007). After passive diffusion internalization, where concentration can be up to 500 fold higher than compared with extracellular levels, the plethora of processes and drug-target interactions by which doxorubicin plays its therapeutic effect are vast (Tacar *et al.*, 2013; Granados-Principal *et al.*, 2010; Gewirtz, 1999). Regardless the most consensual processes described according to literature falls upon two major mechanisms of action: DNA intercalation and generation of free radicals.

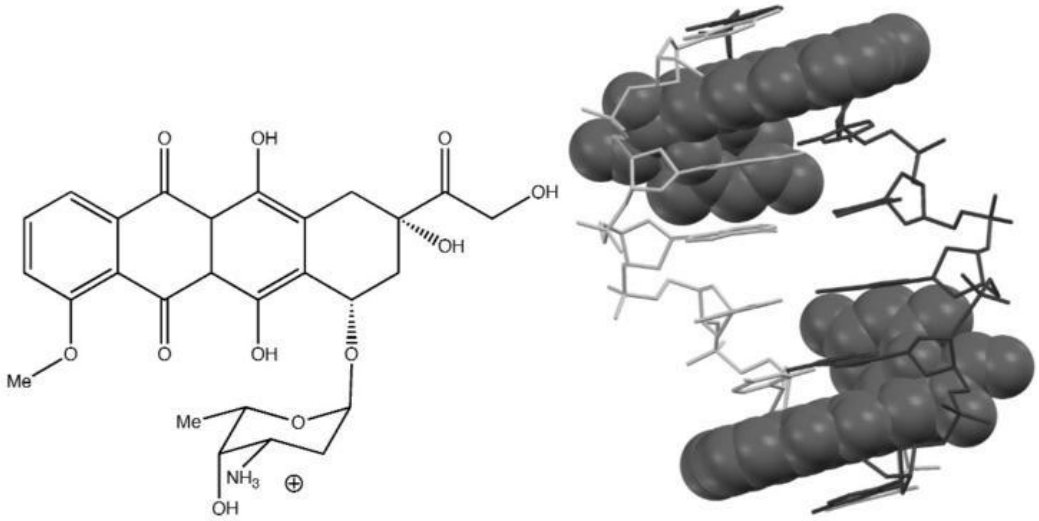

Figure 1.9 – (Left) Doxorubicin chemical structure and (right) doxorubicin's DNA intercalation mechanism through computer modelling tools (Adapted from Hannon, 2007).

Once in the nucleus doxorubicin binds to DNA and intercalates into the base pairs of the DNA's double helix, more particular in 5' GpC sites. Plus doxorubicin presents high affinity towards topoisomerase II (TOPO II) resulting in the assembly of a molecular complex DNA-TOPO II promoting the disruption of DNA/RNA synthesis and of topoisomerase-II-mediated DNA repair system possibly leading to the activation of the p53 mediated apoptosis process (Thorn *et al.*, 2012). On the other hand free radical generation and oxidative stress is intimately connected with four main processes, which include production of semiquinone, activation of nicotinamide adenine dinucleotide phosphate (NADPH) oxidases, non-enzymatic reaction and products from the metabolism of doxorubicin. In short doxorubicin's ability to induce the formation of free radicals ultimately leads to

the morphological and physiological modifications of biological membranes through lipid peroxidation, sequentially inducing cell death (Granados-Principal *et al.*, 2010).

1.4.4.3. Erlotinib

Approved for the treatment of advanced non-small cell lung adenocarcinoma, erlotinib (erlo) is a part of a group of EGFR tyrosine kinase inhibitors, that has shown positive results in clinical studies (Gridelli *et al.*, 2007). Chemically speaking erlotinib is a quinazoline derivative and in monotherapy treatments has shown prolonged survival and delayed disease progression (Friess *et al.*, 2006; Bonomi, 2003).

The mechanism of action is thought to be related with the abrogation of cell growth, through G0/G1 cell cycle arrest. While particular *in vitro* studies have correlated the reduced cell proliferation with decreased levels of phosphorylated Rb (Gridelli *et al.*, 2007; Bonomi, 2003) supporting the evidences of G0/G1 cell cycle arrest, other reports have indicated increased DNA fragmentation in monotherapy treatments as a result of apoptosis (Bonomi, 2003).

Other possible mechanisms of action include inhibition of angiogenic growth factor production, inhibition of invasion and metastasis and potentiation of antitumour activity of cytotoxic drugs and radiotherapy

1.5. Combination Chemotherapy

Even though combination chemotherapy has been the standard in cancer treatment, recent comprehensive studies on tumour's heterogeneity and the consequent unravelling of the genetic and molecular alterations that lead the processes of initiation to drug resistance acquisition, have provided the ground work for the development of new compounds with improved specificity, re-inventing combination regimens (Yardley, 2013). Plus the establishment of new combination regimens and their rational design has been recently "built" upon an effort to target cancer's typical hallmarks with particular focus on anti-resistance combinations (Yardley, 2013; Hanahan and Weinberg, 2011). In fact the rationale behind combination chemotherapy is intimately related with tumour heterogeneity and its implication for drug resistance, as well as with the success of combination chemotherapy, which greatly improves patients' outcomes (Mayer and Janoff, 2007; Emil Frei and Eder, 2003).

The fundamental principles considered for combination chemotherapy have been to: i) use drugs with non-overlapping toxicities so that each drug can be administered at near-maximal dose; ii) combine agents with different mechanisms of action and minimal cross-resistance in order to inhibit the emergence of broad spectrum drug resistance; iii) preferentially use drugs with proven activity as single drugs and iv) administer the combination at early stage disease (Pinto *et al.*, 2010; Mayer and

Janoff, 2007; Zoli *et al.*, 2001). In an effort to assess the potential of each combination regimen several mathematical modelling frameworks have been established, allowing for the characterization of the combined drug effect (Chou and Talalayi, 1984). The combination regimens clinically employed are vast and usually specific for each cancer type ("Combination Chemotherapy Regimen by Type of Cancer," 2013). Nonetheless, those that have been screened so far were reported to be only additive or, at most, minimally synergistic emphasizing the need for further investigation (Yardley, 2013).

The main physiological advantages reported when considering combination regimens are the possible emergence of synergistic interactions between the compounds administered and the ability to reverse multidrug resistance or to delay it (Pinto *et al.*, 2010). A myriad of compounds, like verapamil and several other lipid-soluble, are actually able to target and inhibit p-glycoprotein (*Multi Drug Resistance I* gene product), the efflux pump responsible for multi-drug resistance (Emil Frei and Eder, 2003).

1.6. Aims and Objectives

As the main objective the work presented intended to proceed to the full characterization of the cytotoxic potential and mechanisms of action of newly synthesized chlorogold compounds with phosphine or N,O donor ligands. In order to accomplish the established objective a series of post genomic techniques were performed across a library of tumoural and non-tumoural cell lines available, out of which two non-small cell lung adenocarcinoma cell lines were selected for further studies. Parameters such as antiproliferative activity, compound selectivity, macromolecule interactions, cell death mechanisms, cell cycle disorders and proteomic profiles were assessed and duly characterized. It was also intended to pay special attention to the identification of proteins related with cell signalling, cell death, drug efflux pumps and DNA damage response mechanisms. As a secondary objective, it was expected to establish and characterize new combination therapies, employing both chlorogold compounds and reference chemotherapeutic drugs, such as Doxorubicin and Erlotinib. Furthermore, it was planned to establish two multidrug resistance cell lines as study tools for the implications of new combination chemotherapy programs and to perform comparisons with monotherapy treatments.

It should be stated herein that, due to time limitations some post genomic analysis and other experiments were not performed in their entirety and consequently this work should be seen as a future on-going study platform.

2. Materials and Methods

2.1. Compounds

All chlorogold complexes studied were synthesized in the Center of Chemistry of Instituto Superior Técnico by Drª. Luísa Martins. Compounds were weighed using an analytical balance and dissolved in dimethyl sulfoxide (DMSO) in order to obtain stock solutions at a final concentration of 10 mg ml^{-1}. Respective stock solutions were aliquoted and stored at room temperature (≈ 25 ºC) until their further need for assays, as well as the remaining solid state compounds.

The general characteristics of the complexes as well as the information needed for the preparation of the stock solutions are summarized in Table 2.1.

In addition to chlorogold complexes, other classical compounds such as Cetuximab, Erlotinib and Doxorubicin were also used during the development of this work, in an attempt to establish new chemotherapeutic combination strategies.

Table 2.1 – Molecular and structural characteristics of the studied compounds, and necessary information for preparation of the respective stock solutions.

Code	Molecular Formula	Molecular Weight ($gmol^{-1}$)	Solvent
A	$C_6H_5AuCl_2NO_2$	389.97	DMSO
B	C_3H_9AuClP	308.5	DMSO
C	$C_{27}H_{37}AuClN_2$	621.01	DMSO
D	$C_{18}H_{15}AuClP$	494.03	DMSO

2.2. Human Cell Lines

Human tumour cell lines used in this work were morphologically comprised of two types; (I) adherent, and (II) non-adherent or in suspension. HCT116, HEPG2 and MCF7, corresponding respectively to colorectal carcinoma, hepatocellular carcinoma and mammary adenocarcinoma cell lines were kindly offered by Drª. Cecília Rodrigues from the Research Institute for Medicine and Pharmaceutical Sciences (iMed), from Faculdade de Farmácia of Universidade de Lisboa. All other cell lines used were obtained directly from ATCC ("ATCC: The Global Bioresource Center," 2014).

Furthermore as control of cell viability assays, fibroblasts, a non-tumour foreskin derived cell line, was used, to evaluate and infer about compound toxicity over healthy cells. Details and cell line general characteristics are summarized in Table 2.2.

Table 2.2 – Details and characteristics of human cell lines used in this work. Cell lines are discriminated by cell designation, type; morphology, culture properties and growth media. (DMEM - Dulbecco's Modified Eagle Medium; FBS - Fetal Bovine Serum; NEA - Non-essential amino acids; Pen/Strep - Penicilin-Streptomicin).

Cell Designation	Cell Type	Morphology	Culture Properties	Growth media % in (v/v)
A549	Non-small cell lung adenocarcinoma	Epithelial	Adherent	DMEM; 10 % FBS; 1 % Pen/Strep
HCT-116	Colorectal carcinoma	Epithelial	Adherent	DMEM; 10 % FBS; 1 % Pen/Strep
H1975	Non-small cell lung adenocarcinoma	Epithelial	Adherent	RPMI; 10 % FBS; 1 % Pen/Strep
HEP G2	Hepatocellular carcinoma	Epithelial	Adherent	DMEM; 10 % FBS; 1 % Pen/Strep; 1 % NEA
K562	Chronic myelogenous leukemia (CML)	Lymphoblast	Suspension	DMEM; 10 % FBS; 1 % Pen/Strep
MCF7	Mammary adenocarcinoma	Epithelial	Adherent	DMEM; 10 % FBS; 1 % Pen/Strep
MNT 1	Melanoma	Epithelial	Adherent	DMEM; 10 % FBS; 1 % Pen/Strep
Fibroblasts	Skin (epidermis)	Spindle-shaped/ bipolar and refractile	Adherent	DMEM; 10 % FBS; 1 % Pen/Strep; 1 % NEA

Adapted from: ("ATCC: The Global Bioresource Center," 2014)

2.3. Cell Line Handling and Maintenance

All cell lines were cultivated and maintained in either 25 or 75 cm^2 BD vented cell culture flasks (BD Biosciences, New Jersey, EUA), in Dulbecco's Modified Eagle Medium (DMEM; Invitrogen, New York, EUA) supplemented with 10 % (v/v) Fetal Bovine Serum (FBS; Invitrogen) and 1 % (v/v) of antibiotic/antimicotic Penicilin-Streptomicin (Pen–Strep + Antimicotic; Invitrogen, New York, EUA), with exception for H1975 cell line which was cultivated in Roswell Park Memorial Institute medium (RPMI; Invitrogen, New York, EUA).

In addition, HepG2, MCF7 and Fibroblasts culture medium was further supplemented with 1 % (v/v) of non-essential amino acids (NEA) 100x (Sigma, St. Louis Missouri, EUA). Cell culture flasks were maintained in a CO_2 incubator (SANYO CO_2 Incubator, Electric Biomedical Co., Osaka, Japan) at 37 ^oC and at an atmosphere of 99 % (v/v) humidity and 5 % (v/v) CO_2.

Culture cell renewal was performed approximately when an 80 % confluence was reached in the culture flask (Olympus CXX41inverted microscope, Tokyo, Japan) which represents the critical point when cells start to detach from the flask and to degenerate due to lack of nutrients, and due to contact inhibition. The depleted medium was removed and discarded with the aid of mechanical pump, which was followed by the addition of 2 mL of trypsin (TrypLE™, Invitrogen, New York, EUA) to help cell detachment. After an incubation period of 5 min in the CO_2 incubator, trypsin activity was blocked by the addition of 2 mL cell medium. The cell suspension solution was transferred to 15 mL BD Falcons (BD Biosciences) and centrifuged at 1500 rpm for 5 min at approximately 15 ºC (Sigma 3-16K 10280, Tuttlingen, Germany). The supernatant was then discarded and the remaining pellet was resuspended in 2 mL of fresh medium. For each 75 cm^2 cell culture flask, carrying 10 mL of fresh medium it was added roughly 50 µL of the cell suspension, being subsequently incubated at 37 ºC and at an atmosphere of 99 % (v/v) humidity and 5 % (v/v) CO_2.

2.4. Quality Control: *Mycoplasma* Analysis of Cell Lines

Cell lines were periodically evaluated for possible mycoplasma contaminations as a quality control check, by a Polymerase Chain Reaction (PCR) detection method. Cell samples from each cell line were collected by trypsinization as described in section 2.3. centrifuged at 1500 rpm for 5 min, and the cell pellet resuspended in Phosphate buffered saline 1x (PBS1x)(composition PBS10x: 1.37 M NaCl, 0.027 M KCl, 0.1 M Na_2HPO_4, 0.018 M KH_2PO_4). Deoxyribonucleic Acid (DNA) extraction protocol was performed using the High Pure PCR Template Preparation Kit (Roche Diagnostic, Indianapolis, USA) following the procedure described by the manufacturer. Total DNA concentration was assessed using Nanodrop2000 (Thermo Scientific, Waltham, MA, USA) as well as Abs260/Abs280 and Abs260/Abs230 ratios as DNA purity parameters (as described by the manufacturer). A master mix was prepared for all samples, considering a final volume of 20 µL per reaction, containing 75mU/µL of Taq Red DNA Polymerase (Bioline), PCR Buffer 10x, High Specific, 1 mM from each dNTP (Bioline), 2 mM of magnesium chloride ($MgCl_2$; Bioline), primers forward and reverse and the sample DNA at a final concentration of 20 ng/µL. The primer set used, (Table 2.2), were designed to be highly specific to the 16S rRNA coding region in the mycoplasma genome, thus allowing for the detection of the most frequent mycoplasma contaminants in cell culture environment.

Table 2.3 – Primer set used in *Mycoplasma* analysis, detailing forward and reverse primer sequences, as well as the expected size of the specific amplicon for the 16S rRNA gene.

Gene	Primer forward (5'- 3')	Primer reverse (5´- 3')	Amplicon (bp)
16S rRNA	*GAGGGCAAGTACGAGTGGCAA*	*CTGCGCATTGCTCCGCTAACC*	≈700 bp

Amplification of the reaction mix, was performed with the conditions described in Table 2.3, in an Tpersonal termocycler (Biometra GmbH, Goettingen, Germany). All amplification products were further separated by gel electrophoresis, in a 0.8 % (w/v) agarose gel (Thermo Scientific, Waltham, MA, USA), stained with 2 % (v/v) of gel red (10000x) (Biotarget, Portugal). A 110 voltage was used during a 50 min run, in Tris base, acetic acid and EDTA buffer 1x (TAE 1x buffer) (composition TAE 10x: 1.7 M NaCl, 0.03 M KCl, 0.1 M Na_2HPO_4 and 0.01 M K_2HPO_4). An already know contaminated cell line was used as a positive control, and as negative control it was used eukaryotic cat DNA. Hyperladder IV (Bioline) was used as molecular weight marker.

Table 2.4 – PCR amplification program for the *16S rRNA* gene in mycoplasma detection protocol.

Step	Temperature (ºC)	Time (min)	Cycles
Initial denaturation	95 ºC	5 min	30
Denaturation	95 ºC	0.5 min	
Annealing	58 ºC	1.5 min	
Extension	72 ºC	1.5 min	
Final Extension	72 ºC	10 min	

2.5. Growth Inhibition Assays

In vitro cytotoxicity assays were performed for each cell line available and for each compound mentioned (sections 2.1 and 2.2), through the use the CellTiter 96® AQueous Non-Radioactive Cell Proliferation Assay (Promega, Madison, USA), a colorimetric method for determining the number of viable cells.

At 80 % confluence, cells were harvested and centrifuged as mentioned in section 2.3. The supernatant was discarded, and the cell pellet resuspended in 2 mL of medium. For growth inhibition assays, $0.75x10^5$ cells/mL were plated into flat bottomed 96-well plates (Costar, Corning, NY) and incubated at 37 ºC, 99 % (v/v) humidity and 5 % (v/v) CO_2. Cell density was evaluated as the total number of viable cells within the grids on the hemacytometer (Hirschmann, Eberstadt, Germany) using trypan blue exclusion method. For this procedure 350 µL of medium was pipetted to a 2 mL eppendorf together with 50 µL of the 2 mL cell suspension followed by 100 µL of 0.4 % (v/v) trypan blue solution (Sigma). The hemacytometer was loaded and examined immediately under the microscope at low resolution, and cell viability was determined through the following equation (1):

$$\frac{\text{Nº of cells}}{\text{ml}} = \frac{\sum \text{cells per quadrant}}{4} * 10^4 \ (\text{Chamber Volume} * \text{Dilution factor}) \qquad (1)$$

After 24 h, a range of concentrations of the specific drug in question were added (after removal of depleted medium), and the cells were incubated for an additional 48 h (37 ºC, 99 % humidity and 5% (v/v) CO_2). Subsequently a reaction mix of medium, MTS (3-(4,5-dimethylthiazol-2-yl)-5-(3-carboxymethoxyphenyl)-2-(4-sulfophenyl)-2H-tetrazolium, inner salt), and PMS (phenazine

methosulfate) in a ratio of 100:19:1 was added to each well and further incubated for 45 min. During this period, MTS is reduced into formazan by dehydrogenases present in metabolically active cells, which in turn is susceptible of being measured at 490 nm absorbance by Tecan Infinite F200 Microplate Reader (Tecan, Männedorf, Switzerland), directly from the 96-well assay plate, so that the quantity of formazan product measured is directly proportional to the number of living cells in culture. The cell viability results for each concentration assayed were normalized relative to the control samples and obtained accordingly to the following equation (2):

$$\frac{\text{Sample Absorvance (490 nm)}}{\text{Control Absorvance (490 nm)}} * 100 = \text{Cell Viability (\%)} \quad (2)$$

The concentration of each compound resulting in 50 % growth inhibition (IC_{50}) was expressed as percentage of the untreated controls, and calculated using Excel and GraphPad software (Graph Pad Software Inc., San Diego, CA, USA). Additionally different combination therapies between chlorogold compounds and other classic chemotherapy drugs, such as Doxorubicin (Dox) or Erlotinib (Erlo), were used in an attempt to establish better chemotherapeutic strategies.

Due to the large number of compounds and cell lines under study, initial compound screening was performed by testing a range of concentrations, typically between 1 and 1000 μM on all cell lines available, to obtain data on percentage growth inhibition and relative IC_{50} values. These results were taken into consideration for the rest of the work and further studies on the molecular mechanisms of anticancer activity were restricted to the most active chlorogold complexes, namely compounds B and D. Cell line screening and selection was performed based on the same initial results and the post-established thesis main objective (see section 1.6 and 3.1). Non-small cell lung cancer cell lines (NSCLC), A549 and H1975 were thus selected for further assays.

2.5.1. Combination Chemotherapy: Cell Viability Assessment

Cell viability assessment for combination chemotherapy was proceeded in same way was described in section 2.5 through the use the CellTiter 96® AQueous Non-Radioactive Cell Proliferation Assay (Promega, Madison, USA) with the exception that it was only performed in non-small cell lung cancer cell line, A549. Cells were seeded in 96-well plates, at $0.75x10^5$ cells/ml and incubated at 37 ºC, 99 % humidity and 5% CO_2 (v/v) for a period of 24 h. Twenty-four hours after seeding cells were exposed to both compound B and doxorubicin or to compound B and erlotinib for a total exposure period of 48 h in three distinct sequences: both compounds were administered concomitantly (I), pretreatment with compound B for 24 h with posterior administration of the second drug (II) and pretreatment with doxorubicin or erlotinib for 24 h with posterior administration of compound B (III). The concentrations used in each assay were based on each drug's individual IC_{50} which was pre-determined on single drug viability assays (see Appendix A and B), or in the case of doxorubicin

extracted from literature reports (He *et al.*, 2011). Assays were performed in triplicate and the data represents the result of at least three independent experiments.

2.6. Apoptotic Potential Evaluation

2.6.1. Hoechst Staining

As an early apoptotic potential evaluation assay, Hoechst 33258 fluorescent staining was performed. Hoechst 33258, Phenol, 4-[5-(4-methyl-1-piperazinyl)[2,4'-bi-1H-benzimidazol]-2'-yl]-, trihydrochloride, has a high affinity to nucleic acids (excitation and emission wavelengths of 352 and 461 nm, respectively when bound to DNA) allowing for the identification and visualization by fluorescent microscopy, of early apoptotic hallmarks such as, aberrant nuclear morphology, chromatin condensation and apoptotic body formation (*Hoechst Stains, MP21486, Invitrogen*, 2005).

Both cell lines, A549 and H1975 were collected and centrifuged as described in section 2.4. Cells were then seeded in flat bottomed 24-well plates (Costar, Corning, NY), at a cell density of $1x10^5$ cell/mL and incubated at 37 ºC, 99 % (v/v) humidity and 5 % (v/v) CO_2 for a period of 24 h. Prior to cell seeding, lamellae were sterilized with 70 % (v/v) ethanol, and further rinsed with PBS1x, being sequentially set at the bottom of each well. After 24 h period, the corresponding IC_{50} values of each selected compound (e.g. compound B and compound D), corresponding to their respective IC_{50} values, were added to each well, considering a final volume of 400 µL, and incubated for an additional 48 h period. Solutions were prepared using culture medium and 0.1 % (v/v) DMSO was used as control of the experiment.

The culture medium of the incubated cells was then discarded and cells were rinsed three times with PBS1x. Cells were fixed with 400 µL solution of 4 % (v/v) paraformaldehyde diluted in PBS1x and incubated in the absence of light for a period of 10 min. For Hoechst staining, to each well was added a 400 µL solution of Hoechst 33258 (Sigma), containing 0.8 µL Hoechst 33258 (5 mg/mL) in 400 µL of PBS1x. An incubation of 15 min in the absence of light and at room temperature followed, and sequentially each well was rinsed once again three times with 400 µL PBS1x. Separately slides were prepared with 5 µL droplets of a glycerol solution diluted in PBS1x (1:3 ratio). Inverted lamellae, containing fixed cell samples were carefully placed on top of each droplet, and thereafter visualized and photographed in a Olympus BX51 fluorescent microscope with an attached Olympus DP50 (Olympus) camera. Photographs were acquired with Infarview software.

2.6.2. AnnexinV-FITC and Propidium Iodide Staining

AnnexinV-FITC (Fluorescein Isothiocyanate) and propidium iodide (PI) double staining procedure was carried out has a complementary study of the compound's apoptotic potential over the selected cell lines, using AnnexinV-FITC Apoptosis Kit (Invitrogen). This particular assay takes advantage

over some of the molecular and morphological hallmarks of apoptosis. One of the earliest events of apoptosis consists on the translocation of the phosphatidylserine from the inner membrane leaflet to the outer membrane leaflet, which in turn presents high affinity for Annexin V, a Ca^{2+} dependent phospholipid-binding protein, thus allowing for the detection of exposed phosphatidylserine. On the other hand, propidium iodide, a red-fluorescent nucleic acid binding dye, internalizes dead cells or cells with a compromised plasma membrane thus staining them with red fluorescence. Annexin V and propidium iodide staining is inherently dependent on the plasma membrane integrity, and consequently by taking advantage of apoptosis related molecular events involving it, it provides a rapid and reliable method to quantify viable cells in a cell suspension (*FITC Annexin V / Dead Cell Apoptosis Kit with FITC annexin V and PI , for Flow Cytometry, MP 13242, Invitrogen*, 2010).

For AnexinV-FITC and propidium iodide staining, NSCLC cell line (A549) was seeded at a cell density of $0.75x10^5$ cells/mL in 35 mm plates and incubated at 37 ºC, 99 % (v/v) humidity and 5 % (v/v) CO_2. Twenty-four hours later, the medium was replaced with the medium containing the compounds as indicated (compound B and Dox), and further incubated for another 48 h. Chlorogold compound B, and Dox were used at their respective IC_{50} concentrations, and 0.1 % (v/v) DMSO as control of the experiment. Supernatant and cells were collected (supernatant was collected separately to BD 15 mL Falcons and cells were collected through the addition of 1 mL of trypsin and incubation at 37 ºC, 99 % (v/v) humidity and 5 % (v/v) CO_2 for 5 min), and centrifuged at 1500 rpm for 5 min. Supernatants were discarded and the cell pellets were rinsed three times with 1 mL PBS1x intercalated with 5 min centrifugations at 1500 rpm. Afterwards 100 µL of annexin Binding Buffer 1x was added to all cell samples. Additionally 5 µL of annexin V and 2 µL of propidium iodide were added to the samples, followed by an incubation of 15 min in the absence of light and at room temperature. Sequentially another 400 µL of Anexin Binding Buffer 1x were added, and 500 µL of PBS 1x, to make up to 1 mL solution to each sample. After staining cell populations with FITC annexin V and PI in the in the respective buffer, apoptotic cells show green fluorescence, dead cells show red and live cells show little or no fluorescence (*FITC Annexin V / Dead Cell Apoptosis Kit with FITC annexin V and PI , for Flow Cytometry, MP 13242, Invitrogen*, 2010).

Cell samples were analyzed by flow cytometry on an Attune® Acoustic Focusing Flow Cytometer (Life Technologies, Carlsbad, California), through the acquisition of at least 10000 events for each experimental condition.

2.7. DNA Interaction Studies

2.7.1. UV/Vis Spectrophotometric Analysis

Many metal based chemotherapeutic drugs are known to interact and influence the overall molecular structure of the DNA molecule, often comprehending their main mechanisms of action by which they

exert their therapeutic effects. UV/Vis spectrophotometry assays allowed to draw conclusions about the drug interaction with DNA (Shahabadi *et al.*, 2011). Assays were performed using Calf Thymus-DNA (CT-DNA; Invitrogen), which it's concentrations were determined by NanoDrop reading at 260 nm, considering both the DNA molar extinction coefficient (6600 M^{-1} cm^{-1}) and lambert beer's law (Equation (3)):

$$A = \varepsilon . l . c \qquad (3)$$

Where A is the absorbance measured at 260 nm, ε the molar extinction coefficient in M^{-1} cm^{-1}, l the optical path in cm, and c the sample concentration in $molL^{-1}$ (Ahmadi, 2011; Gallego *et al.*, 2011).

The UV-Vis spectra for DNA with chlorogold compounds interactions were obtained using an Evolution 300 UV-Vis spectrophotometer (Thermo Scientific). Absorption titration experiments were carried out by keeping the concentration of DNA constant (20 μM) while varying the complex concentration from 1 to 100 μM. Samples were prepared in 5 mM Tris-HCl (Merck), 50 mM NaCl (Panreac), pH 7 buffer, and were incubated at 37 °C for 24 h. DMSO was used as reference solution in the same concentrations as that used for samples.

Maximum absorbance values were corrected by the subtraction of the respective values obtained for the reference samples (DMSO) in the same wavelength and fitted in the following equation (4) in order to obtain intrinsic binding constant, Kb, of the respective compounds:

$$\frac{[DNA]}{(\varepsilon a - \varepsilon f)} = \frac{[DNA]}{(\varepsilon b - \varepsilon f)} + \frac{1}{Kb(\varepsilon b - \varepsilon f)} \qquad (4)$$

where εa, εf , and εb are the apparent, free and bound complex extinction coefficients, respectively. In particular, εf was determined by a calibration curve of the isolated metal complex in aqueous solution; following the Beer's law, εa was determined as the ratio between the measured absorbance and the chlorogold complexes concentration. The inability to obtain tangible and reproducible results through this assay, possibly due to a lack of compound stability in the mentioned buffer, led to its discontinuity and no significant results are shown for this particular assay (see appendix C).

2.7.2. DNA cleavage assay

DNA interaction studies were further evaluated through DNA cleavage assays. In these assays double-stranded closed circular high copy plasmid pUC18 DNA (Fermentas, Maryland, EUA) concentration was maintained constant (10 ng/μL), while compound concentration varied differently from each chlorogold compound, namely compound B concentrations varied from 10 μM to 200 μM , whereas compound D concentrations varied from 10 μM to 300 μM .

10 ng/μL of pUC18 were incubated either in the presence of the respective compound concentrations, or in the presence of 0.62 % or 2.23 % (v/v) of DMSO as reference solutions (compound B and D respectively) considering a total reaction volume of 20 μL. Incubation was performed in 5 mM Tris-HCl, 50 mM NaCl buffer (pH 7) for a period of at least 24 h at 37 ºC. After incubation at 37°C, a 20 μL aliquot of each reaction was mixed with 4 μL of 6x loading dye (Fermentas, Maryland, EUA) and electrophoresed on 0.7 % (w/v) agarose gel for 2 h at 70 Volts. As a molecular weight marker λ DNA/HindIII (Fermentas, Maryland, EUA) was used. Sequentially the gel was stained with an ethidium bromide solution (Invitrogen) (0.05 μg/mL in 100 mL of distilled water) for 30 min with agitation. Excess of ethidium bromide was rinsed with 100 mL of distilled water. Gel results were visualized using Molecular Imager® Gel Doc™ XR+ System with Image Lab™ Software (BioRad, Berkley, California) and image acquisition was obtained with GelDoc software. Data treatment was performed using GelAnalyzer software and as a result of three independent assays.

2.8. Cell Cycle Progression Assay

The tightly regulated cell cycle progression, with its numerous checkpoints, composes an optimal bio-indicator of cell health, as any deviation or delay in its distinct phases may point out deficient processes and pathways as a result of an extrinsic (or intrinsic) input such as chemotherapeutic drugs (Malumbres and Barbacid, 2009). Cell cycle alterations are consequently a good indicator of chemotherapeutic drug's ability to target cell cycle intervenients, ultimately leading to cell cycle arrest or apoptosis. For cell cycle progression analysis, NSCLC cell line (A549) was seeded in 25 cm^2 cell culture flasks, at a cell density of $2x10^5$ cells/mL and incubated at 37 ºC, 99 % (v/v) humidity and 5 % (v/v) CO_2. Thymidine, a commonly used S-phase blocker in cell cycle progression studies was used to slow down and arrest cells in S-phase progression. For a clear synchronization at early S-phase a double thymidine block procedure described by Borralho and coworkers (2009) was performed.

After 8 h of cell seeding, the first thymidine block was performed by the addition of 2 mM thymidine (Sigma) in culture medium. Culture flasks were then incubated for a further 14 h at 37 ºC, 99 % (v/v) humidity and 5 % (v/v) CO_2. Afterwards depleted medium was removed and culture flasks were incubated without thymidine for an additional 10 h, at the end of which it was added 2 mM thymidine; followed by incubation at 37 ºC, 99 % (v/v) humidity and 5 % (v/v) CO_2 for 14 h followed. At the end of the thymidine block procedure, depleted medium containing thymidine was removed and replaced either by chlorogold compound solutions and/or doxorubicin, at their respective IC_{50} concentrations, or by 0.1 % (v/v) DMSO (control), diluted in fresh medium. Exposure times to the respective compounds were established to be 3, 6 and 9 h.

Cell samples were collected by trypsinization as described in section 2.4 in 15 mL falcons, and centrifuged at 2000 rpm for 5 min at 4 ºC. Supernatant was removed and the cell pellet was

resuspended in cold PBS 1x and centrifuged at 2000 rpm once more. Supernatant was discarded and the remaining sediments were resuspended in 1 mL PBS1x followed by fixation with a 1 mL of an 80 % (v/v) ethanol solution previously made and stored at -20 ºC. The ethanol solution was added carefully and progressively into the cell suspension, and with gentle agitation in vortex. Cell samples were then maintained in ice for a period of 30 min to improve fixation efficiency, after which samples were stored at 4 ºC for at least 18 h prior to analysis. As a synchronization control, cells from a separate culture flask were immediately collected and fixated after the end of the thymidine block procedure, and were considered as the initial time point.

Falcons were centrifuged at 2000 rpm for 5 min at 4 ºC, and the supernatant was discarded, The remaining cell pellet was resuspended in 1 mL of a propidium iodide solution (50 µg/mL propidium iodide, 200 mL distilled water, 0.1 % sodium citrate, 0.02 ng/mL RNAse, 0.20 % Nonidet P-40; pH=7) and incubated at room temperature for 30 min. Cell cycle progression analysis was performed in a Attune® Acoustic Focusing Flow Cytometer through the acquisition of at least 10000 events per sample. Data treatment was carried out using Excel software as the result of three independent assays.

2.9. Proteomic Studies: Two-dimensional (2-D) Gel Electrophoresis

2.9.1. Sample Preparation, and Compound Exposure

Proteomic studies were carried out in NSCLC A549 and HCT-116 cell lines exposed to DMSO. Cell lines were collected by trypsinization as described in section 2.4 and centrifuged at 1500 rpm for 5 min. Cells were then resuspended in medium and seeded in 25 cm^2 culture flasks at a cell density of $2x10^5$ cell/mL, and incubated at 37 ºC, 99 % (v/v) humidity and 5 % (v/v) CO_2 for a period of 24 h. Next cell medium was discarded and replaced by 0.1 % (v/v) DMSO, both diluted in fresh medium. Time exposure to DMSO was established to be 48 h. Culture flasks were incubated in the same conditions described above.

After 48 h incubation period cells were collected by trypsinization and centrifuged at 2500 rpm for 5 min and at 4 ºC. Cell sediments were rinsed three times with PBS1x, and centrifuged in between, in the same conditions as mentioned above.

2.9.2. Whole Protein Extraction: Ultrasonication

For whole protein extraction, previously harvested cells were resuspended in a cell lysis solution (100 µL per $4x10^6$ cells/mL) comprised of NaCl-Tris-EDTA buffer (150 mM NaCl; 50 mM Tris, pH=8; 5 mM EDTA), phosphatase inhibitors 1x (PhosStop, Roche), protease inhibitors 1x (cOmplete ULTRA Tablets, Mini, EASYpack, Roche, Basel, Switzerland), 0.1 % (w/v) dithiothreitol (DTT) (AMRESCO, USA), 1 mM of phenylmethylsulfonyl fluoride (PMSF) (Sigma), 2 % (w/v) Nonidet P-40 (Thermo Scientific, Massachusetts, EUA). Sequentially cell suspensions were submitted to ultrasonication

protein extraction protocol (Table 2.4), by which cells are disrupted by high-frequency sound waves that generate low pressure regions, ultimately leading to cell membrane rupture and protein extravasation.

Table 2.5 – Ultrasonication protein extraction protocol.

Cycles	Bursts	Output (%)
3	5	60
5	10	70
15	20	70

* Samples were maintained in ice for 30 seconds between cycles to avoid overheating and protein loss due to shear forces.

2.9.3. Whole Protein Precipitation and Purification: 2-D Clean-Up Kit

Cell lysates were centrifuged 14000 xg for 15 min and supernatants were recovered and stored at -80 ºC. For whole protein precipitation and purification 2-D Clean-Up Kit (GE Healthcare, Little Chalfont, United Kingdom) was used accordingly with manufacturer protocol except for wash additive and wash buffer step were cell lysates were incubated overnight at -20 ºC. Plus centrifugations were performed for 15 min instead of the indicated 10 min.

Following centrifugation, 100 µL of re-hydration buffer (7 M urea (BDH Prolabo, VWR International), 2 M Tiourea (Merck, Frankfurt, Germany), 2 % (w/v) (3-[(3-Cholamidopropyl)dimethylammonio]-1 propanesulfonate) (CHAPS) (GE Healthcare), phosphatase inhibitors 1x, protease inhibitors 1x, bromophenol blue (Merck), 1 µL 10 % (w/v) DTT and 1µL of 100 mM PMSF) was used to resuspend the whole protein extract. After 2 h incubation at room temperature whole protein extract was centrifuged at 14000 xg for 15 min and the resulting supernatant recovered. Selective protein precipitation is greatly improved through the employment of such reagents while circumventing interfering sources such as salts, nucleic acids, lipids, and phenolic compounds by promoting their suspension in solution, consequently improving 2-D gel quality results (*GE Healthcare 2-D Clean-Up Kit*, 2009).

2.9.4. Whole Protein Quantification: Pierce Reagent 660 nm

Protein quantification was carried out by employing Pierce Protein Assay Kit (ThermoScientific). Prior to protein quantification a calibration curve was established using know standard Bovine Serum Albumin (BSA) solutions, with concentrations ranging from 0 to 500 µg/mL. To 50 µL of replicate standard solution it was added 750 µL of protein assay reagent (1:15 ratio) and the mixture gently stirred by vortex. For unknown sample solutions, 5 µL of whole protein extract was added to 45 µL of deionized water, plus 750 µL of protein assay reagent. Samples were incubated at room temperature for 5 min prior to spectrophotometer reading at 660nm.

2.9.5. 2-D Gel Electrophoresis: Isoelectric Focusing

2-D gel electrophoresis first dimension, isoelectric focusing (IEF), was performed by in-gel rehydration using the Ettan IPGphor3 IEF System (GE Healthcare). Sample loading into sample cups was carried out by uniformly distributing 200 μg of whole protein extract, resuspended in 125 μL of rehydration solution supplemented with 0.5 % Immobilized pH gradient (IPG) (GE Healthcare) and 0.5 % de destreak (GE Healthcare), into each 7 cm IPG strip holder (GE Healthcare). Immediately after, a 7 cm long Immobiline DryStrip pH 3-10 NL (GE Healthcare) was placed over the sample and special attention was taken to ensure that no bubbles were formed between the gel and the sample. Furthermore 750 μL of Drystrip Cover Fluid (GE Healthcare) were added over the strip to ensure full immersion. A 5 step program, displayed in Table 2.5 was used for IEF.

Table 2.6 –2-D gel electrophoresis IEF five step program.

Steps	Voltage (V)	Time (h)	Temperature (°C)
1	30	14	20
2	100	0.5	20
3	500	0.5	20
4	1000	0.5	20
5	5000	1	20

2.9.6. 2-D Gel Electrophoresis: SDS-PAGE

Immediately after IEF and prior to the second-dimension run, immobiline drystrip gel equilibration was performed in order to promote saturation with the Sodium dodecyl sulfate (SDS) buffer system required for second-dimension separation. A 5 mL solution comprised of 70 mM Tris-HCl pH 8.8, 6M Urea, 30 % (v/v) glycerol, 2 % (w/v) SDS and 1 % (w/v) DTT (GE Healthcare) was used as a first equilibration step for 15 min, followed by a second supplemented with 2.5 % (w/v) iodoacetamide (GE Healthcare) for another 15 min.

For the second-dimension run a SDS-PAGE Mini-PROTEAN® 3 System was used. Plus a lab-cast 12 % (v/v) polyacrylamide gel was also prepared, comprised of 4 mL of a 30 % (w/v) acrylamide/bis-acrylamide mix, 3.5 mL of deionized water, 2.5 mL of Tris-HCl buffer (Merck) 1.5 M pH 8.8, 75 μL of a 10 % (v/v) ammonium persulfate (APS) (Biorad, California, USA) and 10 μL of tetramethylethylenediamine (TEMED) (Sigma). After gel polymerization (approximately 30 min) IPG strips were put on top of each gel and sealed with an agarose solution (0.5 % (w/v) agarose diluted in running buffer (3.79 g/L Tris, 18 g/L glycine, 1.25 g/L SDS, and evidences of bromophenol blue).

Initially electrophoresis run was performed at a Voltage of 30 V, for roughly 30 min in order to promote protein transfer from IPG strips to SDS-polyacrylamide gel, and in a second step for 150 V for 90 min until no evidences of bromophenol blue was left in the gel

2.9.7. Detection and Digital Imaging

Gel staining was performed using 3 PhasTGelTM Blue R tablets (Coomassie R350) (GE Healthcare) diluted in 1 L, 10 % (v/v) acetic acid. The gel containing solution was further heated in the microwave oven for 2 min at 900 watts (W), and the process was repeated every 20 min three times. Microwave heated deionized water (2 min at 900 watts) was used for rinsing the gel until appropriate contrast was obtained for protein spot detection. Images of the 2-DE gels were acquired through Magic Scan software in Tiff and Lab Scan format, and protein spot analysis was carried out by Melanie 7.0 software (GeneBio, Genebra, Switzerland). Protein spot comparison was conducted between gels in order to evaluate abundance level variation, considering the different analyzed conditions. Abundance level variation was calculated through the ratio between intensity of each sample spot and its homologous spot in the control gel. Abundance levels ≤ 0.7 and ≥ 1.5 were considered significant.

2.10. Multidrug Resistance Induction

Multi-drug resistance acquisition is still largely unexplored and somewhat controversial; thusly cell line models offer a sturdy *in vitro* platform to study and understand drug resistant tumour cells and associated molecular patterns and pathways. HCT-116 and A549 cell lines, long term exposure to increasing concentrations of Doxorubicin allowed to establish a series of descendent subcultures that were significantly more resistant to this particular drug. Drug resistance induction was established *in vitro* in a step wise increase in doxorubicin concentration in culture medium. HCT-116 and A549 original cell lines were subcultered as described in section 2.3, and were seeded at approximately 20 % confluence, in independent 25 cm^2 culture flasks for drug resistance induction. Drug resistance culture flasks were incubated at 37 ºC, 99 % (v/v) humidity and 5 % (v/v) CO_2 for 24 h at the end of which, cell lines were exposed to a pre-determined doxorubicin concentration that varied between cell lines. HCT-116 cell line was submitted to a step wise increase in doxorubicin concentration that ranged from 0.001 μg/mL to 0.5 μg/mL, while A549 cell lined doxorubicin concentration ranged from 0.0058 μg/mL to 0.029 μg/mL. Cell lines were maintained in the same concentration for 5 subcultures to allow cells to adapt to drug concentration and to develop resistance molecular patterns. A total of 15 out of 30 planed subcultures were carried out. The total number of subcultures (30) under drug exposure was considered, accordingly to literature reports, to be enough to induce a resistance phenotype.

3. Results and Discusion

3.1. Cytotoxic Potential Evaluation

The antiproliferative potential was evaluated through assessment of the cytotoxicity of chlorogold compounds B and D in non-small cell lung (A549; H1975), human colorectal (HCT116), hepatocellular (HepG2), breast (MCF-7) and melonotic (MNT-1) carcinoma cell lines as well as in chronic myelogenous leukaemia (K562) and human normal fibroblasts. After a 48 h exposure period to chlorogold compounds B and D, spectrophotometric quantification of the amount of formazan, resulting from MTS reduction by mitochondrial dehydrogenases of metabolically active cells, using the CellTiter 96 ® AQueous non-radioactive cell proliferation assay, allowed to establish a correlation between the colour intensity of the formazan dye and the number of viable cells (Wang *et al.*, 2010; Riss *et al.*, 2013). From the results obtained, it was possible to determine important pharmacological parameters, namely the absolute and the relative IC_{50} values (among other parameters), which prove themselves fundamental for the validation and characterization of the compounds, as well as for the understanding of which mechanistic studies, *in vitro* and *in vivo* should be performed to assess potential therapeutic applications before effective translation into the clinics is made possible (McGowan *et al.*, 2011). When considering the concepts of absolute and the relative IC_{50} values this are somewhat controversial and important guidelines should be followed (Sebaugh, 2010). While the absolute IC_{50} corresponds to the concentration that represents the halfway point between 100 % and 0 % viability, the relative IC_{50} is the concentration required to bring the dose-response curve down to the point halfway between the top and bottom plateaus of the curve. The full quantification of a drug's potency in relation to its target is logically unfeasible when applying the concept of absolute IC_{50} as some drugs often develop their therapeutic action in a non-dose dependent way. In this sense the concept of an absolute IC_{50} is not standard, and many find it not to be useful. The concept of relative IC_{50} on the other hand is considered to be the most common definition in accordance with pharmacological analysis (Neubig *et al.*, 2003) and it will be considered the norm hereon forward. All values were calculated from dose-response curves resorting to GraphPad software.

Observation of the data shown in Table 3.1 outlines that both compounds, B and D induced a varying but substantial degree of cytoxicity in all cell lines screened, yielding IC_{50} values in the 10^{-6} to 10^{-5} M range after continuous exposure to various concentrations for a period of 48 h. Furthermore dose-response curves, showed in Appendix A, highlight the ability of the compounds to inhibit cell proliferation in a dose-dependent manner. Relative IC_{50} are displayed in upper right corner of each chart, which in turn are specific for each compound and for each cell line.

Table 3.1 – IC_{50} values for chlorogold compounds B and D, in non-small cell lung (A549; H197), human colorectal (HCT-116), hepatocellular (HepG2), breast (MCF-7) and melonotic (MNT-1) carcinoma cell lines as well as on chronic myelogenous leukemia (K562) and human fibroblasts. Data values are referent to those reported in Appendix A, and are represented as means of at least three independent experiments.

Cell Line	Relative IC50 (μM); 48 h	
	Compound B	Compound D
A549	44.40	30.09
HCT-116	9.51	9.02
H1975	3.36	5.43
HEP G2	9.97	9.79
K562	5.13	8.02
MCF-7	11.65	13.06
MNT-1	17.88	11.64
Fibroblasts	7.74	19.10

Among all the tested cell lines, compound B and D elicited the strongest inhibitory effect on the proliferation on H1975 NSCLC cell line, exhibiting IC_{50} values of 3.36 and 5.43 μM respectively. On the other hand H1975 NSCLC cell line counterpart, A549, displayed values of 44.40 and 30.09 μM respectively in what was the weakest antiproliferative effect in all cell lines available. Indeed compound B and D's activity on H1975 is approximately 13.2 and 5.5 times higher than when compared with A549, clearly evidencing not only different mechanisms of action differing between cell lines but also consequently different susceptibilities. Of relevance from the remaining tumoural cell lines, HCT-116 and HEP G2 exhibited very similar responses for both compounds and in between cell lines (HCT-116 - 9.51; 9.02 μM / HEP G2 – 9.97; 9.79 μM for compound B and D respectively). Moreover MCF-7 and MNT-1 displayed the second highest IC_{50} values for both compounds, after A549 (MCF-7 – 11.65; 13.06 μM / MNT-1 – 17.88; 11.64 μM for compound B and D respectively). A relevant particularity when observing Table 3.1 is the variability of distinct tumoural cell line response when exposed to the same compounds. This simultaneously puts in perspective the plethora of morphological and molecular differences typical of each cancer cell line, as result of differentiation and mutational processes, and the different possible drug-target interactions by which the chlorogold compounds may "take advantage of" to play their cytotoxicity.

In particular viability rates obtained for both A549 and H1975 are evidence in Figure 3.1 and 3.2 respectively, after a 48 h exposure treatment with compound B and D. A closer analysis in both cell lines allows the observation of a gradual decrease in cell viability as compound concentrations rose. The effect is particularly more evident for concentrations above 20 μM in A549 and for concentrations roughly above 2.5 μM in H1975, for both compounds. Taking into consideration doxorubicin´s IC_{50} values for the same cell lines, namely 9.20 μM for A549 and 0.066 μM for H1975, the (He *et al.*, 2011; Brechbuhl *et al.*, 2013), chlorogold compounds are unable to achieve growth inhibition in that

order of magnitude. Nonetheless the results displayed either in Table 3.1 or in Figures 3.1 and 3.2 suggest that chlorogold compounds confer antiproliferative properties *in vitro* for both tumoural cell lines, however the drug concentrations necessary to inhibit cell growth are substantially higher than those of renowned chemotherapeutic drugs such as doxorubicin or cisplatin (He *et al.*, 2011). Despite these differences the chlorogold compounds in question seem to target the proliferative nature of cancer, one of the main basal cell functions. Since basal cell functions are always supported by specialized pathways, chlorogold compounds most likely affect specific regulators opening new possibilities for potential novel therapies in cancer treatment. However prudence must be taken into consideration as results *in vitro* may not be fully depictured in the same way as *in vivo*. Fundamental pharmacokinetic properties such as rates of absorption, biotransformation, distribution and excretion, that influences compound exposure *in vivo* can't be adequately represented in *in vitro* assays (Holohan *et al.*, 2013).

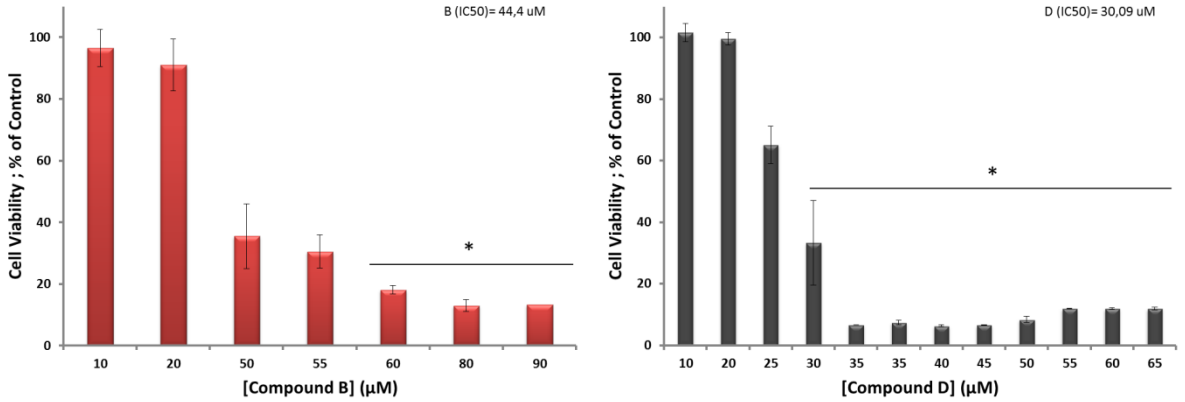

Figure 3.1 – Dose dependent cytotoxicity of chlorogold compounds, B (left) and D (right), on non-small cell lung adenocarcinoma cell line (A549). The respective relative IC_{50} of each compound is displayed in the upper right corner of each chart. The data are represented as means ± SEM of at least three independent experiments; *p < 0.05, as compared with the control group. Cell viability values were normalized in relation to the control group without compounds (only DMSO).

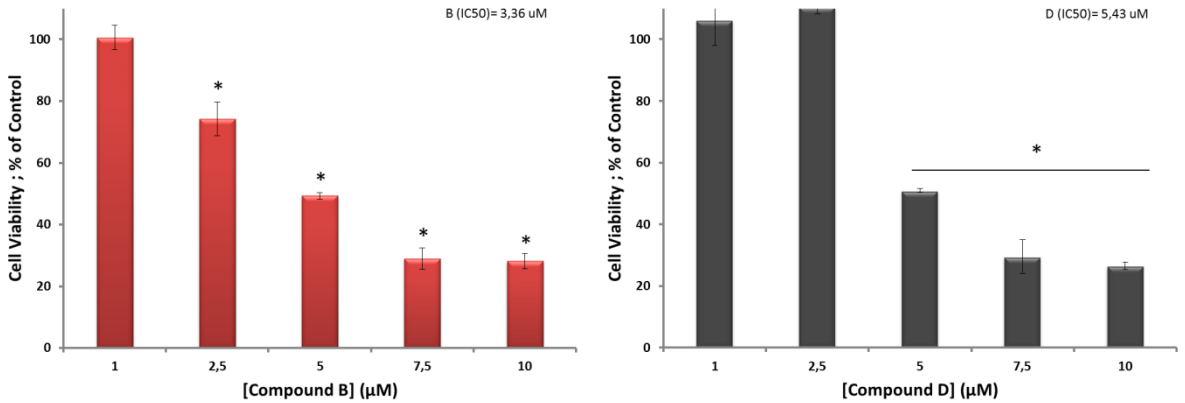

Figure 3.2 – Dose dependent cytotoxicity of chlorogold compounds, B (left) and D (right), on non-small cell lung adenocarcinoma cell line (H1975). The respective relative IC_{50} of each compound is displayed in the upper right corner of each chart. The data are represented as means ± SEM of at least three independent experiments; *p < 0.05, as compared with the control group. Cell viability values were normalized in relation to the control group without compounds (only DMSO).

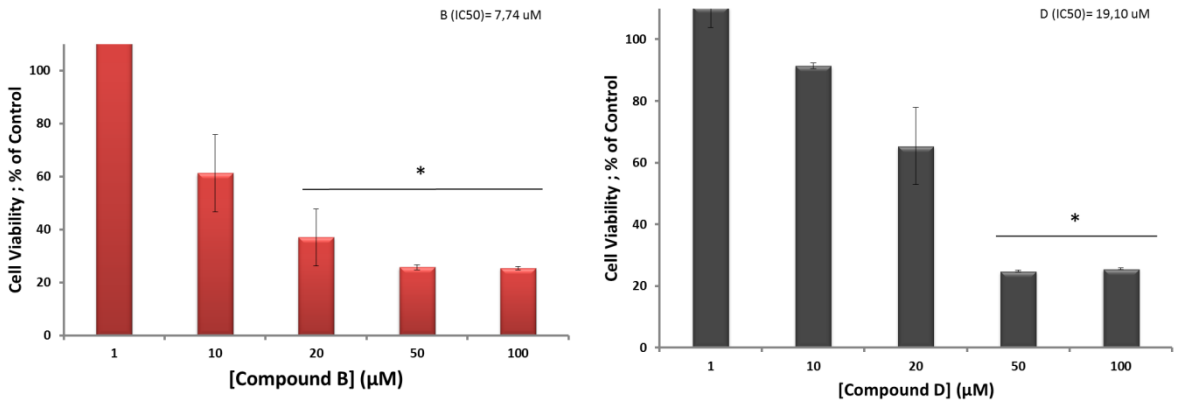

Figure 3.3 – Dose dependent cytotoxicity of chlorogold compounds, B (left) and D (right), on fibroblast cell line. The respective relative IC_{50} of each compound is displayed in the upper right corner of each chart. The data are represented as means ± SEM of at least two independent experiments; *p < 0.05, as compared with the control group. Cell viability values were normalized in relation to the control group without compounds (only DMSO).

Information on the relative toxicity spectrum on non-tumoural cells was also assessed. In this sense investigation was proceeded towards determination of the effects of chlorogold compounds B and D, on cell growth and cell survival in a fibroblast healthy cell line. Analysis of Figure 3.3 evidences a substantial dose-dependent cytotoxicity observed for both compound B and D, being significant for concentrations ≥ 20 µM for compound B and for concentrations ≥ 50 µM for compound D ($p < 0.05$). The IC_{50} values obtained for both compounds are actually lower than when compared with A549 cell line (5.7 and 1.6 fold lower), meaning that lower concentrations tend to induce more cell death in fibroblast healthy cell line than in A549. The IC_{50} value comparison for H1975 is not as dramatic as to its counterpart; nonetheless results only evidence a slightly higher IC_{50} value for compound B and D in fibroblasts comparing with H1975 values (Table 3.1).

Considering extrapolation of these results into a hypothetical clinical translation, as potential chemotherapeutic agents of NSCLC, would have to be done with diligences as these compounds reveal substantial toxicity towards healthy cells at their respective IC_{50} values for the treatment of NSCLCs. Ideally chlorogold compounds should have pertained a higher "predisposition" to target tumour cell lines than healthy cell lines, this being noticeable by a far higher IC_{50} values in fibroblasts cell line. In these sense one possibility to circumvent broad toxicity, would be to consider these chlorogold compounds in targeted therapies for NSCLC, such as antibody drug conjugates or nanocarriers as drug delivery platforms (Martins *et al.*, 2014b; R. Fernandes and Viana Baptista, 2013; Iyer and Kadambi, 2011; Singh and Lillard, 2009). Nonetheless in view of chlorogold compound's potency against H1975 and the weaker results in A549, both cell lines were selected for further assays in an attempt to unravel the governing mechanisms of action of each compound that determine the different therapeutic responses in each cell line.

3.2. Combination Chemotherapy and Implications in NSCLC Treatment

The inability of current chemotherapeutic single agents to effectively manage non-small cell lung cancer death in first world countries has halted the progress in the treatment of this disease. Reaching this plateau in the development of effective strategies, as led to experimentation with different combination processes in order to tackle such problem (Van Schaeybroeck *et al.*, 2006). Cell viability assay in NSCLC A549 cell line in response to compound B and doxorubicin in combination therapy (Figure 3.4), was performed in order to assess its potential as a novel possible combination therapy for this disease.

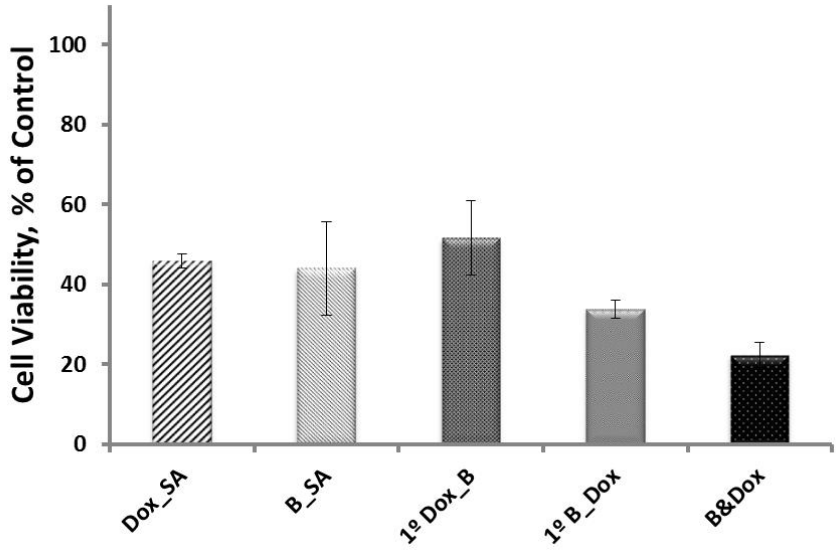

Figure 3.4 – Cell viability in NSCLC A549 cell line in response to compound B and doxorubicin in combination therapy. Combination strategies' (1º Dox_B; 1º B_Dox; B&Dox) effectiveness was compared to single agent (SA) treatments (Dox_SA; B_SA). All strategies resorted to the IC_{50} values of each compound (see section 3.1). The data are represented as means ± SEM of at least three independent experiments; *$p < 0.05$, as compared with the control group. Cell viability values were normalized in relation to the control group without compounds (only DMSO).

A broad analysis of Figure 3.4 evidences that not all combination strategies employed using these compounds exhibited a considerable cytotoxicity in comparison with the single agent (SA) treatments of doxorubicin (Dox_SA) and compound B (B_SA) at their respective IC_{50} values. A closer look allows to observe that the first treatment strategy, pretreatment with doxorubicin for 24 h with posterior administration of compound B for 24 h (1º Dox_B), decreases the loss in cell viability compared to single agent treatments (e.g. 45 % to 51 % of cell viability increase compared to doxorubicin). This result might give an indication of possible antagonism when employing such strategy. Pretreatment with compound B for 24 h with posterior administration of doxorubicin for 24 h (1º B_Dox) and/or the administration of both compounds concomitantly for 48 h (B&Dox), have evidenced a reduction in cell viability compared to single agent treatments (cell viability of 33.8 and 22.3 % respectively). In fact the administration strategies, 1º B_Dox and B&Dox are approximately

1.5 and 2.3 fold more cytotoxic compared to Dox_SA, respectively. In contrast with the first treatment strategy (1º Dox_B) pretreatment with compound B for 24 h in 1º B_Dox strategy, has apparently enhanced doxorubicin-induced cytotoxicity in A549 cell line, possibly by cellular redox homeostasis impairment. Compound B administration could eventually augment doxorubicin's main mechanisms of action, namely DNA biosynthesis inhibition and formation of ROS (Thorn *et al.*, 2012). In addition, simultaneous administration further attests for this cooperative effect, visible by an even lower cellular viability value (22.2 % in comparison with 45.2 % for Doxorubicin alone). Albeit none of the results are statistically significant, these provide initial evidences as for their possible mechanisms action and more importantly the pharmacodynamic properties between doxorubicin and compound B. Further exploitation and adjustments on drug-ratio concentrations could strengthen the full therapeutic potential of this drug combination (Mayer and Janoff, 2007) lowering the amount of compounds/drugs needed for the same cytotoxic effect and providing for novel therapeutic strategies and "avenues" in cancer treatment.

In parallel with the above mentioned combination study, two other combinations were tested and duly analysed. Particularly cell viability assay in NSCLC A549 cell line, in response to the combination of erlotinib and compound B, or erlotinib and doxorubicin were assessed as potential tools for chemotherapy (Figure 3.5). Taking into consideration that as much as 80 % of all NSCLC patients display EGFR overexpression (Van Schaeybroeck *et al.*, 2006), selection of erlotinib as the preeminent drug in these strategies was a seemingly logical approach and a key intermediate for the success of the established strategies. In fact erlotinib's application in clinical research has provided substantial

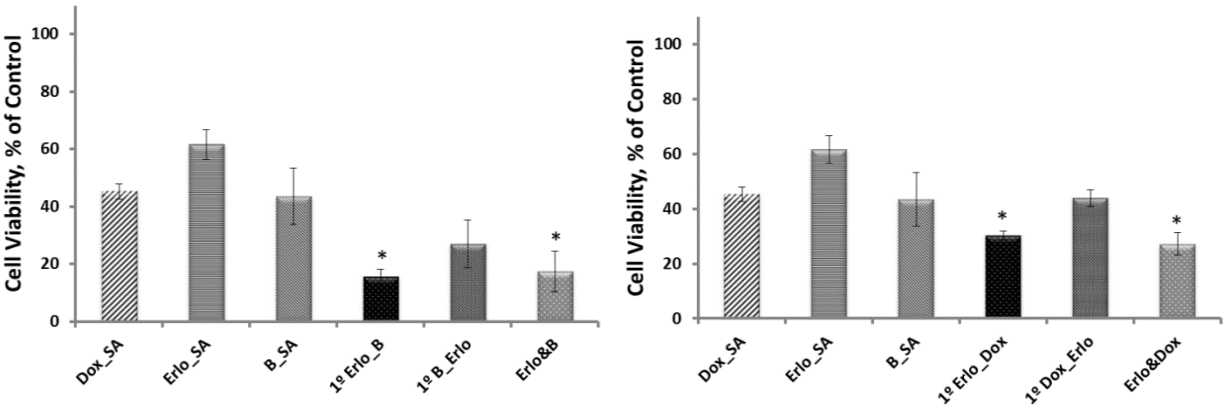

Figure 3.5 – Cell viability in NSCLC A549 cell line in response to erlotinib and compound B (Left) and erlotinib plus doxorubicin (Right) in combination therapy. Combination strategies' (1º Erlo_B; 1º B_Erlo; Erlo&B; Erlo_Dox; Dox_Erlo; Erlo&Dox) effectiveness was compared to single agent (SA) treatments (Dox_SA; Erlo_SA; B_SA). All strategies resorted to the IC_{50} values of each compound (see section 3.1). The data are represented as means ± SEM of at least three independent experiments; *$p < 0.05$, as compared with the control group. Cell viability values were normalized in relation to the control group without compounds (only DMSO).

positive results in several areas, such as in adjuvant treatment, in the first-line therapy of advanced disease and in combination with cytotoxic treatments (Gridelli *et al.*, 2007). The success of phase I/II clinical trials combining erlotinib and bevacizumab, or sorafenib and erlotinib on constraining and abrogating antiproliferative growth on several NSCLC patients, has raised awareness and interest in the potentiality of other combinations employing erlotinib and other molecular target drugs (Gridelli *et al.*, 2007).

Examination of cell viability assay in NSCLC A549 cell line in response to erlotinib and compound B (left chart-Figure 3.5) puts in evidence the feasibility of this combination of compounds, as all the strategies employed and illustrated (1º Erlo_B; 1º B_Erlo; Erlo&B), indicate a substantial reduction in cell proliferation in comparison single agent treatments (Dox_SA; Erlo_SA; B_SA). A more thorough analysis, reveals that pretreatment with erlotinib for 24 h with posterior administration of compound B for another 24 h (1º Erlo_B) presents a total cell viability count in the order of 15.6 %, while pretreatment with compound B for 24 h with posterior administration of erlotinib (1º B_Erlo) a cell viability count in the order of 29.9 %. Similarly, simultaneous administration of both compounds (Erlo&B) exhibited a cell viability of 17.3 %. In comparison with Dox_SA (45.2 % cell viability) these values represent a reduction in cell viability, in an order of magnitude of 2.9, 1.7 and 2.6 fold, respectively. Of these strategies only 1º Erlo_B and Erlo&B are statistically significant in comparison with SA treatments, which seems to be in accordance with what is published in literature regarding the active role of erlotinib in combination therapies and its' action principle. Apparently pretreatment with erlotinib, or concomitant administration with compound B, might block key molecular pathways and regulators for cancer growth and progression such as EGFR pathway or abrogation of RB leading to cell cycle arrest (Bonomi, 2003). These processes compromises the cells' integrity becoming further susceptible to a second drug, in this case compound B, which results in increased cell death and a lower cell viability.

Similarly NSCLC A549 cell line's response to erlotinib and doxorubicin (right chart-Figure 3.5), has shown equivalent results although in a less pronounced fashion. While pretreatment with doxorubicin for 24 h with posterior administration of erlotinib for another 24 h (1º Dox_Erlo) showed no significant alterations, its counterpart, pretreatment with erlotinib for 24 h with posterior administration of doxorubicin for 24 h (1º Erlo_Dox) or concomitant administration of both compounds for 48 h (Erlo&Dox) have respectively reduced cell viabilities to 30.3 and 27.2 %. Indeed these combinations are approximately 1.5 and 1.7 times more active than Dox_SA (45.2 % cell viability). However by contrast, the previous combination study employing compound B and erlotinib have shown to be 2.9 and 2.6 more active for the same conditions. In view of such results, out of the three analysed combination studies, erlotinib plus compound B in combiantion significantly demonstrated the most promising results even surpassing the conventional chemotherapeutic drug,

doxorubicin under the same conditions. Future studies employing it should be performed in order to determine more precisely fundamental parameters such as pharmacodynamics and the possible mechanisms of action by identification of main drug-target interactions.

Despite the observed results judgment should be kept in mind when trying to evaluate the possible interactions between compound B, doxorubicin and erlotinib in their respective combination strategies. In fact dose-effect relationships between compounds, such as synergistic, additive or antagonistic, can only be intuitively extracted from the above results, as no generalized method for analyzing dose-effect relationships was used for such cellular systems and strategies (Pinto *et al.*, 2010). The median effect analysis developed by Chou and Talalayi has been the most renowned and currently used method for quantitative evaluation of compound combinations (Chou and Talalayi, 1984). The method offers a mathematical model based on enzyme kinetic systems and Michaelis–Menten and Hill equations that allows to correlate the drug dose and the corresponding effect (Chou and Talalayi, 1984) and should in future studies be employed to better understand dose-effect relationships and how it effects the pharmacokinetic properties of the respective compounds. In other words parameters such as synergistic, additive or antagonistic dose-effect relationships should be determined alongside with clinical relevant factors like absorption, distribution, metabolism, and excretion of the respective compounds and how the concomitantly administration itself affects these same factors.

3.3. Evaluation of the Apoptotic Potential

In view of the initial antiproliferative results obtained for chlorogold compounds B and D in NSCLC cell lines (A549; H1975) (section 3.1), Hoechst 33258 labeling plus anexinV-FITC and propidium iodide double labeling technics were used to explore the underlying mechanisms related to cell viability loss.

3.3.1. Hoechst 33258 Labeling: Nuclear Morphology Alterations

Hoechst 33258 fluorescence sensitivity to DNA conformation and chromatin aberrations enable its use to detect multiple forms of nuclear damage, being a good indicator of cellular death processes such as apoptosis (*Hoechst Stains, MP21486, Invitrogen*, 2005). Hoechst 33258 ability to bind to AT-rich dsDNA strands was used for nuclear staining of NSCLC cell lines, A549 and H1975, when exposed to chlorogold compounds (Figure 3.6 and 3.7 respectively), in order to evaluate two main parameters: the effects of continuous exposure to chlorogold compounds B and D for 48 h on overall nuclear morphology (I) and the underlying mechanism of cell death responsible for cell viability loss when exposure to the same compounds (II).

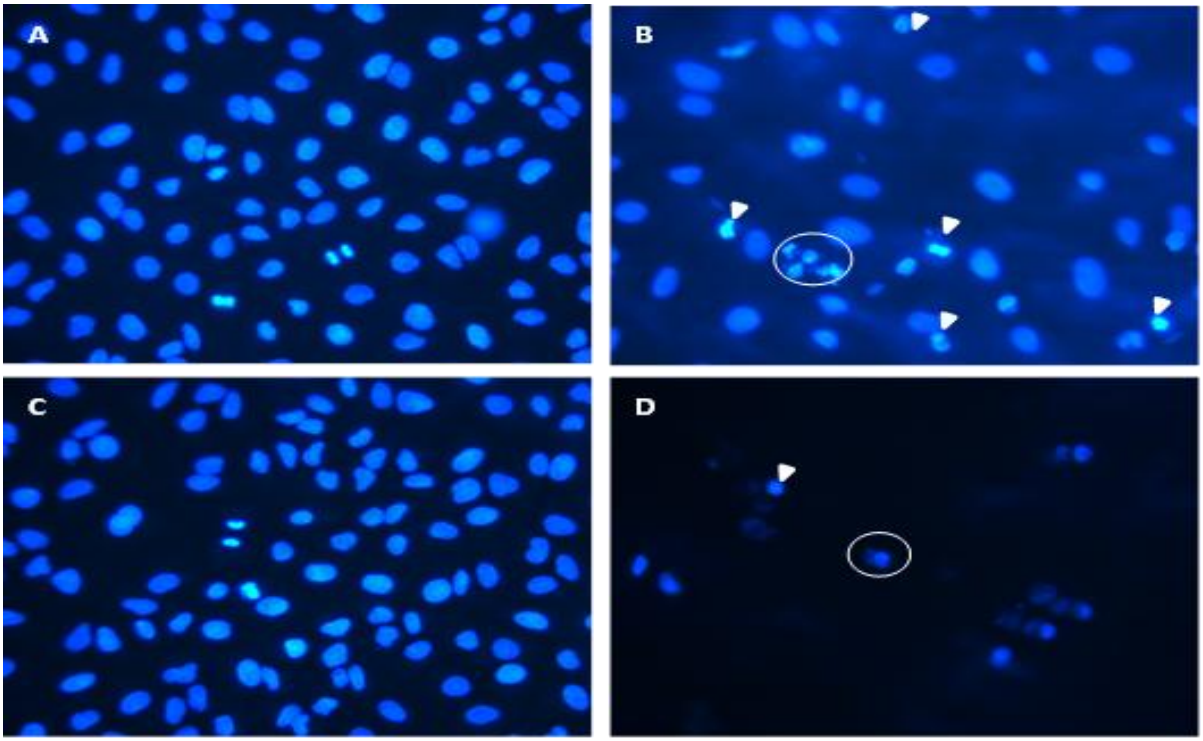

Figure 3.6 – NSCLC A549 cell line nuclear staining with Hoechst 33258 in response to 44.4 μM of compound B (B) and 30.0 μM of compound D (D) bringing to evidence nuclear morphological alterations indicative of apoptosis. Qualitative results were compared with the respective solvent of the compounds: 0.1 % (v/v) DMSO (A;C). White arrows point out evidences of initial apoptosis hallmarks such as chromatin condensation or aberrant nuclear morphology. White circles indicate nuclear fragmentation.

NSCLC A549 cell line nuclear staining, in response to 44.4 μM of compound B, illustrates several nuclei exhibiting clear hallmarks of programmed cell death by apoptosis. Nuclei present themselves shrunken with an overall aberrant nuclear morphology and condensed chromatin (Figure 3.6; B; arrowheads). Furthermore nuclear fragmentation is also evident as well as the formation of apoptotic bodies (Figure 3.6; B; circles). Regarding NSCLC A549 cell line nuclear staining, in response to 30.0 μM of compound D similar results were observed although to a lesser extent. Paradoxically when exposed to compound D, a lower cellular density was observed when in comparison with compound B, which in part could be explained considering a hypothetical fast acting mechanism of action for compound D consequently justifying for the low number of nuclei. This effect is also visible for compound B but less pronounced. These results become considerably more noticeable when in contrast with control samples, exposed only to the compounds' solvent, DMSO. Nuclei in control samples present a uniform distribution of fluorescence indicating uncondensed chromatin and normal metabolic activity (Silva *et al.*, 2012). One noteworthy fact is the observation of active dividing cells in control samples which are not apparent when under compound exposure. The induction of nuclear fragmentation and/or the activation of cell cycle arrest processes by possible mechanisms of action of the compounds, could offer an explanation for such observations.

Similarly the effects of H1975 exposure to compound B and D, on nuclear morphology resemble the same as those evidenced for A549. Exposure to 3.36 μM of compound B and 5.43 μM of compound D leads to the observation of clear nuclear morphological alterations such as chromatin condensation (Figure 3.7; B-D; arrowheads) and nuclear fragmentation (Figure 3.7; B-D; circles). Additionally the difference in cell density between control samples and samples exposed to compounds, further emphasize the compounds' capacity to induce cell death, most likely by apoptosis given the presence of the exhibited apoptotic hallmarks for the remaining nuclei.

All in all the results observed in Figures 3.6 and 3.7 correlate with the above cell viability results presented in Figure 3.1 and 3.2. There is a clear and marked decrease in cell viability in the presence of compound B and D, for both cell lines, which is likely to be intimately correlated with an increased cell death by apoptosis (although necrosis cannot be overruled by this assay).

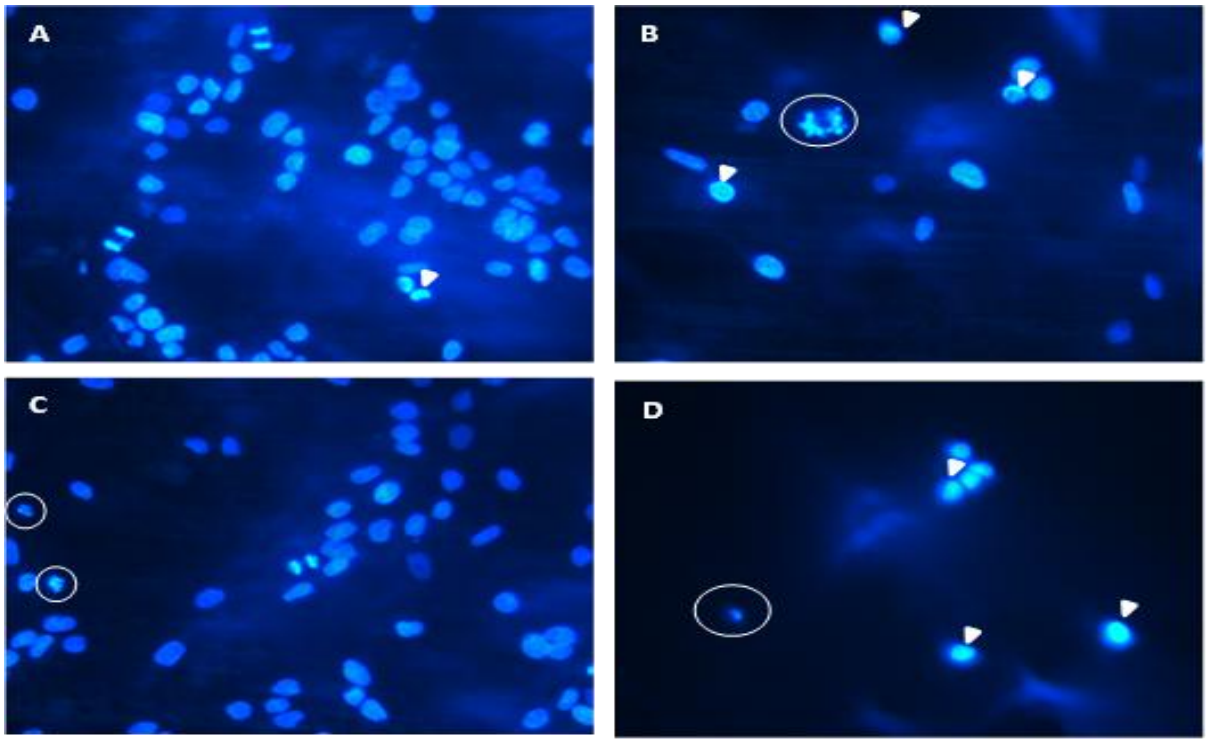

Figure 3.7 – NSCLC H1975 cell line nuclear staining with Hoechst 33258 in response to 3.36 μM of compound B (B) and 5.43 μM of compound D (D) bringing to evidence nuclear morphological alterations indicative of apoptosis. Qualitative results were compared with the respective solvent of the compounds: 0.1 % (v/v) DMSO (A;C). White arrows point out evidences of initial apoptosis hallmarks such as chromatin condensation or aberrant nuclear morphology. White circles indicate nuclear fragmentation.

3.3.2. Annexin-FITC and Propidium Iodide Double Labeling: Necrotic vs Apoptotic Cells

To consolidate the results obtained for Hoechst staining and in order to get further insights into the cytotoxic action of chlorogold compounds in tumour cells, PI and Annexin V-FITC double staining was performed to better differentiate between apoptotic and necrotic cell death. Apoptosis is distinguished from necrosis by a set of specific molecular and biochemically complex energy dependent alterations, involving cytoplasm and chromatin condensation, nuclear aberrations and loss of membrane asymmetry. In response to external or internal stimuli, early apoptotic cells rapidly lose the asymmetric distribution of the phospholipids in both leaflets typical of viable cells, however without losing membrane integrity (Schutte *et al.*, 1998; Brumatti *et al.*, 2008). This early hallmark of apoptosis is epitomized by the translocation of the phosphatidylserine from the inner membrane leaflet to the outer membrane leaflet which is prone to bind to Annexin V, the Ca^{2+} dependent phospholipid-binding protein (*FITC Annexin V / Dead Cell Apoptosis Kit with FITC annexin V and PI , for Flow Cytometry, MP 13242, Invitrogen*, 2010). Plasma and nuclear membrane integrity on the other hand decreases in late apoptotic and necrotic cells allowing the nuclear dye PI to pass through membranes and intercalate with nucleic acids (Rieger *et al.*, 2011). Flow cytometry employing double staining with annexin-FITC and PI can hence discriminate between early and late apoptotic cells from necrotic cells. While early apoptotic cells present an $FITC^+/PI^-$ ratio and late apoptotic cells an $FITC^+/PI^+$, necrotic cells present an $FITC^-/PI^+$ ratio in view of their membrane integrity characteristics. At risk of stating the obvious, viable cells present no staining from both dyes ($FITC^-/PI^-$) (Brumatti *et al.*, 2008; Sabbadini *et al.*, 2012).

Flow cytometry results of NSCLC A549 cell line when exposed to compound B and/or doxorubicin are illustrated in Table 3.2 and in Figure 3.8. Regarding the control sample, cells exposed only to 0.1 % (v/v) DMSO, showed an intact cytoplasmic membrane, evidenced by a demarking large percentage of viable cells (89.9 %), with only a small percentage of apoptotic cells. In respect to the exposure of NSCLC A549 cell line to 44.4 μM of compound B, the percentage of non-stained ($FITC^-/PI^-$) viable cells decreases significantly from 89.9 % to 55.4 % in what represents a total 1.6 fold change. Parallel to the decrease in cell viability, a considerable subpopulation of cells, exhibiting hallmarks of late apoptosis ($FITC^+/PI^+$) experience a substantial increase in an order of magnitude of approximately 5.4 fold higher (7.5 to 40.8 %) when compared with 0.1 % (v/v) DMSO. These results become even more pronounced with a 1.5 fold increase in compound B concentration. A 66.6 μM compound B exposure induces high numbers of late apoptotic cells ($FITC^+/PI^+$), reaching a total number of 74.7 %. Indeed when compared to 0.1 % (v/v) DMSO this value represents an astonishing 10 fold increase in the number of late apoptotic cells. For the remaining subpopulations ($FITC^+/PI^-$, $FITC^-/PI^+$) no significant alterations were observed (Table 3.2), however for all three conditions analysed (0.1 % (v/v) DMSO;

compound B 44.4 and 66.6 μM) the bulk of apoptotic cells were found to increase in a dose-dependent way and to mainly have late apoptosis hallmarks, hence exhibiting a double staining pattern ($FITC^+/PI^+$). The relevance of such noteworthy evidence, comes from the fact that a higher proportion of cells in latter stages of apoptosis is indicative of the compound's ability to induce apoptosis in a more readily fashion, and consequently of a potentially faster mechanism of action.

Both the hypotheses of a potentially faster mechanism of action as well as the induction of cell death by apoptosis (and not necrosis) are strongly corroborated with the initial results presented for Hoechst 33258. In face of the results obtained for cell viability assays, Hoechst 33258 staining and flow cytometry data, a substantial increase in the sub-population of late apoptotic cells seems to be linked to the underlying mechanism of cell death of chlorogold compounds. Based on these evidences, chlorogold compounds are able to induce cell death by apoptosis in a dose-dependent fashion and through potentially faster mechanism of action.

Table 3.2 – Total percentage of viable, early apoptotic, late apoptotic and necrotic cells, in NSCLC A549 cell line, when exposed to different concentrations of compound B and doxorubicin or when exposed to both compounds in combination at their respective IC_{50} values. Cells treated with 0.1% (v/v) DMSO were used as control. Data was analysed by flow cytometry after Annexin-V/FITC and PI double staining. Data values are referent to those reported in Figure 3.8, and are represented as means ± SEM of at least three independent experiments.

	0.1% DMSO	Compound B (44.4 μM)	Compound B (66.6 μM)	Doxorubicin (9.20 μM)	Doxorubicin (13.8 μM)	Compound B & Doxorubicin
Viable Cells	89.95 (± 2.07)	55.36 (± 14.53)	21.19 (± 14.54)	5.26 (± 2.42)	10.59 (± 7.81)	4.23 (± a)
Early Apoptotic Cells	1.87 (± 1.68)	1.48 (± 0.27)	2.67 (± 0.76)	25.17 (± 15.36)	26.96 (± 16.15)	17.63 (± a)
Late Apoptotic Cells	7.51 (± 1.75)	40.84 (± 13.89)	74.77 (± 15.11)	46.35 (± 9.58)	39.86 (± 7.23)	75.68 (± a)
Necrotic Cells	0.67 (± 0.46)	2.31 (± 0.79)	1.36 (± 0.53)	23.22 (± 15.07)	22.59 (± 15.23)	2.46 (± a)

a – Not available

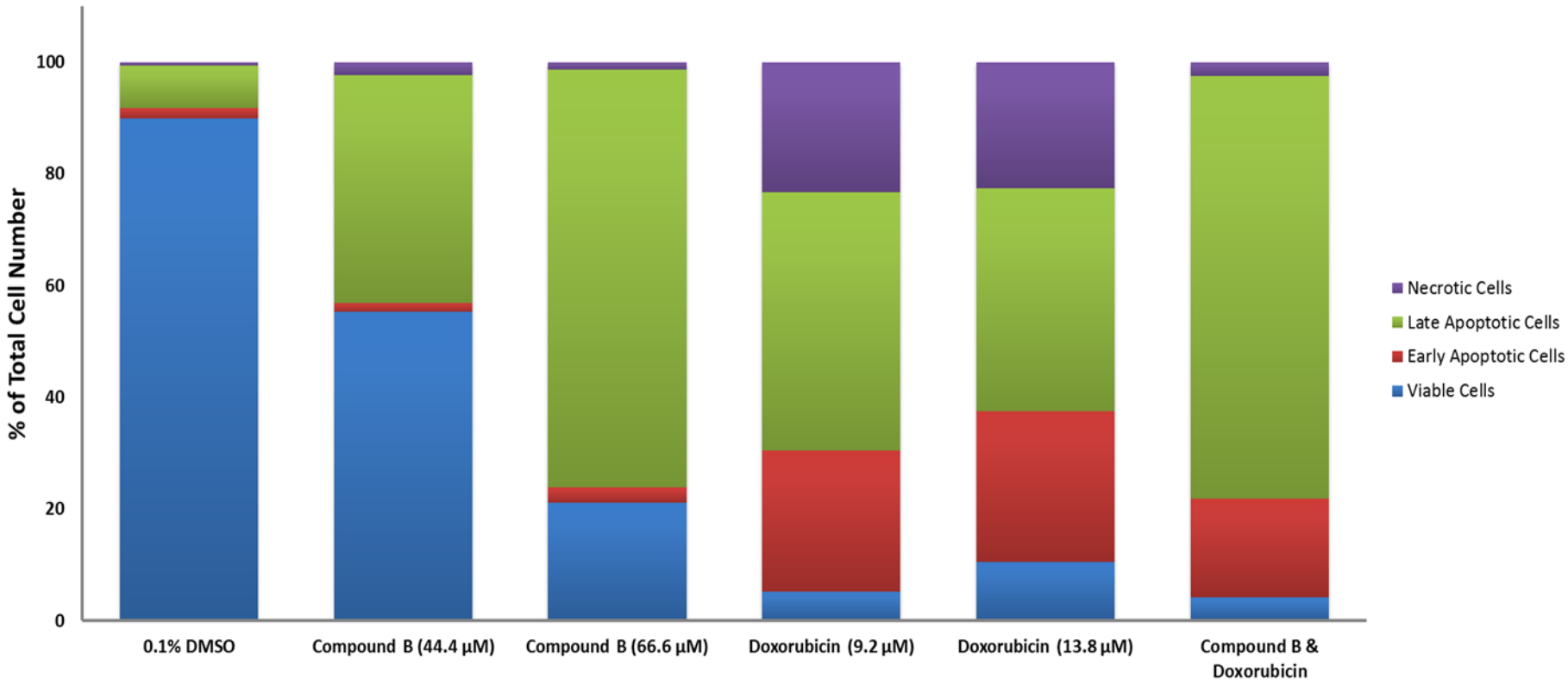

Figure 3.8 – Proportion of viable, apoptotic and necrotic cells in NSCLC A549 cell line, when exposed to different concentrations of compound B and doxorubicin or when exposed to both in combination at their respective IC_{50} values. Cells treated with 0.1% (v/v) DMSO were used as control. Data was analysed by flow cytometry after Annexin-V/ FITC and PI double staining. The data is represented as means ± SEM of at least three independent experiments.

Regarding the exposure effects of NSCLC A549 cell line to doxorubicin the evidenced results show a very distinct distribution of viable, apoptotic and necrotic cells when compared with compound B's results. Administration of 9.20 μM of doxorubicin (IC_{50} value) promotes an abrupt decrease in cell viability when compared with 0.1 % (v/v) DMSO, presenting only an approximately 5 % of cells with intact cytoplasmic membrane ($FITC^-/PI^-$). Plus the bulk of apoptotic and necrotic cells present an increase of 7.6 and 34.6 fold respectively. In comparison with administration of 44.4 μM of compound B (IC_{50} value), doxorubicin exhibited 50 % less viable cells, which were followed by an increase of 23.7, 5.5, and 20.9 % more early apoptotic ($FITC^+/PI^-$), late apoptotic ($FITC^+/PI^+$) and necrotic cells ($FITC^-/PI^+$) respectively. Also of interest, the administration of doxorubicin's IC_{50} value (He *et al.*, 2011), paradoxically induces cell death values substantially above 50 % which even considering the concept of relative IC_{50} values is an odd fact. Such result can be explained as part of the limitations of MTS cell viability assay. In particularly the rationality behind the MTS assay stems from the spectrophotometric readings of the formazan resultant from the reduction of the set of tetrazolium reagents, by metabolically active cells (Wang *et al.*, 2010). This fact alone translated into other words means that IC_{50} values obtained through MTS cell viability assay are often overestimated, consequently explaining this paradigm. Furthermore a 1.5 fold increase in doxorubicin's concentration, opposed to what was observed for compound B, did not dramatize the initial effects obtain for the respective IC_{50} value. In fact unlike what was expected the percentage of viable cells actually increased from 5.2 to 10.6 % and late apoptotic cells actually decreased (Table 3.2). Despite these results the distinct distribution of viable, apoptotic and necrotic cells when compared with compound B, seems to point out to the distinct mechanisms of action between the two compounds.

In view of these results and taking into consideration the use of agents with different mechanisms of action as one of the fundamental principles for combination chemotherapy (Mayer and Janoff, 2007), the rational step of analysing the combination therapy of doxorubicin and compound B by flow cytometry was performed in order to assess its effect in NSCLC A549 cell line as complementary study of combination therapies already mentioned above. The concomitant administration of doxorubicin and compound B at their respective IC_{50} values evidenced clear patterns of the mechanisms of action of both compounds (Figure 3.8). Indeed as shown in Table 3.2, only 4.2 % of the cells are considered as viable, in a total decrease of 85.7 % in cell viability compared with 0.1 % (v/v) DMSO. Similar values were obtained for doxorubicin at its IC_{50} value (approximately 84.7 %). Plus the numbers of early apoptotic cells also seem to follow a pattern similar to that obtained for doxorubicin either at 9.20 μM or 13.8 μM. Evidencing a total value of 17.6 % of early apoptotic cells, only 9.3 % separate it from doxorubicin's value at 13.8 μM, while when compared with compound B at 66.6 μM this difference increases to approximately 15 %. Conversely a more thorough analysis on late apoptotic and necrotic cells, evidences patterns almost identical to those presented for compound B at 66.6 μM. By putting in contrast both tested conditions, compound B at 66.6 μM and the

simultaneous administration of doxorubicin and compound B at the respective IC_{50} values, early apoptotic cells' values are only set apart by 0.9 % thus emphasizing the possible influence of chlorogold compound B in inducing a fast acting apoptotic process when in combination. Considering necrotic cell value variance between the mentioned conditions these are also not substantial, being apart only by 1.1 %.

Again these results "push" towards an hypothesis were the administration of both compounds simultaneously is accompanied by the observation of a hybrid therapeutic effect (here evidenced by flow cytometry), characterized by the merging of the different mechanisms of action of both compounds.

3.4. Cell Cycle Evaluation: Cell Cycle Arrest

The intricacy of the biochemical events and molecular mechanisms that regulate cell cycle and apoptosis are intimately linked (Al-Rubeai and Singh, 1998). The delicate balance between the regulatory processes that govern cell cycle can either prevent or induce an apoptotic response. Tumour suppressor genes *TP53* and *RB*, *C-MYC* oncogene and CDKs (Pucci *et al.*, 2000), comprise the main orchestrators that supervise and regulate such responses, and that ultimately establish the link between cell cycle and apoptosis responses. For instances p53 may mediate cell cycle arrest in response to DNA damage and eventually in face of un-repairable damage entry of the cell into apoptosis (Vousden and Prives, 2009).

Cell cycle evaluation was performed in order to better understand the molecular mechanisms underlying the therapeutic activity of chlorogold compounds, while simultaneously assessing its applicability and effects on cell cycle progression, alone and in combination with doxorubicin. These cell cycle studies also allowed to understand whether loss of viability through the induction of apoptosis could be preceded by alterations in cell cycle progression and in cell cycle checkpoints.

Table 3.3 – Total percentage of NSCLC A549 cells at different stages of the cell cycle, when exposed to compound B and doxorubicin at their respective IC_{50} values either in single agent treatment or in combination therapy. Data was analysed by flow cytometry after propidium iodide (PI) staining of DNA. Cells treated with 0.1% (v/v) DMSO were used as control. Data values are referent to those reported in Figure 3.9, and are represented as means ± SEM of at least two independent experiments.

	3h Exposure			6h Exposure			9h Exposure		
	0.1 % DMSO	B	B & Dox	0.1 % DMSO	B	B & Dox	0.1 % DMSO	B	B & Dox
G1/G0	32.2 (± 3.35)	38.96 (± 2.59)	57.52 (± 3.23)	29.34 (± 2.87)	38.19 (± 7.25)	44.14 (± 6.54)	62.78 (± 1.77)	40.84 (± 6.39)	50.29 (± 0.92)
S	53.47 (± 2.92)	51.55 (± 2.39)	32.06 (± 0.45)	18.34 (± 3.30)	46.1 (± 5.56)	44.52 (± 9.24)	9.1 (± 0.84)	27.71 (± 2.56)	38.96 (± 2.33)
G2/M	13.32 (± 2.77)	9.49 (± 1.46)	10.42 (± 2.78)	52.33 (± 1.70)	15.71 (± 2.16)	11.34 (± 2.69)	28.13 (± 1.26)	31.45 (± 8.91)	10.75 (± 1.41)

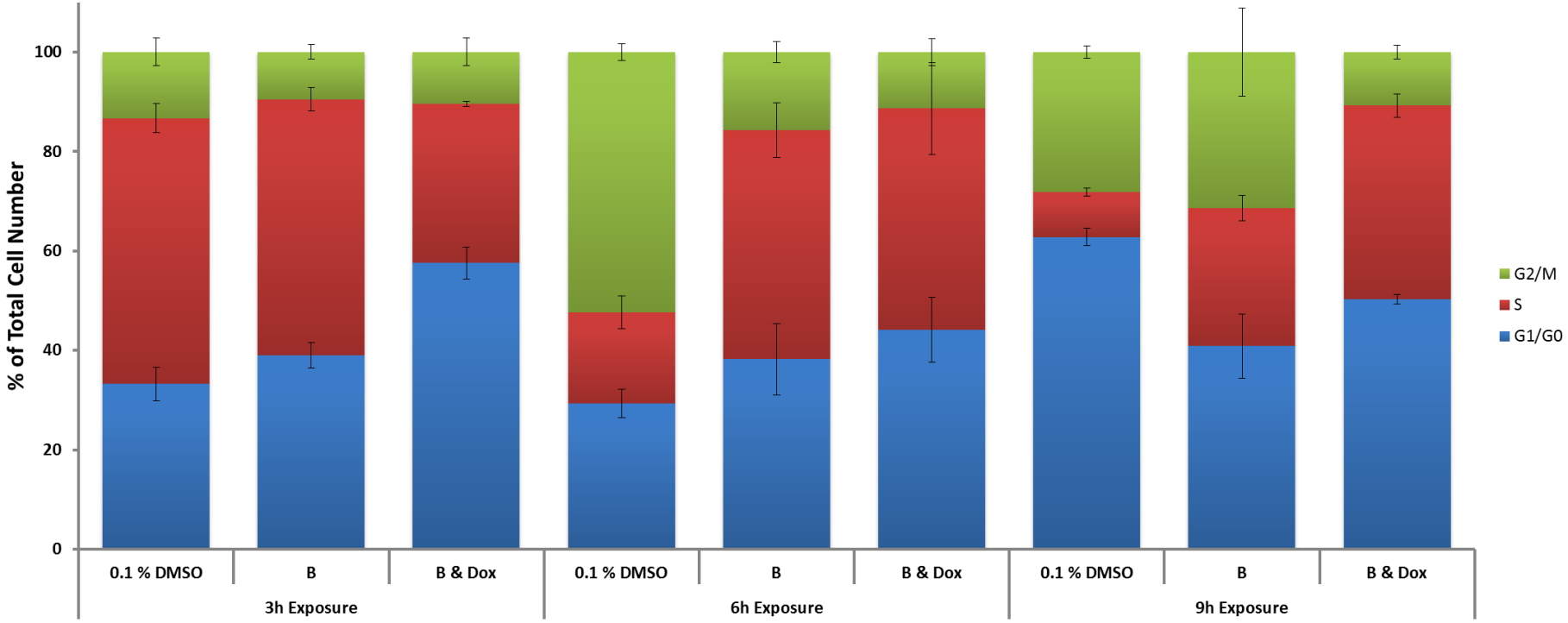

Figure 3.9 – Effect of compound B in single agent treatment and of compound B and doxorubicin in combination therapy on NSCLC A549 cell cycle. Cells were treated with 0.1% (v/v) DMSO as control of the experiment or with 44.4 µM compound B and compound B & Dox at their respective IC_{50} values during different time points (3, 6, 9 h). DNA was stained with propidium iodide, and DNA content was analysed by flow cytometry. The data are represented as means ± SEM of at least two independent experiments.

Exposure of NSCLC A549 cell line to 0.1 % (v/v) DMSO for a period of 3 h evidences the majority of the cells in S-phase (53.5 %) and a small subpopulation under G1/G0 phase (32.2 %) (Table 3.3 and Figure 3.9). This pattern evidenced for the control sample is probably a reminiscent effect of the synchronization at early S-phase with the double thymidine block procedure. The 3 h exposure period for compound B exhibits a similar effect to that evidenced for 0.1 % (v/v) DMSO with 51.5 % cells in S-phase and approximately 38.9 % in G1/G0 phase. Combination therapy employing compound B and doxorubicin on the other hand exhibited the most contrasting results, with a significant proportion of cells under G1/G0 phase reaching 57.5 % of the total number, while S-phase exhibited approximately 32.0 %. Considering doxorubicin's ability to bind to TOPO II and consequently disrupting DNA/RNA synthesis and topoisomerase-II-mediated DNA repair system the last results presented fit to the described mechanism of action. DNA damage induced by doxorubicin could induce p53 activation causing G1 arrest by inducing p21 expression and consequent inhibition of CDKs/Cyclin D complexes (Pucci *et al.*, 2000). Samples that were submitted under 6 h exposure period showed substantial differences compared to the control sample 0.1 % (v/v) DMSO (6 h) (Table 3.3; Figure 3.9). Conversely compound B exposure and compound B plus doxorubicin in combination, evidence similar results, and differences throughout cell cycle phases between each condition do not exceed a 1.38 fold discrepancy. When compared with 0.1 % (v/v) DMSO (6 h), the same conditions show differences in S- and in G2/M phase. While compound B demonstrates a 2.5 fold increase and a 3.3 fold decrease for S- and in G2/M phase respectively, combination therapy manifested a 2.4 fold increase and a 4.6 fold decrease, being these differences initial indications of cell cycle arrest, especially when compared with 3 h exposure samples. The fact that no significant alterations were observed between 3 h and 6 h exposure samples, namely for the samples exposed either to compound B or the combination therapy reinforces the concept of abrogation of cell cycle progression (Figure 3.9). At 9 h exposure period, the proportion of subpopulations throughout the different cell cycle stages also exhibit differences in comparison with 0.1 % (v/v) DMSO (9 h), emphasizing the idea of the continuity of the cell cycle progression for the control samples, while the remaining test samples present a non-linear cell cycle progression with contrasting "anomalies" (Figure 3.9). A more detailed analysis demonstrates that the most significant differences are evidenced for the percentage values between S-phases. In fact compound B and combination therapy display a 2.9 and a 4.3 fold increase respectively when compared with 0.1 % (v/v) DMSO (9 h) (Figure 3.9). Putting in contrast compound B at 6 h and at 9 h exposure a 1.7 fold decrease is evidenced between the S-phase and a 2.0 fold increase for G2/M phase indicating that despite an apparent S-phase delay, the cell cycle continues to advance (Figure 3.9). The same is not the case for compound B and doxorubicin in combination where no significant differences were observed between the 3 and 6 h exposure samples. Indeed the differences presented do not exceed the 1.1 fold discrepancy throughout all the cell cycle phases. This effect shown for the combination therapy suggests that the delay effect demonstrated for compound B

in single agent treatment is actually not only is maintained in combination therapy with doxorubicin as well as it is potentiated, the latter being more evident for 9 h exposure period (Figure 3.9).

Comparing the percentage values of the different cell cycle phases for all control samples (3, 6 and 9 h) it is apparent that the cell populations that were in S- and G2/M phase progressed towards G1/G0, and the ones that were in G1/G0 progressed to S- and G2/M phase (Figure 3.9). The transition between cell cycle phases is not so evident and linear when cell populations' were exposed to either compound B or the combination therapy (Figure 3.9). Overall the results here presented for the different time-points seem to point out for the progression of the cell cycle for the control samples, while cells submitted to either compound B or doxorubicin demonstrated clear signs of cell cycle "drag" and cell cycle arrest, this effect being, especially evident for S-phase.

In view of these results the apparent stalled cell cycle progression during S-phase could indicate the possible molecular targets of compound B and of the combination therapy. Namely the formation of CDK2/cyclin A complex by complexation of both regulators, is a master orchestrator of secondary specific and intricate mechanisms responsible for DNA polymerases, histones and proliferating cell nuclear antigen, inextricably involved in DNA synthesis (Lapenna and Giordano, 2009). Stalled cell cycle progression in S-phase may result from the possible targeting of any of these regulators involved in DNA replication that trigger the intra-S-phase checkpoint responsible for the transition S — G2/M. In fact several chemotherapeutic drugs are known to induce the intra-S-phase checkpoint pathway, consequently blocking S-phase progression (Karnani and Dutta, 2011). Some reports have shown that the intra-S-phase checkpoint is responsible for regulating replication fork progression. In this sense any DNA lesion or hindrances of the molecular machinery responsible for the replication process could induce checkpoint activation and consequently cell cycle delay/arrest (Grallert and Boye, 2008). This checkpoint signaling could eventually result in the activation of apoptotic pathways if the respective cellular damage cannot be repaired (Pietenpol and Stewart, 2002).

In order to understand whether cell cycle arrest occurs and to verify the possibility of an intra-S-phase checkpoint pathway activation, quantitative RealTime-PCR (qRT-PCR) studies on the genes involved in the replication machinery and in intra-S-phase checkpoint would be fundamental. Comparative proteomic studies would also be paramount to understand the intricacy of the regulators involved. Reported proteins involved in intra-S-phase checkpoint that would be critical to understand these results include the CDK2/cyclin A complex and other cellular factors directly phosphorylated by ataxia telangiectasia mutated (ATM), such as BRCA1, E2F-1 and others (Bartek and Lukas, 2001).

3.5. Compound-DNA Interactions

3.5.1. UV-Vis Spectroscopy Analysis

For the large percentage of the chemotherapeutic drugs currently employed, DNA is often the primary intracellular target, and the consequent interactions generally cause broad spectrum damage leading to a myriad of cellular responses that frequently culminate in either cell cycle arrest or in cell death. UV/Vis absorption spectrophotometry was performed in order to draw conclusions on the possible interactions of chlorogold compounds with the DNA molecule, further contributing for the understanding of the molecular mechanisms involved in cell cycle arrest and apoptotic responses. Recurrent interactions between metal complexes and double helix DNA include intercalation, groove binding or external electrostatic binding (Palchaudhuri and Hergenrother, 2007; Shahabadi and Mohammadi, 2012; Satyanarayana *et al.*, 1993). DNA interactions through intercalation or in an electrostatic dependent manner are typically characterized by alterations of the spectral features of DNA regarding its double helix structure. Namely these types of interactions are generally characterized by hypochromism and red shift (bathochromism). Hypochromism corresponds to a decrease in the samples' absorption spectra associated with intercalation, while hyperchromism, an increase in the samples' absorption spectra, is typically ascribed to electrostatic binding or to uncoiling of the DNA double helix (Shahabadi *et al.*, 2011; Cox *et al.*, 2009).

UV/Vis absorption spectrophotometry studies aimed at the analysis of specific parameters such as hyperchromic/hypochromic and bathochromic effects in order to determine the specific modes of interaction between chlorogold compounds and CT-DNA, while simultaneously evaluating the respective intrinsic affinity binding constants (Kb) of each compound, obtained through the shift in absorbance values for the maximum wavelength value (Yousuf *et al.*, 2014). According to the data shown the absorption spectra of the compounds B and D in the presence or absence of CT-DNA displayed in Appendix C, did not reveal a peak of absorbance values for a specific wavelength making it impossible to determine and characterize the type of interaction with the DNA as well as the intrinsic binding affinity constants. The integrity of the chlorogold compounds' structure in solution (5 mM Tris-HCl (Merck), 50 mM NaCl (Panreac), pH 7 buffer) is possibly a key interfering factor in the absorption spectra of each compound. In view of the inability to obtain significant results through UV-Vis spectroscopy these studies were not further investigated. In the future, studies regarding the stability and hydrosolubility of compounds B and D should be emplaced in order to further understand the reason for such results.

3.5.2. DNA cleavage assay

Initial compound-DNA interaction studies based on UV-Vis spectroscopy analysis retrieved no significant results possibly as consequence of weak compound stability in aqueous solution. In an

attempt to obtain further insights on the possibility of chlorogold compounds (B and D) interacting with DNA, supplementary studies were employed. In this regard the ability of chlorogold compounds to bind and cleave the DNA molecule was assessed, through the exposure of plasmid DNA (pDNA) pUC18 to increasing concentrations of the tested compounds for 24 h at 37 ºC and consequently submitting the corresponding products to agarose gel 0.7% (w/v) electrophoresis (Figure 3.10 and Figure 3.11). The rationale behind this DNA cleavage assay is based on the fact that the intact double-stranded plasmid DNA is normally in a compact circular closed formation known as the supercoiled isoform. Under physical aggression supercoiled DNA strands can be cleaved, being the end result distinct whether one, or two strands are damaged. Assuming that the supercoiled DNA sustains only one break in one of the strands the DNA acquires a more relaxed conformation known as open circular DNA or Nicked DNA isoform. The DNA will remain circular however the break allows for rotation along its own central axis, the phosphodiester backbone, hence releasing the supercoils. Following a cleavage event on the complementary strand near the first cleavage site the conformation is reduced to a linear isoform (Palchaudhuri and Hergenrother, 2007; Silva *et al.*, 2011). Accordingly to the conformation acquired by the pDNA molecule, dependent on the interaction with the compounds, different migration rates are observed when these are subjected to agarose gel electrophoresis. A small compact supercoiled DNA isoform experiences considerably less friction against the agarose matrix than compared to an open circular DNA isoform which is translated to a relatively fast migration observed for the supercoiled DNA. Linear isoform one the other hand runs through a gel end first and consequently sustains less friction than the open circular DNA isoform but more than the supercoiled, positioning itself between these two isoforms in the agarose gel matrix (Neves, 2001).

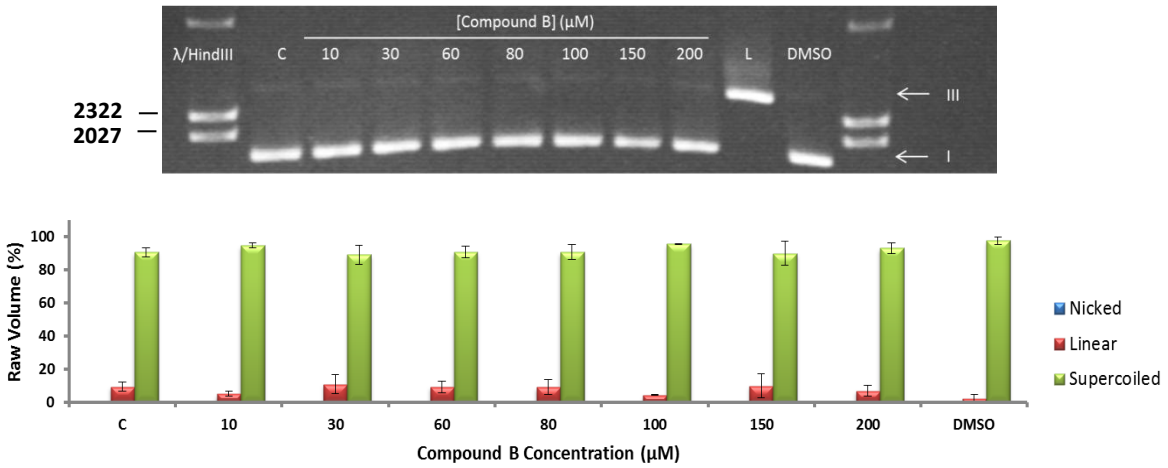

Figure 3.10 – Exposure effect of 200 ng of pUC18 plasmid DNA to either 0.62 % (v/v) DMSO or to increasing concentrations of compound B (0, 10, 30, 60 80, 100, 150, 200 μM). Resulting products of a 24 h exposure period at 37 ºC were submitted to electrophoresis in agarose gel 0.7 % (w/v) (upper panel). λ/HindIII – molecular weight marker; C – control with plasmidic DNA pUC18; DMSO – control with DMSO at 0.62 % (v/v) without compound; L – Linearized pUC18 with EcoRI. I – Supercoiled isoform; II – Nicked isoform (not shown); III – Linear isoform. pUC18 plasmidic DNA isoform distribution, illustrated in the bar chart (lower panel) was obtained through software analysis tool *GelAnalyzer*.

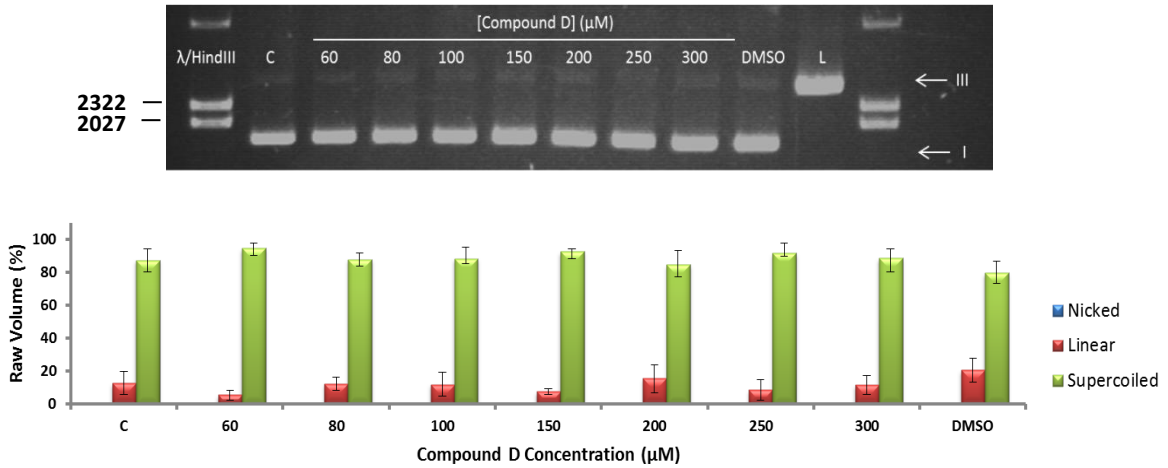

Figure 3.11 – Exposure effect of 200 ng of pUC18 plasmid DNA to either 2.23 % (v/v) DMSO or to increasing concentrations of compound D (0, 60, 80, 100, 150, 200, 250, 300 µM). Resulting products of a 24 h exposure period at 37 ºC were submitted to electrophoresis in agarose gel 0.7 % (w/v) (upper panel). λ/HindIII – molecular weight marker; C – control with plasmidic DNA pUC18; DMSO – control with DMSO at 0.62 % (v/v) without compound; L – Linearized pUC18 with EcoRI. I – Supercoiled isoform; II – Nicked isoform (not shown); III – Linear isoform. pUC18 plasmidic DNA isoform distribution, illustrated in the bar chart (lower panel) was obtained through software analysis tool *GelAnalyzer*.

A closer analysis over compound B (Figure 3.10) and compound D's (Figure 3.11) effect on the conformation of pUC18 plasmid DNA reveals that these compounds do not present the ability to either bind/cleave the DNA molecule or to change its conformation in any form. The absent interaction of chlorogold compounds B and D, with the pDNA molecule is evident throughout increasing concentrations on both cases. In fact a 20 fold concentration increase for compound B (from 10 to 200 µM) and a 5 fold concentration increase for compound D (from 60 to 300 µM) does not increase the extent of pDNA degradation and hence no substantial differences in the proportion of pDNA isoform conformations were observed, with exception for slight variations of the linear isoform, a pattern similar for both compounds. This effect however is unlikely to be the direct result of the chlorogold compounds' ability to induce double strand breaks on pDNA since this pattern is highly inconstant over the increasing concentrations and not significantly different from the control sample values (0.62 and 2.23 % (v/v) DMSO for compound B and D respectively). The possibility of an intact and undamaged form of supercoiled pDNA to give rise to circular or linear isoforms by random cleavage, through either enzymatic or chemical aggression (freeze/thaw cycles), of one or both strands (Li *et al.*, 2011; Iuliano *et al.*, 2002) offers the most reasonably explanation for such results and observed patterns. In short these results demonstrate no interactions between chlorogold compounds and the pDNA molecule for the tested concentrations and hence the molecular mechanism underlying the antiproliferative activity so far revealed by the same compounds are implausible to be related to any, adduct, intercalating or electrostatic type interaction, and can be considered to occur by DNA-independent processes. In fact recent mechanistic studies employing a wide variety of cytotoxic gold

compounds, have similarly demonstrated their ability to induce broad apoptosis, however manifesting considerably lower affinity for DNA when compared with blockbuster platinum(II) compounds, thus suggesting a DNA-independent mechanism of action (Bindoli *et al.*, 2009). In similarity to other cytotoxic gold compounds the results here obtain for compound B and D push towards the hypothesis of the existence of preferential protein targets for such compounds. Key protein targets such as TrxR involved in the redox potential homeostasis, or the proteasome system involved in protein and organelle turnover, have been the most consensual targets listed in the literature (Bindoli *et al.*, 2009; Lima and Rodriguez, 2011). Enzymatic assays employing such targets should be considered paramount for the understanding of the molecular mechanisms that govern the cytotoxicity of these chlorogold compounds.

3.6. Proteome Evaluation: Comparative Proteomics

Proteome evaluation through the use of 2-DE gel electrophoresis was established as a mean to construct a broader scale comparative proteome profile between NSCLC cell lines (A549 and H1975) when subjected to chlorogold compound exposure in order to better understand the molecular mechanisms underlying the biological activity of these coordination compounds while identifying the major affected biochemical pathways. Due to time limitation factors and methodology-related hindrances such as the difficulty in obtaining sufficient amounts of biological material to perform the analysis, comparative proteome profiling was performed only between A549 and HCT-116 cell line under the exposure of 0.1% (v/v) DMSO for a period of 48 h. The rationale behind the use of HCT-116 cell line in this study stems from the fact that the majority of the identified proteins in our research group were performed in this cell line, and as such it was used as a support platform for facilitating protein identification in NSCLC A549 cell line.

The two dimensional gel electrophoresis of the whole protein extract from the two cell lines were performed twice and the representative protein patterns of HCT-116 and A549 cell lines are illustrated in Figure 3.12. Protein quantitative analysis was performed by the normalization of the volume percentage of each spot, relatively to the total spots per sample. The Melanie 7.0 program allowed to detect approximately a total of 482 and 417 protein spots in HCT-116 and A549 respectively. Furthermore image analysis identified a total of 405 spots shared between the two cell lines out of which 25.17 % are found to be less abundant in A549 and 30.46 % more abundant relatively to HCT-116 cell line. The total number of proteins that were possible to be identified by previous characterized gels and that exhibited significant differences in abundance are depicted in Table 3.4.

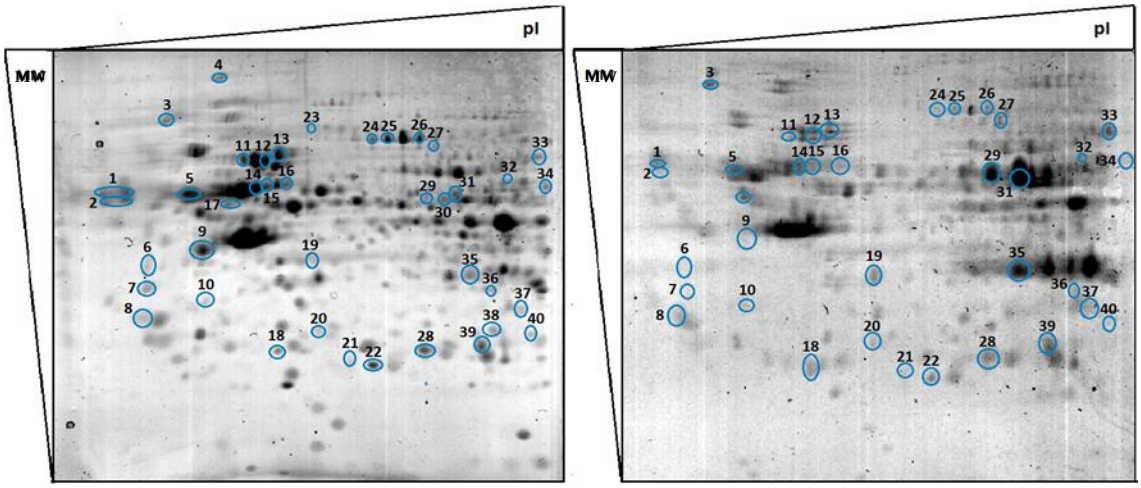

Figure 3.12 – Comparative proteome profiling of HCT-116 (left) and A549 (right) cell lines when subjected to 0.1 % (v/v) DMSO for an exposure period of 48 h. 2-DE gels were obtained from at least 200 µg of whole protein extract and resulting spots were stained with Comassie Blue. Spots whose abundance variance levels were considered significantly altered were marked and number tagged.

Table 3.4 – Proteome evaluation: Total number of proteins identified in 2-D gel electrophoresis, with the indication of the spot ID referent to figure 3.7, UniProt ID, protein identification, isoelectric point, molecular weight, function and abundance variance levels between HCT-116 and A549 cell lines. Proteins whose abundance variance levels were considered significantly altered were highlighted. Values under 0.7 (red) and above 1.5 fold (green) were taken into account.

Spot ID	UniProt ID	Protein Identification	pI	MW (KDa)	Fold Change	Protein Function
1	CALR_HUMAN	*Calreticulin*	4.29	48.11	**0.58**	Chaperone/Stress response
2	CALR_HUMAN	*Calreticulin*	4.29	48.11	**0.14**	Chaperone/Stress response
3	TCPQ_HUMAN	*T-complex protein 1 subunit theta*	5.42	59.58	**2.08**	Cytoskeleton mobility
4	HS90B_HUMAN	*Heat shock protein HSP 90-beta*	4.97	83.21	-	Chaperone/Stress response
5	P4HB_HUMAN	*Protein disulfide-isomerase*	7.17	36.69	**0.52**	Protein binding/Folding
6	ENOA_HUMAN	*Alpha-enolase*	7.01	47.13	**1.94**	Metabolism
7	RANG_HUMAN	*Ran-specific GTPase-activating protein*	5.19	23.29	**2.04**	Signal transduction
8	1433Z_HUMAN	*14-3-3 protein zeta/delta*	4.73	27.73	**2.25**	Signal transduction
9	DHE3_HUMAN	*Glutamate dehydrogenase 1, mitochondrial*	7.66	61.36	**0.66**	Component turnover/Detox
10	PHB_HUMAN	*Prohibitin*	5.57	29.79	**1.82**	Protein binding/Folding
11	HSP7C_HUMAN	*Heat shock cognate 71 kDa protein*	5.37	70.85	**0.32**	Chaperone/Stress response
12	HS90B_HUMAN	*Heat shock protein HSP 90-beta*	4.97	83.21	**0.54**	Chaperone/Stress response
13	GRP75_HUMAN	*Stress-70 protein, mitochondrial*	5.87	73.63	**0.63**	Chaperone/Stress response
14	CH60_HUMAN	*60 kDa heat shock protein, mitochondrial*	5.08	45.44	**0.39**	Protein binding/Folding
15	HSP71_HUMAN	*Heat shock 70 kDa protein 1A/1B*	5.48	70.01	**0.65**	Chaperone/Stress response

16	HSP71_HUMAN	*Heat shock 70 kDa protein 1A/1B*	5.48	70.01	**0.59**	Chaperone/Stress response
17	ATP5B_HUMAN	*ATP synthase subunit beta, mitochondrial*	5.57	40.20	-	Metabolism
18	PRDX2_HUMAN	*Peroxiredoxin-2*	6.27	49.77	**9.69**	Signal transduction
19	RSSA_HUMAN	*40S ribosomal protein SA*	4.79	32.83	**0.57**	Other
20	GDIR1_HUMAN	*Heat shock protein beta-1*	5.84	45.95	**1.86**	Chaperone/Stress response
21	SODC_HUMAN	*Superoxide dismutase [Cu-Zn]*	5.70	15.93	**2.16**	Component turnover/Detox
22	TPIS_HUMAN	*Triosephosphate isomerase*	5.65	30.77	**1.59**	Metabolism
23	EZRI_HUMAN	*Ezrin*	5.94	69.37	-	Cytoskeleton mobility
24	HSP71_HUMAN	*Heat shock 70 kDa protein 1A/1B*	5.48	70.01	**0.28**	Chaperone/Stress response
25	ENPL_HUMAN	*Endoplasmin*	4.76	92.41	**0.54**	Chaperone/Stress response
26	EZRI_HUMAN	*Ezrin*	5.94	69.37	**0.58**	Cytoskeleton mobility
27	XRCC6_HUMAN	*X-ray repair cross-complementing protein 6*	6.23	69.79	**1.73**	Other
28	RBBP7_HUMAN	*Histone-binding protein RBBP7*	4.89	47.82	**1.52**	Signal transduction
29	PA2G4_HUMAN	*Proliferation-associated protein 2G4*	6.13	43.76	**9.81**	Signal transduction
30	IF4A2_ HUMAN	*Eukaryotic initiation factor 4A-II*	6.74	95.30	-	Other
31	PA2G4_HUMAN	*Proliferation-associated protein 2G4*	6.13	43.76	**5.70**	Signal transduction
32	TCPB_HUMAN	*T-complex protein 1 subunit beta*	6.01	57.45	**1.80**	Protein binding/Folding
33	ENOA_HUMAN	*Alpha-enolase*	7.01	47.14	**2.28**	Metabolism
34	EZRI_HUMAN	*Ezrin*	5.94	69.37	**0.52**	Cytoskeleton mobility
35	SGTA_HUMAN	*Small glutamine-rich tetratricopeptide repeat-containing protein alpha*	4.81	44.08	**4.04**	Chaperone/Stress response
36	ANXA2_ HUMAN	*Annexin A2*	6.79	98.92	**1.78**	Chaperone/Stress response
37	P5CR1_HUMAN	*Pyrroline-5-carboxylate reductase 1, mitochondrial*	7.18	33.34	**1.54**	Chaperone/Stress response
38	ECH1_HUMAN	*Delta (3,5) -Delta(2,4)-dienoyl-CoA isomerase, mitochondrial*	8.16	35.80	-	Metabolism
39	PRDX6_HUMAN	*Peroxiredoxin-6*	6.00	25.02	-	Component turnover/Detox
40	1433Z_HUMAN	*14-3-3 Protein zeta/delta*	4.73	27.73	**1.87**	Signal transduction
Spot ID	UniProt ID	Protein Identification	pI	MW (KDa)	Fold Change	Protein Function
1	CALR_HUMAN	*Calreticulin*	4.29	48.11	**0.58**	Chaperone/Stress response
2	CALR_HUMAN	*Calreticulin*	4.29	48.11	**0.14**	Chaperone/Stress response
3	TCPQ_HUMAN	*T-complex protein 1 subunit theta*	5.42	59.58	**2.08**	Cytoskeleton mobility
4	HS90B_HUMAN	*Heat shock protein HSP 90-beta*	4.97	83.21	-	Chaperone/Stress response
5	P4HB_HUMAN	*Protein disulfide-isomerase*	7.17	36.69	**0.52**	Protein binding/Folding

6	ENOA_HUMAN	*Alpha-enolase*	7.01	47.13	**1.94**	Metabolism
7	RANG_HUMAN	*Ran-specific GTPase-activating protein*	5.19	23.29	**2.04**	Signal transduction
8	1433Z_HUMAN	*14-3-3 protein zeta/delta*	4.73	27.73	**2.25**	Signal transduction
9	DHE3_HUMAN	*Glutamate dehydrogenase 1, mitochondrial*	7.66	61.36	**0.66**	Component turnover/Detox
10	PHB_HUMAN	*Prohibitin*	5.57	29.79	**1.82**	Protein binding/Folding
11	HSP7C_HUMAN	*Heat shock cognate 71 kDa protein*	5.37	70.85	**0.32**	Chaperone/Stress response
12	HS90B_HUMAN	*Heat shock protein HSP 90-beta*	4.97	83.21	**0.54**	Chaperone/Stress response
13	GRP75_HUMAN	*Stress-70 protein, mitochondrial*	5.87	73.63	**0.63**	Chaperone/Stress response
14	CH60_HUMAN	*60 kDa heat shock protein, mitochondrial*	5.08	45.44	**0.39**	Protein binding/Folding
15	HSP71_HUMAN	*Heat shock 70 kDa protein 1A/1B*	5.48	70.01	**0.65**	Chaperone/Stress response
16	HSP71_HUMAN	*Heat shock 70 kDa protein 1A/1B*	5.48	70.01	**0.59**	Chaperone/Stress response
17	ATP5B_HUMAN	*ATP synthase subunit beta, mitochondrial*	5.57	40.20	-	Metabolism
18	PRDX2_HUMAN	*Peroxiredoxin-2*	6.27	49.77	**9.69**	Signal transduction
19	RSSA_HUMAN	*40S ribosomal protein SA*	4.79	32.83	**0.57**	Other
20	GDIR1_HUMAN	*Heat shock protein beta-1*	5.84	45.95	**1.86**	Chaperone/Stress response
21	SODC_HUMAN	*Superoxide dismutase [Cu-Zn]*	5.70	15.93	**2.16**	Component turnover/Detox
22	TPIS_HUMAN	*Triosephosphate isomerase*	5.65	30.77	**1.59**	Metabolism
23	EZRI_HUMAN	*Ezrin*	5.94	69.37	-	Cytoskeleton mobility
24	HSP71_HUMAN	*Heat shock 70 kDa protein 1A/1B*	5.48	70.01	**0.28**	Chaperone/Stress response
25	ENPL_HUMAN	*Endoplasmin*	4.76	92.41	**0.54**	Chaperone/Stress response
26	EZRI_HUMAN	*Ezrin*	5.94	69.37	**0.58**	Cytoskeleton mobility
27	XRCC6_HUMAN	*X-ray repair cross-complementing protein 6*	6.23	69.79	**1.73**	Other
28	RBBP7_HUMAN	*Histone-binding protein RBBP7*	4.89	47.82	**1.52**	Signal transduction
29	PA2G4_HUMAN	*Proliferation-associated protein 2G4*	6.13	43.76	**9.81**	Signal transduction
30	IF4A2_ HUMAN	*Eukaryotic initiation factor 4A-II*	6.74	95.30	-	Other
31	PA2G4_HUMAN	*Proliferation-associated protein 2G4*	6.13	43.76	**5.70**	Signal transduction
32	TCPB_HUMAN	*T-complex protein 1 subunit beta*	6.01	57.45	**1.80**	Protein binding/Folding
33	ENOA_HUMAN	*Alpha-enolase*	7.01	47.14	**2.28**	Metabolism
34	EZRI_HUMAN	*Ezrin*	5.94	69.37	**0.52**	Cytoskeleton mobility
35	SGTA_HUMAN	*Small glutamine-rich tetratricopeptide repeat-containing protein alpha*	4.81	44.08	**4.04**	Chaperone/Stress response
36	ANXA2_ HUMAN	*Annexin A2*	6.79	98.92	**1.78**	Chaperone/Stress response
37	P5CR1_HUMAN	*Pyrroline-5-carboxylate reductase 1,*	7.18	33.34	**1.54**	Chaperone/Stress response

		mitochondrial				
38	ECH1_HUMAN	*Delta (3,5) -Delta(2,4)-dienoyl-CoA isomerase, mitochondrial*	8.16	35.80	-	Metabolism
39	PRDX6_HUMAN	*Peroxiredoxin-6*	6.00	25.02	-	Component turnover/Detox
40	1433Z_HUMAN	*14-3-3 Protein zeta/delta*	4.73	27.73	**1.87**	Signal transduction

Moreover through bioinformatics analysis and database mining, the identified proteins were classified based on their function into various categories, namely chaperone/stress response, metabolism cytoskeleton mobility, protein turnover/detoxification, signal transduction and other as shown in Figure 3.13. The classification of the respective proteins into specific categories was mainly done by recurring to databases such STRING 9.1. The majority of the proteins with substantial abundance differences were considered involved in chaperone/stress response mechanisms (35 %) followed by

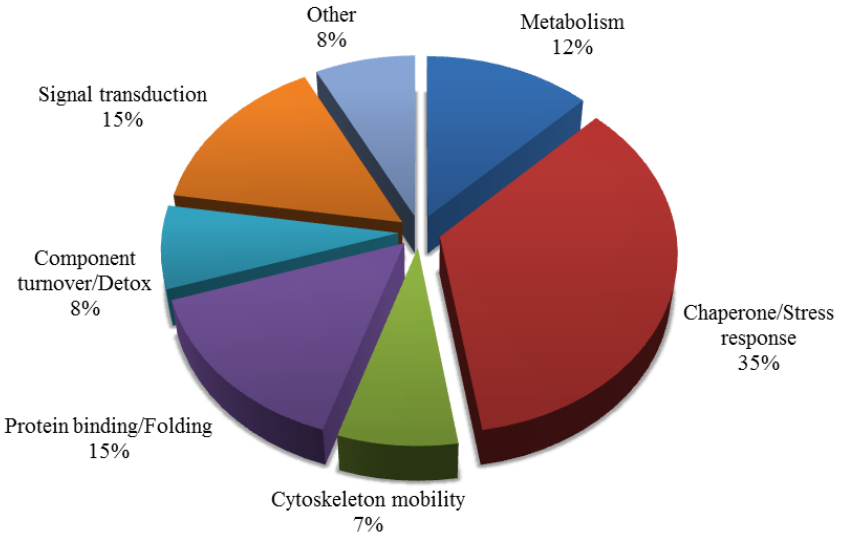

protein binding/folding (15 %), signal transduction (15 %) and metabolism (12 %) (Figure 3.13).

Figure 3.13 – Categorization of the proteome profiling of HCT-116 and A549 into functional categories such as, chaperone/stress response, metabolism cytoskeleton mobility, protein turnover/detoxification, signal transduction and other. Protein functional properties were based on STRING 9.1 database. The data is referent to table 3.4.

Analysis of Table 3.4 reveals a total of fifteen proteins with abundance variance levels 1.5 fold higher and nineteen proteins with abundance variance levels 0.7 fold lower in A549. Given the extensive number of proteins with substantial differences in abundance levels only a few will be addressed here and special attention will be given to overexpressed proteins. For instance prohibitin (spot nº10), has been found to be 1.82 fold higher in A549 compared with HCT-116 cell line. This protein has been correlated with an active role in regulation of cell proliferation but perhaps more importantly to play an important part as a regulator of mitochondrial respiration activity and aging. More specifically in a

recent study it was evidenced that TNFα and interferon gamma (IFNγ) induced autophagy, was inversely correlated with prohibitin protein expression levels. Moreover abrogation of prohibitin expression levels through gene silencing methods, in epithelial cells lead to ROS mediated-mitochondrial autophagy (Kathiria *et al.*, 2012). Translation of this striking correlation between prohibitin and abrogation of mitochondrial autophagy, indicates that the higher fold expression level evidenced for A549 cell line renders it less susceptible to mitochondrial damage and cytotoxicity. These data is in concordance with early assessed IC_{50} values for both cell lines when exposed to chlorogold compounds B and D, where HCT-116 is substantially more impaired than A549 cell line. Targeting such protein could in theory promote an increase in mitochondrial autophagy and hence reduce the intrinsic resistant nature of NSCLC A549 cell line. As such further investigation on prohibitin protein as a potential biomarker and therapeutic target for NSCLC would prove to be fundamental and paramount for opening new avenues in cancer therapeutics.

With an active role in the redox regulation of the cell, peroxiredoxin 2 (protein spot nº 18) was strikingly found to be 9.69 times more abundant in A549 when in comparison with HCT-116. Apart from redox regulation they have been known to be involved in the process of elimination of peroxides generated during metabolism and perhaps more importantly in signaling transduction pathways such as of growth factors and TNFα cascades, by regulating the intracellular concentrations of H_2O_2 (Kim *et al.*, 2007). Other literature reports revealed that peroxiredoxin 2 is present both in cytoplasm and nucleus of cancer cells where it takes part in a protective role against chemotherapeutic agents (Ishii *et al.*, 2012). Peroxiredoxin 2 in the nucleus demonstrated to induce or to facilitate the activation of the JNK/c-Jun pathway involved in repair of damaged DNA (Lee *et al.*, 2011). Moreover peroxiredoxin 2 ability to enhance the aggressive survival phenotype of cancer cells was corroborated by the induction of increased cell death and sensitivity to chemotherapeutic agents after recurring to gene silencing by siRNA (Ishii *et al.*, 2012; Lee *et al.*, 2011). This information is in line with the findings here evidenced and with previous hypothesis also validated by our group, indicating that NSCLC A549 cell line is considerably less susceptible to chemotherapeutic treatments.

Superoxide dismutase [Cu-Zn] (protein spot nº 21) a conserved antioxidant protein responsible for the elimination of superoxide radical, resultant from the metabolism plays a protective role against ROS (Silva *et al.*, 2013). Indeed the abundance levels in A549 were found to be 2.16 times higher when compared to HCT-116. Studies have related the overexpression of superoxide dismutase 1 activity in lung cancer cells with an increased growth proliferation rate however without a relationship with cell cycle disturbances. Furthermore it was found to related to lower frequencies of programed cell death by apoptosis suggesting that the promotion of increased growth proliferation rates are linked to an increased survival (Somwar *et al.*, 2011). It is assumed that in view of this data that A549 cell line is

considerably less prone to damage induction by ROS, and consequently less susceptible to forms of programed cell death such as apoptosis.

Protein spot number 29 associated with the proliferation-associated protein 2G4 reportedly plays a role in ErbB3-regulated signal transduction pathway of growth regulatory signals. Reaching an abundance variance of 9.81 fold higher compared to HCT-116, its effect may be intimately connected in growth regulation and the promotion of oncogenic functions (Kim *et al.*, 2012). Recent studies on a long isoform of the ErbB3 binding protein, when overexpressed evidenced the capacity to induce differentiation processes involved in malignant transformation (Kim *et al.*, 2012). This fact might help explain the aggressive nature of p53 positive NSCLC cell lines such as A549.

Furthermore α-enolase (protein spot nº 33) expression levels are also substantially different (2.28 fold increase). Considered to be a multifunctional enzyme, playing diverse roles such as growth control, hypoxia tolerance and allergic responses, it is although more renowned for its part as metabolic enzyme involved in glycolysis and in the consequent synthesis of pyruvate (Chang *et al.*, 2006; Capello *et al.*, 2011). The overexpression profile of this protein in A549 it is not itself a surprising evidence as the re-modulation of energy metabolism is typically considered a transition hallmark from normal cells to tumour cells, where glycolysis develops into the main metabolic pathway to sustain and support the synthesis of nucleotides, fatty acids, amino acids and other macromolecules for the accelerated mitosis (Warburg effect) (Marie and Shinjo, 2011). However recent studies have correlated the expression status of α-enolase with different clinical outcomes regarding tumour malignancy, survival and tumour recurrence in NSCLC. Moreover the substantial difference observed in A549 in comparison with HCT-116 offers new possibilities for prognostic strategies and new targeted therapy for NSCLC (Chang *et al.*, 2006)

Small glutamine-rich tetratricopeptide repeat-containing protein alpha (SGTA) (Protein spot number 35) was similarly found to be overexpressed by 4.04 fold in comparison with HCT-116. Interestingly these results seem to be in accordance with recent literature data, reporting high expression values in NSCLC (Xue *et al.*, 2013). Furthermore overexpression of this protein has shown to be significantly correlated with critical processes involved in tumour growth and differentiation. Suppression of SGTA expression dramatically influenced the proliferation rate of A549 cell line and cell cycle progression. In fact cell cycle analysis transiently suppressed by siRNA revealed an accumulation of cells in the G0/G1 phase and helped to correlate the expression of cell cycle proteins such as cyclin A and cyclin D1 with the expression of SGTA (Xue *et al.*, 2013).

All in all comparative proteomic studies were initially ought to be performed for A549 cell line when subjected to chlorogold compounds' exposure in order to compare proteome profiles of cell samples with and without chemotherapeutic stress, thus helping to trace the molecular mechanisms involved in

the cytotoxic activity of such coordination compounds. As mentioned above, methodology-related hindrances did not allow the successful realization of the initially established goals. However A549 and HCT-116 cancer cell line comparison by two-dimensional gel electrophoresis allowed to point out significant differences between these distinct cancer cell lines, opening new possibilities in targeted therapies and in the identification of new potential biomarkers for prediction of prognosis in NSCLC. Being the leading cause of cancer related death worldwide (Gridelli *et al.*, 2007), the importance of these and other similar studies could have not been more stressed. The findings here presented and discussed for prohibitin, peroxiredoxin 2, superoxide dismutase [Cu-Zn], proliferation-associated protein 2G4 and for SGTA may have potentially new applications in the field of oncology.

3.7. Morphological Characterization of Human Colorectal and Lung Adenocarcinoma Cell Lines with Multidrug Resistance

Accordingly with the secondary objective established in this work it was expected to set up the foundations for a study platform for multidrug resistance, in order to decipher the underlying mechanism that orchestrate it, and to understand the implications of newly established combination chemotherapies as means to overcome drug resistance.

By long term exposure of HCT-116 and A549 cell lines to doxorubicin, it was established a series of subcultures that were considered to be at the initial stages of acquired multidrug resistance. HCT-116 cell line exposure to a step wise increase in doxorubicin concentration that ranged from 0.001 μg/mL to 0.5 μg/mL, and from 0.0058 μg/mL to 0.029 μg/mL for A549 cell line, induced the acquisition of morphological features that accordingly to literature reports are consistent with early signs of multidrug resistance. In fact compared with parent cells, resistant cell lines A549/R were in general smaller at low confluence mixed with considerably large cells in different sizes (results not shown) which is in accordance with similar studies (Wang *et al.*, 2006). HCT-116/R cells on the other hand were substantially smaller and presented a higher tendency to grow in organized cell clusters (results not shown).

As a result of the unfinished process of multidrug resistance induction, (only a total of 15 out of 30 subcultures were carried out under the presence of doxorubicin) parameters such as the chemoresistance indexes were not evaluated. Future studies in view include the assessment of such chemoresistance indexes as well as the performance of genomic and post-genomic analysis regarding the amplification of the human *MDRI* expression, and/or the relative increase in the amount of membrane P-glycoproteins or their activity.

4. Conclusions and Future Perspectives

The interdisciplinary and constantly evolving nature of chemotherapeutics consistently offers new and ingenious possibilities for targeting cancer, however pre-clinical, clinical research and eventually clinical translation often poses as a great challenge for the validation and integration of such "possibilities". The conceptualized hierarchical system of *in vitro* studies as an integrating part of the pre-clinical and clinical research is paramount for the biological evaluation of new anticancer agents and strategies. In this work biological evaluation of newly synthesized chlorogold complexes through a selected set of *in vitro* studies followed the same logic, in order to understand and describe whether or not the compounds were effective against cancer cells while simultaneously unraveling related mechanisms of action.

The antiproliferative evaluation of chlorogold complexes bearing phosphine or N,O-donor ligands, was carried out across a panel of tumoural and non-tumoural cell lines available. The most active compounds Chloro(trimethylphosphine)gold(I) (compound B) and Chloro(triphenylphosphine)gold(I) (compound D) displayed the ability to inhibit cell proliferation in a dose-dependent manner across the panel of tumoural cell lines. A549 cell line exposure to compound B and compound D displayed an IC_{50} value of 44.4 and 30.0 μM, plus 3.3 and 5.4 μM in H1975 cell line respectively suggesting that chlorogold compounds confer antiproliferative properties *in vitro* for both tumoural cell lines. Nonetheless it is worth noting that for these cell lines both compounds revealed to less active than clinically employed renowned agents such as doxorubicin or cisplatin. Cytotoxicological analysis of compound B and D, further performed in normal human dermal fibroblast revealed IC_{50} values of 7.74 and 19.10 μM respectively translating into a 5.7 and a 1.6 fold higher toxicological effect for healthy cell lines when compared with tumoural cell line A549. Such analysis would suggest that these chlorogold compounds present some significant setbacks when considering systemic toxicity; hence a hypothetical translation into clinical setting would have to take into consideration strategies to circumvent such hindrances. Targeted therapies, such as nanocarriers as drug delivery platforms show great potential for overcoming these toxicity related issues, and the viability of their employment should be assessed in future studies.

Combination chemotherapy studies were performed upon an effort to target cancer's typical hallmarks with particular focus on resistance to chemotherapeutics in order to improve patient's outcomes. It was tested different combination therapies in three distinct sequences defined in section 2.5.1. Particularly cell viability assay in NSCLC A549 cell line, in response to the combination of compound B and doxorubicin, erlotinib and compound B, or erlotinib and doxorubicin were assessed as potential tools for combination chemotherapy. In summary the investigated combination therapies revealed variable degrees of antiproliferative potential. More specifically pretreatment with doxorubicin for 24 h with

posterior administration of compound B for another 24 h revealed to be the most effective combination while pretreatment with erlotinib for 24 h with posterior administration of compound B elicited the weakest antiproliferative effect. To gain further insights on the quantitative evaluation of the compounds combinations future studies based on the median effect analysis developed by Chou and Talalayi should be employed.

After selection of compound B and D as the most active compounds from the initial screen, further *in vitro* analysis based on a number of properties associated with the mechanisms of action were determined. The apoptotic potential, evaluated by Hoechst 33258 for A549 and H1975 cell lines revealed the ability of the compounds to induce chromatin condensation as well as nuclear fragmentation on both cell lines, being indicative of apoptotic cell death. A549 cell line double staining with PI and Annexin V-FITC after exposure to 44.4 and 66.6 μM of compound B evidenced that chlorogold compounds are able to induce cell death by apoptosis in a dose-dependent fashion and potentially through a fast acting mechanism. Administration of 9.20 and 13.8 μM of doxorubicin in turn revealed an abrupt decrease in cell viability as well with a parallel increase in the bulk of apoptotic and necrotic cells. Combination chemotherapy employing both compounds was accompanied by the observation of a hybrid therapeutic effect possibly characterized by the merging of the different mechanisms of action of both compounds.

A549 cell line exposure to compound B and the combination therapy with compound B plus doxorubicin throughout different time points evidenced demonstrated clear signs of cell cycle "drag" and cell cycle arrest, this effect being, especially evident for S-phase. Moreover the assessment of the compounds' ability to interfere with cell cycle main regulators and in intra-S-phase, such as Cyclin E/ CDK2 and Cyclin A/ CDK2 through RT-PCR could eventually prove to be paramount to obtain further insights into the mechanism of action of the complexes, more specifically regarding the process by which the cell cycle is impaired. Plus other cellular factors directly phosphorylated by ataxia telangiectasia mutated (ATM), such as BRCA1, E2F-1 could provide more insights on the subject.

The attempts to obtain tangible and reproducible absorption spectroscopic data were proven unsuccessful and information regarding the type of interaction with the DNA as well as the intrinsic binding affinity constants was "unachievable". The integrity of the chlorogold compounds' structure in solution is possibly a key interfering factor in the absorption spectra of each compound and hence additional avenues must be explored as means to obtain these data. DNA cleavage assays on the other hand indicated that compound interaction with the DNA molecule was proven to be either weak or inexistent, revealed by the compounds' inability to compromise plasmid DNA conformation.

Proteomic studies envisaged a further investigation into the mode of action of the chlorogold compounds with a particular interest to identify target proteins involved stress response, multidrug resistance, apoptosis, cellular signaling as well as cell cycle regulation and overall cellular homeostasis. Time limitation factors and methodology-related hindrances such as the difficulty in obtaining sufficient amounts of biological material to perform the analysis were at core of the impotence to obtain enough data regarding the molecular mechanisms and the target through which chlorogold compounds develop their cytotoxic activity. Despite not conclusive regarding chlorogold compounds' mechanism of action, the few data gathered allowed for the identification of potential important biomarkers for prediction of prognosis in non-small-cell lung carcinoma. Proteins such as prohibitin, peroxiredoxin 2, superoxide dismutase [Cu-Zn], proliferation-associated protein 2G4 and for SGTA may open new avenues and lay the ground work for potentially new applications in the field of oncology. In the future to fully understand the molecular targets of the chlorogold compounds it is imperative to trace the proteome profiles in A549 and H1975 cell lines.

Also given the extensive literature on the ability of gold compounds to interact with TrxR it would be interesting to assess the compounds' ability to promote enzyme inhibition plus the ability to induce ROS by a glutathione s-transferase assay.

Overall the unique cellular and biochemical aspects of each tumor, such as their heterogeneity and continuously evolving nature continue to hinder the success of currently established therapies and the emergence of new strategies. Well-established *in vitro* studies as those here employed are increasingly more important as demands for a better quality of treatment for one the epidemics of the twenty-first century become progressively stricter. Parallel to the development of novel more effective drugs and to meet up with demands new drug delivery systems based on nanoscale devices showing new and improved pharmacokinetic and pharmacodynamics properties like enhanced bioavailability, high drug loading or systemic stability have surged in the past decade as promising solutions to the required therapeutic efficacy. Merging chlorogold compounds with the toolbox of nanotechnology and nanoscale drug delivery devices offers a virtually endless number of possibilities to target cancer and should be conceptualized for future work.

5. References

Ahmadi, S.M. 2011. *In Vitro* Studies on Calf Thymus DNA interaction with Quercetin-Palladium (II) Complex. *In* International Conference on Bioscience, Biochemistry and Bioinformatics. pp. 110–113.

Alarcon-Vargas, D., Ronai, Z. 2002. p53-Mdm2--the affair that never ends. Carcinogenesis 23: 541–547.

Alley, S.C., Okeley, N.M., Senter, P.D. 2010. Antibody-drug conjugates: targeted drug delivery for cancer. Current opinion in chemical biology 14: 529–537.

Al-Rubeai, M., Singh, R.P. 1998. Apoptosis in cell culture. Current Opinion in Biotechnology 9: 152–156.

Anand, P., Kunnumakkara, A.B., Kunnumakara, A.B., Sundaram, C., Harikumar, K.B., Tharakan, S.T., Lai, O.S., Sung, B., Aggarwal, B.B. 2008. Cancer is a preventable disease that requires major lifestyle changes. Pharmaceutical research 25: 2097–2116.

Ashkenazi, R., Gentry, S.N., Jackson, T.L. 2008. Pathways to Tumorigenesis — Modeling Mutation Acquisition in Stem Cells and Their Progeny 10: 1170–1182.

ATCC: The Global Bioresource Center. 2014. http://www.lgcstandards-atcc.org/?geo_country=pt (accessed 8.29.14).

Baan, R., Grosse, Y., Straif, K., Secretan, B., El Ghissassi, F., Bouvard, V., Benbrahim-Tallaa, L., Guha, N., Freeman, C., Galichet, L., Cogliano, V. 2009. A review of human carcinogens—Part F: Chemical agents and related occupations. The Lancet Oncology 10: 1143–1144.

Baba, A.I., Câtoi, C. 2007. Principles of anticancer therapy. The Publishing House of the Romanian Academy.

Baptista, P. V 2009. Cancer Nanotechnology - Prospects for Cancer Diagnostics and Therapy. Current Cancer Therapy Reviews 5: 80.

Bartek, J., Lukas, J. 2001. Mammalian G1- and S-phase checkpoints in response to DNA damage. Current Opinion in Cell Biology 13: 738–747.

Bergers, G., Benjamin, L.E. 2003. Tumorigenesis and the angiogenic switch. Nature reviews. Cancer 3: 401–410.

Berman, B.P., Weisenberger, D.J., Aman, J.F., Hinoue, T., Ramjan, Z., Liu, Y., Noushmehr, H., Lange, C.P.E., van Dijk, C.M., Tollenaar, R. a E.M., Van Den Berg, D., Laird, P.W. 2012. Regions of focal DNA hypermethylation and long-range hypomethylation in colorectal cancer coincide with nuclear lamina-associated domains. Nature genetics 44: 40–46.

Berners-Price, S.J., Filipovska, A. 2011. Gold compounds as therapeutic agents for human diseases. Metallomics : integrated biometal science 3: 863–873.

Bertram, J.S. 2001. The molecular biology of cancer. Molecular aspects of medicine 21: 167–223.

Besaratinia, A., Tommasi, S. 2013. Genotoxicity of tobacco smoke-derived aromatic amines and bladder cancer: current state of knowledge and future research directions. FASEB journal :

official publication of the Federation of American Societies for Experimental Biology 27: 2090–100.

Bindoli, A., Rigobello, M.P., Scutari, G., Gabbiani, C., Casini, A., Messori, L. 2009. Thioredoxin reductase: A target for gold compounds acting as potential anticancer drugs. Coordination Chemistry Reviews 253: 1692–1707.

Bonomi, P. 2003. Erlotinib: a new therapeutic approach for non-small cell lung cancer. Expert opinion on investigational drugs 12: 1395–401.

Bouvard, V., Baan, R., Straif, K., Grosse, Y., Secretan, B., Ghissassi, F. El, Benbrahim-Tallaa, L., Guha, N., Freeman, C., Galichet, L., Cogliano, V. 2009. A review of human carcinogens—Part B: biological agents. The Lancet Oncology 10: 321–322.

Brechbuhl, H., Kachadourian, R., Min, E., Chan, D., Day, B. 2013. Chrysin enhances doxorubicin-induced cytotoxicity in human lung epithelial cancer cell lines: the role of glutathione. Toxicol Appl Pharmacol. 258: 1–9.

Brooks, S. a, Lomax-Browne, H.J., Carter, T.M., Kinch, C.E., Hall, D.M.S. 2010. Molecular interactions in cancer cell metastasis. Acta histochemica 112: 3–25.

Brumatti, G., Sheridan, C., Martin, S.J. 2008. Expression and purification of recombinant annexin V for the detection of membrane alterations on apoptotic cells. Methods (San Diego, Calif.) 44: 235–240.

Cancer of the Lung and Bronchus - SEER Stat Fact Sheets. 2010. URL http://seer.cancer.gov/statfacts/html/lungb.html (accessed 8.6.14).

Capello, M., Ferri-Borgogno, S., Cappello, P., Novelli, F. 2011. α-Enolase: a promising therapeutic and diagnostic tumor target. The FEBS journal 278: 1064–1074.

Chabner, B.A., Jr, T.G.R. 2005. Chemotherapy and the war on cancer. Nature Reviews 5: 65–72

Chang, G.-C., Liu, K.-J., Hsieh, C.-L., Hu, T.-S., Charoenfuprasert, S., Liu, H.-K., Luh, K.-T., Hsu, L.-H., Wu, C.-W., Ting, C.-C., Chen, C.-Y., Chen, K.-C., Yang, T.-Y., Chou, T.-Y., Wang, W.-H., Whang-Peng, J., Shih, N.-Y. 2006. Identification of alpha-enolase as an autoantigen in lung cancer: its overexpression is associated with clinical outcomes. Clinical cancer research : an official journal of the American Association for Cancer Research 12: 5746–5754.

Chipuk, J.E., Green, D.R. 2006. Dissecting p53-dependent apoptosis. Cell death and differentiation 13: 994–1002.

Chou, T., Talalayi, P. 1984. Quantitative analysis of dose-effect relationships: The combined effects of multiple drugs or enzime inhibitors. Adv Enzyme Regul 22: 27–5.

Combination Chemotherapy Regimen by Type of Cancer. 2013. URL http://www.hci.utah.edu/patientdocs/hci/drugs/Chemoregimen/combocancer.html (accessed 8.31.14).

Cortés-Funes, H., Coronado, C. 2007. Role of anthracyclines in the era of targeted therapy. Cardiovascular toxicology 7: 56–60.

Cox, P.J., Psomas, G., Bolos, C. a 2009. Characterization and DNA-interaction studies of 1,1-dicyano-2,2-ethylene dithiolate Ni(II) mixed-ligand complexes with 2-amino-5-methyl thiazole, 2-amino-2-thiazoline and imidazole. Crystal structure of [Ni(i-MNT)(2a-5mt)(2)]. Bioorganic & medicinal chemistry 17: 6054–6062.

Crawford, S. 2013. Is it time for a new paradigm for systemic cancer treatment? Lessons from a century of cancer chemotherapy. Frontiers in pharmacology 4: 1–18.

Cross, D., Burmester, J.K. 2006. Gene therapy for cancer treatment: past, present and future. Clinical medicine & research 4: 218–227.

Dawson, M. a, Kouzarides, T. 2012. Cancer epigenetics: from mechanism to therapy. Cell 150: 12–27.

Devi, G.R. 2006. siRNA-based approaches in cancer therapy. Cancer gene therapy 13: 819–829.

Díaz, M., Vivas-Mejia, P. 2013. Nanoparticles as Drug Delivery Systems in Cancer Medicine: Emphasis on RNAi-Containing Nanoliposomes. Pharmaceuticals 6: 1361–1380.

Doll, R., Peto, R. 1981. The causes of cancer: quantitative estimates of avoidable risks of cancer in the United States today. Journal of the National Cancer Institute 66: 1191–1308.

Doody, J.F., Wang, Y., Patel, S.N., Joynes, C., Lee, S.P., Gerlak, J., Rolser, R.L., Li, Y., Steiner, P., Bassi, R., Hicklin, D.J., Hadari, Y.R. 2007. Inhibitory activity of cetuximab on epidermal growth factor receptor mutations in non small cell lung cancers. Molecular cancer therapeutics 6: 2642–2651.

Du, C., Fang, M., Li, Y., Li, L., Wang, X. 2000. Smac, a mitochondrial protein that promotes cytochrome c-dependent caspase activation by eliminating IAP inhibition. Cell 102: 33–42.

El Ghissassi, F., Baan, R., Straif, K., Grosse, Y., Secretan, B., Bouvard, V., Benbrahim-Tallaa, L., Guha, N., Freeman, C., Galichet, L., Cogliano, V. 2009. A review of human carcinogens—Part D: radiation. The Lancet Oncology 10: 751–752.

Elmore, S. 2007. Apoptosis: a review of programmed cell death. Toxicologic pathology 35: 495–516.

Emil Frei, I., Eder, J.P. 2003. Combination Chemotherapy. *In*: Cancer Medicine (Kufe DW, Pollock RE, Weichselbaum RR, et al., eds), 6th edition. Hamilton (ON): BC Decker; 2003.

Esteller, M., Corn, P.G., Baylin, S.B., Herman, J.G. 2001. A gene hypermethylation profile of human cancer. Cancer research 61: 3225–3229.

Fadeel, B., Garcia-Bennett, A.E. 2010. Better safe than sorry: Understanding the toxicological properties of inorganic nanoparticles manufactured for biomedical applications. Advanced drug delivery reviews 62: 362–374.

Farnebo, M., Bykov, V.J.N., Wiman, K.G. 2010. The p53 tumor suppressor: a master regulator of diverse cellular processes and therapeutic target in cancer. Biochemical and biophysical research communications 396: 85–89.

Ferrari, M. 2005. Cancer nanotechnology: opportunities and challenges. Nature reviews. Cancer 5: 161–171.

FITC Annexin V / Dead Cell Apoptosis Kit with FITC annexin V and PI , for Flow Cytometry, MP 13242, Invitrogen 2010.

Forbes, N.S. 2010. Engineering the perfect (bacterial) cancer therapy. Nature reviews. Cancer 10: 785–794.

Friess, T., Scheuer, W., Hasmann, M. 2006. Erlotinib antitumor activity in non-small cell lung cancer models is independent of HER1 and HER2 overexpression. Anticancer research 26: 3505–3512.

Fulda, S., Debatin, K.-M. 2006. Extrinsic versus intrinsic apoptosis pathways in anticancer chemotherapy. Oncogene 25: 4798–4811.

Gallego, B., Kaluđerović, M.R., Kommera, H., Paschke, R., Hey-Hawkins, E., Remmerbach, T.W., Kaluđerović, G.N., Gómez-Ruiz, S. 2011. Cytotoxicity, apoptosis and study of the DNA-binding properties of bi- and tetranuclear gallium(III) complexes with heterocyclic thiolato ligands. Investigational new drugs 29: 932–944.

Galluzzi, L., Vitale, I., Abrams, J.M., Alnemri, E.S., Baehrecke, E.H., Blagosklonny, M. V, Dawson, T.M., Dawson, V.L., El-Deiry, W.S., Fulda, S., Gottlieb, E., Green, D.R., Hengartner, M.O., Kepp, O., Knight, R. a, Kumar, S., Lipton, S. a, Lu, X., Madeo, F., Malorni, W., Mehlen, P., Nuñez, G., Peter, M.E., Piacentini, M., Rubinsztein, D.C., Shi, Y., Simon, H.-U., Vandenabeele, P., White, E., Yuan, J., Zhivotovsky, B., Melino, G., Kroemer, G. 2012. Molecular definitions of cell death subroutines: recommendations of the Nomenclature Committee on Cell Death 2012. Cell death and differentiation 19: 107–120.

Garattini, S. 2007. Pharmacokinetics in cancer chemotherapy. European journal of cancer (Oxford, England : 1990) 43: 271–282.

Garber, J.E., Offit, K. 2005. Hereditary cancer predisposition syndromes. Journal of clinical oncology : official journal of the American Society of Clinical Oncology 23: 276–292.

GE Healthcare 2-D Clean-Up Kit 2009.

Gerber, D.E. 2008. Targeted therapies: a new generation of cancer treatments. American family physician 77: 311–319.

Gewirtz, D.A. 1999. A Critical Evaluation of the Mechanisms of Action Proposed for the Antitumor Effects of the Anthracycline Antibiotics Adriamycin and Daunorubicin 57: 727–741.

Gianferrara, T., Bratsos, I., Alessio, E. 2009. A categorization of metal anticancer compounds based on their mode of action. Dalton transactions (Cambridge, England : 2003) 7588–7598.

GLOBOCAN: International Agency for Research on Cancer, World Health Organization. 2012. URL http://globocan.iarc.fr/Default.aspx (accessed 8.6.14).

Gordon, D.J., Resio, B., Pellman, D. 2012. Causes and consequences of aneuploidy in cancer. Nature reviews. Genetics 13: 189–203.

Grallert, B., Boye, E. 2008. The multiple facets of the intra-S checkpoint. Cell Cycle 7: 2315–2320.

Granados-Principal, S., Quiles, J.L., Ramirez-Tortosa, C.L., Sanchez-Rovira, P., Ramirez-Tortosa, M.C. 2010. New advances in molecular mechanisms and the prevention of adriamycin toxicity

by antioxidant nutrients. Food and chemical toxicology : an international journal published for the British Industrial Biological Research Association 48: 1425–1438.

Green, D.R., Kroemer, G. 2009. Cytoplasmic functions of the tumour suppressor p53. Nature 458: 1127–1130.

Gridelli, C., Bareschino, M.A., Schettino, C., Rossi, A., Maione, P., Ciardiello, F. 2007. Erlotinib in non-small cell lung cancer treatment: current status and future development. The oncologist 12: 840–849.

Grivennikov, S.I., Greten, F.R., Karin, M. 2010. Immunity, inflammation, and cancer. Cell 140: 883–899.

Grosse, Y., Baan, R., Straif, K., Secretan, B., El Ghissassi, F., Bouvard, V., Benbrahim-Tallaa, L., Guha, N., Galichet, L., Cogliano, V. 2009. A review of human carcinogens—Part A: pharmaceuticals. The Lancet Oncology 10: 13–14.

Hanahan, D., Weinberg, R.A. 2011. Hallmarks of cancer: the next generation. Cell 144: 646–674.

Hannon, M.J. 2007. Metal-based anticancer drugs: From a past anchored in platinum chemistry to a post-genomic future of diverse chemistry and biology. Pure and Applied Chemistry 79: 2243–2261.

He, H.-Y., Zhao, J.-N., Jia, R., Zhao, Y.-L., Yang, S.-Y., Yu, L.-T., Yang, L. 2011. Novel pyrazolo[3,4-d]pyrimidine derivatives as potential antitumor agents: exploratory synthesis, preliminary structure-activity relationships, and *in vitro* biological evaluation. Molecules (Basel, Switzerland) 16: 10685–10694.

Hoechst Stains, MP21486, Invitrogen 2005.

Holohan, C., Van Schaeybroeck, S., Longley, D.B., Johnston, P.G. 2013. Cancer drug resistance: an evolving paradigm. Nature reviews. Cancer 13: 714–726.

Hu, Z. 2014. Photodynamic Therapy as an Emerging Treatment Modality for Cancer and Non-Cancer Diseases. Journal of Analytical & Bioanalytical Techniques S1: 1–3.

Iii, C.F.S. 1999. Gold-Based Therapeutic Agents 2589–2600.

Ishii, T., Warabi, E., Yanagawa, T. 2012. Novel roles of peroxiredoxins in inflammation , cancer and innate immunity 50: 91–105.

Iuliano, S., Fisher, J.R., Chen, M., Kelly, W.J. 2002. R apid analysis of a plasmid by hydrophobic-interaction chromatography with a non-porous resin 972: 77–86.

Iyer, U., Kadambi, V.J. 2011. Antibody drug conjugates - Trojan horses in the war on cancer. Journal of pharmacological and toxicological methods 64: 207–212.

Jakóbisiak, M., Lasek, W., Gołb, J. 2003. Natural mechanisms protecting against cancer. Immunology Letters 90: 103–122.

Jemal, A., Bray, F., Ferlay, J. 2011. Global Cancer Statistics. CA: a cancer journal for clinicians 61: 69–90.

Jemal, A., Center, M.M., DeSantis, C., Ward, E.M. 2010. Global patterns of cancer incidence and mortality rates and trends. Cancer epidemiology, biomarkers & prevention : a publication of the American Association for Cancer Research, cosponsored by the American Society of Preventive Oncology 19: 1893–1907.

Kandoth, C., McLellan, M.D., Vandin, F., Ye, K., Niu, B., Lu, C., Xie, M., Zhang, Q., McMichael, J.F., Wyczalkowski, M. a, Leiserson, M.D.M., Miller, C. a, Welch, J.S., Walter, M.J., Wendl, M.C., Ley, T.J., Wilson, R.K., Raphael, B.J., Ding, L. 2013. Mutational landscape and significance across 12 major cancer types. Nature 502: 333–339.

Kanvah, S., Joseph, J., Schuster, G.B., Barnett, R.N., Cleveland, C.L., Landman, U. 2010. Oxidation of DNA: damage to nucleobases. Accounts of chemical research 43: 280–287.

Karnani, N., Dutta, A. 2011. The effect of the intra-S-phase checkpoint on origins of replication in human cells 621–633.

Kathiria, A.S., Butcher, L.D., Feagins, L. a, Souza, R.F., Boland, C.R., Theiss, A.L. 2012. Prohibitin 1 modulates mitochondrial stress-related autophagy in human colonic epithelial cells. PloS one 7: e31231.

Kim, C.K., Lee, S.B., Nguyen, T.L.X., Lee, K.-H., Um, S.H., Kim, J., Ahn, J.-Y. 2012. Long isoform of ErbB3 binding protein, p48, mediates protein kinase B/Akt-dependent HDM2 stabilization and nuclear localization. Experimental cell research 318: 136–143.

Kim, J.-H., Bogner, P.N., Ramnath, N., Park, Y., Yu, J., Park, Y.-M. 2007. Elevated peroxiredoxin 1, but not NF-E2-related factor 2, is an independent prognostic factor for disease recurrence and reduced survival in stage I non-small cell lung cancer. Clinical cancer research : an official journal of the American Association for Cancer Research 13: 3875–3882.

Klein, S., McCormick, F., Levitzki, A. 2005. Killing time for cancer cells. Nature reviews. Cancer 5: 573–580.

Lapenna, S., Giordano, A. 2009. Cell cycle kinases as therapeutic targets for cancer. Nature reviews. Drug discovery 8: 547–566.

Lea, N.C., Orr, S.J., Stoeber, K., Williams, G.H., Lam, E.W., Ibrahim, M.A.A., Mufti, G.J., Thomas, N.S.B., Al, L.E.A.E.T., Iol, M.O.L.C.E.L.L.B. 2003. Commitment Point during G 0 3 G 1 That Controls Entry into the Cell Cycle 23: 2351–2361.

Lee, K.W., Lee, D.J., Lee, J.Y., Kang, D.H., Kwon, J., Kang, S.W. 2011. Peroxiredoxin II restrains DNA damage-induced death in cancer cells by positively regulating JNK-dependent DNA repair. The Journal of biological chemistry 286: 8394–8404.

Lemjabbar, H., Li, D., Gallup, M., Sidhu, S., Drori, E., Basbaum, C. 2003. Tobacco smoke-induced lung cell proliferation mediated by tumor necrosis factor alpha-converting enzyme and amphiregulin. The Journal of biological chemistry 278: 26202–26207.

Li, H., Bo, H., Wang, J., Shao, H., Huang, S. 2011. Separation of supercoiled from open circular forms of plasmid DNA, and biological activity detection. Cytotechnology 63: 7–12.

Lima, J.C., Rodriguez, L. 2011. Phosphine-gold(I) compounds as anticancer agents: general description and mechanisms of action. Anti-cancer agents in medicinal chemistry 11: 921–928.

Liu, J., Liu, Q., Wei, H., Yi, J., Zhao, H., Gao, L. 2011. Inhibition of thioredoxin reductase by auranofin induces apoptosis in adriamycin-resistant human K562 chronic myeloid leukemia cells 66: 3–7.

Loeb, L.A., Springgate, C.F., Battula, N., Battala, N. 1974. Errors in DNA Replication as a Basis of Malignant Changes 2311–2321.

Luo, J., Solimini, N., Elledge, S. 2010. Principles of Cancer Therapy: Oncogene and Non-oncogene Addiction 136: 823–837.

Luqmani, Y. a 2005. Mechanisms of drug resistance in cancer chemotherapy. Medical principles and practice : international journal of the Kuwait University, Health Science Centre 14 Suppl 1: 35–48.

Malumbres, M., Barbacid, M. 2001. To cycle or not to cycle: a critical decision in cancer. Nature reviews. Cancer 1: 222–231.

Malumbres, M., Barbacid, M. 2009. Cell cycle, CDKs and cancer: a changing paradigm. Nature reviews. Cancer 9: 153–166.

Manuscript, A. 2010. p21 in cancer: intricate networks and multiple activities. Nature reviews. Cancer 9: 400–414.

Marie, S.K.N., Shinjo, S.M.O. 2011. Metabolism and brain cancer. Clinics 66: 33–43.

Mariño, G., Niso-Santano, M., Baehrecke, E.H., Kroemer, G. 2014. Self-consumption: the interplay of autophagy and apoptosis. Nature reviews. Molecular cell biology 15: 81–94.

Martins, P., Marques, M., Coito, L., Pombeiro, A.J.L., Baptista, P.V., Fernandes, A.R. 2014a. Organometallic Compounds in Cancer Therapy: Past Lessons and Future Directions. Anti-cancer agents in medicinal chemistry [Epub ahead of print].

Martins, P., Rosa, D., Fernandes, A.R., Baptista, P. V 2014b. Nanoparticle Drug Delivery Systems : Recent Patents and Applications in Nanomedicine. Recent Patents on Nanomedicine 3: 1–14.

Mayer, L.D., Janoff, A.S. 2007. Drug ratio-dependent combination chemotherapy. Molecular interventions 7: 216–223.

McCormick, F. 2001. Cancer gene therapy: fringe or cutting edge? Nature reviews. Cancer 1: 130–141.

McCracken, M., Olsen, M., Chen, M.S., Jemal, A., Thun, M., Cokkinides, V., Deapen, D., Ward, E. 2007. Cancer incidence, mortality, and associated risk factors among Asian Americans of Chinese, Filipino, Vietnamese, Korean, and Japanese ethnicities. CA: a cancer journal for clinicians 57: 190–205.

McGowan, E.M., Alling, N., Jackson, E. a, Yagoub, D., Haass, N.K., Allen, J.D., Martinello-Wilks, R. 2011. Evaluation of cell cycle arrest in estrogen responsive MCF-7 breast cancer cells: pitfalls of the MTS assay. PloS one 6: 1–8.

Moolgavkar, S.H., Holford, T.R., Levy, D.T., Kong, C.Y., Foy, M., Clarke, L., Jeon, J., Hazelton, W.D., Meza, R., Schultz, F., McCarthy, W., Boer, R., Gorlova, O., Gazelle, G.S., Kimmel, M., McMahon, P.M., de Koning, H.J., Feuer, E.J. 2012. Impact of Reduced Tobacco Smoking on

Lung Cancer Mortality in the United States During 1975-2000. JNCI Journal of the National Cancer Institute 104: 541–548.

Negrini, S., Gorgoulis, V.G., Halazonetis, T.D. 2010. Genomic instability--an evolving hallmark of cancer. Nature reviews. Molecular cell biology 11: 220–228.

Neubig, R.R., Spedding, M., Kenakin, T., Christopoulos, A. 2003. International Union of Pharmacology Committee on Receptor Nomenclature and Drug Classification . XXXVIII . Update on Terms and Symbols in Quantitative Pharmacology 55: 597–606.

Neves, A. 2001. Hydrolytic DNA cleavage promoted by a dinuclear iron (III) complex. Inorganic Chemistry Communications 4: 388–391.

Nishiyama, M., Eguchi, H. 2009. Recent advances in cancer chemotherapy: current strategies, pharmacokinetics, and pharmacogenomics. Advanced drug delivery reviews 61: 367–368.

Nobili, S., Mini, E., Landini, I., Gabbiani, C., Casini, A., Messori, L. 2009. Gold Compounds as AnticancerAgents : Chemistry , Cellular Pharmacology , and Preclinical Studies 30: 550–580.

Olivier, M., Hollstein, M., Hainaut, P. 2010. TP53 Mutations in Human Cancers: Origins, Consequences, and Clinical Use. Cold Spring Harb Perspect Biol 2: 1–17.

Oren, M., Rotter, V. 2010. Mutant p53 gain-of-function in cancer. Cold Spring Harbor perspectives in biology 2: 1–15.

Orrenius, S., Nicotera, P., Zhivotovsky, B. 2011. Cell death mechanisms and their implications in toxicology. Toxicological sciences : an official journal of the Society of Toxicology 119: 3–19.

Ott, I. 2009. On the medicinal chemistry of gold complexes as anticancer drugs. Coordination Chemistry Reviews 253: 1670–1681.

Ott, I., Gust, R. 2007. Non platinum metal complexes as anti-cancer drugs. Archiv der Pharmazie 340: 117–126.

Ouyang, L., Shi, Z., Zhao, S., Wang, F.-T., Zhou, T.-T., Liu, B., Bao, J.-K. 2012. Programmed cell death pathways in cancer: a review of apoptosis, autophagy and programmed necrosis. Cell proliferation 45: 487–498.

Palchaudhuri, R., Hergenrother, P.J. 2007. DNA as a target for anticancer compounds: methods to determine the mode of binding and the mechanism of action. Current opinion in biotechnology 18: 497–503.

Patel, V.A., Lee, D.J., Longacre-antoni, A., Feng, L., Lieberthal, W., Rauch, J., Ucker, D.S., Levine, J.S. 2010. Apoptotic and necrotic cells as sentinels of local tissue stress and inflammation: Response pathways initiated in nearby viable cells. Autoimmunity 42: 317–321.

Peer, D., Karp, J.M., Hong, S., Farokhzad, O.C., Margalit, R., Langer, R. 2007. Nanocarriers as an emerging platform for cancer therapy. Nature nanotechnology 2: 751–760.

Pietenpol, J. a, Stewart, Z. a 2002. Cell cycle checkpoint signaling: cell cycle arrest versus apoptosis. Toxicology 181-182: 475–481.

Pietras, K., Ostman, A. 2010. Hallmarks of cancer: interactions with the tumor stroma. Experimental cell research 316: 1324–13431.

Pinto, A.C., Moreira, J.N., Simões, S. 2010. Combination Chemotherapy in Cancer : Principles , Evaluation and Drug Delivery Strategies. *In* Current Cancer Treatment – Novel Beyond Conventional Approaches (Öner Özdemir ed). pp. 693–714, InTech.

Portt, L., Norman, G., Clapp, C., Greenwood, M., Greenwood, M.T. 2011. Anti-apoptosis and cell survival: a review. Biochimica et biophysica acta 1813: 238–59.

Propidium iodide staining of cells to assess DNA cell cycle. 2014. http://www.abcam.com/?pageconfig=resource&rid=13432 (accessed 8.20.14).

Pucci, B., Kasten, M., Giordano, a 2000. Cell cycle and apoptosis. Neoplasia 2: 291–299.

R. Fernandes, A., Viana Baptista, P. 2013. Nanotechnology for Cancer Diagnostics and Therapy – An Update on Novel Molecular Players. *In* Current Cancer Therapy Reviews. pp. 164–172, Bentham Science Publishers.

Ricci, M.S., Zong, W.-X. 2006. Chemotherapeutic approaches for targeting cell death pathways. The oncologist 11: 342–57.

Rieger, A.M., Nelson, K.L., Konowalchuk, J.D., Barreda, D.R. 2011. Modified annexin V/propidium iodide apoptosis assay for accurate assessment of cell death. Journal of visualized experiments: JoVE 37–40.

Rise, T. 2013. Human Development Report 2013.

Riss, T.L., Niles, A.L., Minor, L. 2013. Cell Viability Assays: Assay Guidance Manual.

Sabbadini, P.S., Assis, M.C., Trost, E., Gomes, D.L.R., Moreira, L.O., Dos Santos, C.S., Pereira, G.A., Nagao, P.E., Azevedo, V.A.D.C., Hirata Júnior, R., Dos Santos, A.L.S., Tauch, A., Mattos-Guaraldi, A.L. 2012. Corynebacterium diphtheriae 67-72p hemagglutinin, characterized as the protein DIP0733, contributes to invasion and induction of apoptosis in HEp-2 cells. Microbial pathogenesis 52: 165–76.

Sandal, T. 2002. Molecular Aspects of the Mammalian Cell Cycle and Cancer. The Oncologist 7: 73–81.

Satyanarayana, S., Dabrowiak, J.C., Chaires, J.B. 1993. Tris(phenanthroline)ruthenium(II) enantiomer interactions with DNA: mode and specificity of binding. Biochemistry 32: 2573–2584.

Schulze-bergkamen, H., Krammer, P.H. 2004. Apoptosis in Cancer — Implications for Therapy. Seminars in Oncology 31: 90–119.

Schutte, B., Nuydens, R., Geerts, H., Ramaekers, F. 1998. Annexin V binding assay as a tool to measure apoptosis in differentiated neuronal cells. Journal of neuroscience methods 86: 63–69.

Schwartz, G.K., Shah, M. a 2005. Targeting the cell cycle: a new approach to cancer therapy. Journal of clinical oncology : official journal of the American Society of Clinical Oncology 23: 9408–9421.

Sebaugh, J.L. 2010. Guidelines for accurate EC50/IC50 estimation. Pharmaceutical statistics 10: 128–134.

Secretan, B., Straif, K., Baan, R., Grosse, Y., El Ghissassi, F., Bouvard, V., Benbrahim-Tallaa, L., Guha, N., Freeman, C., Galichet, L., Cogliano, V. 2009. A review of human carcinogens—Part E: tobacco, areca nut, alcohol, coal smoke, and salted fish. The Lancet Oncology 10: 1033–1034.

Shahabadi, N., Mohammadi, S. 2012. Synthesis Characterization and DNA Interaction Studies of a New Zn(II) Complex Containing Different Dinitrogen Aromatic Ligands. Bioinorganic chemistry and applications 2012: 1–8.

Shahabadi, N., Mohammadi, S., Alizadeh, R. 2011. DNA Interaction Studies of a New Platinum (II) Complex Containing Different Aromatic Dinitrogen Ligands 2011: 1–8.

Sherr, C.J. 1996. Cancer cell cycles. Science 274: 1672–1677.

Siddik, Z.H. 2003. Cisplatin: mode of cytotoxic action and molecular basis of resistance. Oncogene 22: 7265–7279.

Silva, A., Luís, D., Santos, S., Silva, J., Mendo, A.S., Coito, L., Silva, T.F.S., da Silva, M.F.C.G., Martins, L.M.D.R.S., Pombeiro, A.J.L., Borralho, P.M., Rodrigues, C.M.P., Cabral, M.G., Videira, P. a, Monteiro, C., Fernandes, A.R. 2013. Biological characterization of the antiproliferative potential of Co(II) and Sn(IV) coordination compounds in human cancer cell lines: a comparative proteomic approach. Drug metabolism and drug interactions 28: 167–176.

Silva, P.P., Guerra, W., Silveira, J.N., Ferreira, A.M.D.C., Bortolotto, T., Fischer, F.L., Terenzi, H., Neves, A., Pereira-Maia, E.C. 2011. Two new ternary complexes of copper(II) with tetracycline or doxycycline and 1,10-phenanthroline and their potential as antitumoral: cytotoxicity and DNA cleavage. Inorganic chemistry 50: 6414–6424.

Silva, T.F.S., Martins, L.M.D.R.S., Guedes da Silva, M.F.C., Fernandes, A.R., Silva, A., Borralho, P.M., Santos, S., Rodrigues, C.M.P., Pombeiro, A.J.L. 2012. Cobalt complexes bearing scorpionate ligands: synthesis, characterization, cytotoxicity and DNA cleavage. Dalton transactions (Cambridge, England : 2003) 41: 12888–12897.

Singh, R., Lillard, J.W. 2009. Nanoparticle-based targeted drug delivery. Experimental and molecular pathology 86: 215–223.

Somwar, R., Erdjument-Bromage, H., Larsson, E., Shum, D., Lockwood, W.W., Yang, G., Sander, C., Ouerfelli, O., Tempst, P.J., Djaballah, H., Varmus, H.E. 2011. Superoxide dismutase 1 (SOD1) is a target for a small molecule identified in a screen for inhibitors of the growth of lung adenocarcinoma cell lines. Proceedings of the National Academy of Sciences of the United States of America 108: 16375–16380.

Steele, R.J.C., Lane, D.P. 2005. p53 in cancer: A paradigm for modern management of cancer. The Surgeon 3: 197–205.

Straif, K., Benbrahim-Tallaa, L., Baan, R., Grosse, Y., Secretan, B., El Ghissassi, F., Bouvard, V., Guha, N., Freeman, C., Galichet, L., Cogliano, V. 2009. A review of human carcinogens—Part C: metals, arsenic, dusts, and fibres. The Lancet Oncology 10: 453–454.

Sullivan, K.D., Gallant-Behm, C.L., Henry, R.E., Fraikin, J.-L., Espinosa, J.M. 2012. The p53 circuit board. Biochimica et biophysica acta 1825: 229–244.

Suzuki, M., Takahashi, T. 2013. Aberrant DNA replication in cancer. Mutation research 743-744: 111–7.

Tacar, O., Sriamornsak, P., Dass, C.R. 2013. Doxorubicin: an update on anticancer molecular action, toxicity and novel drug delivery systems. The Journal of pharmacy and pharmacology 65: 157–70.

Takahashi, H., Ogata, H., Nishigaki, R., Broide, D.H. 2011. Tobacco smoke promotes lung tumorigenesis by triggering IKKβ and JNK1 dependent inflammation. Cancer Cell 17: 1–19.

Takeda, K., Stagg, J., Yagita, H., Okumura, K., Smyth, M.J. 2007. Targeting death-inducing receptors in cancer therapy. Oncogene 26: 3745–3757.

Taylor, R.C., Cullen, S.P., Martin, S.J. 2008. Apoptosis: controlled demolition at the cellular level. Nature reviews. Molecular cell biology 9: 231–241.

Thorn, C., Oshiro, C., Marsh, S., Hernandez-Boussard, T., Mcleod, H., Klein, T., Altman, R. 2012. Doxorubicin pathways: pharmacodynamics and adverse effects 21: 440–446.

Tomasetti, C., Vogelstein, B., Parmigiani, G. 2013. Half or more of the somatic mutations in cancers of self-renewing tissues originate prior to tumor initiation. Proceedings of the National Academy of Sciences of the United States of America 110: 1999–2004.

Van Schaeybroeck, S., Kyula, J., Kelly, D.M., Karaiskou-McCaul, A., Stokesberry, S. a, Van Cutsem, E., Longley, D.B., Johnston, P.G. 2006. Chemotherapy-induced epidermal growth factor receptor activation determines response to combined gefitinib/chemotherapy treatment in non-small cell lung cancer cells. Molecular cancer therapeutics 5: 1154–11565.

Vanden Berghe, T., Linkermann, A., Jouan-Lanhouet, S., Walczak, H., Vandenabeele, P. 2014. Regulated necrosis: the expanding network of non-apoptotic cell death pathways. Nature reviews. Molecular cell biology 15: 135–147.

Vermeulen, K., Van Bockstaele, D.R., Berneman, Z.N. 2003. The cell cycle: a review of regulation, deregulation and therapeutic targets in cancer. Cell proliferation 36: 131–149.

Vincenzi, B., Schiavon, G., Silletta, M., Santini, D., Perrone, G., Di Marino, M., Angeletti, S., Baldi, a, Tonini, G. 2006. Cell cycle alterations and lung cancer. Histology and histopathology 21: 423–435.

Vousden, K.H., Prives, C. 2009. Blinded by the Light: The Growing Complexity of p53. Cell 137: 413–431.

Waldmann, T., Schneider, R. 2013. Targeting histone modifications--epigenetics in cancer. Current opinion in cell biology 25: 184–189.

Wang, P., Henning, S.M., Heber, D. 2010. Limitations of MTT and MTS-based assays for measurement of antiproliferative activity of green tea polyphenols. PloS one 5: 1–10.

Wang, Z., Zha, G., Don, Z. 2006. Establishment and characterization of lung adenocarcinoma cell lines with multi drug resistance. Life Science Journal 4: 13–16.

Waris, G., Ahsan, H. 2006. Reactive oxygen species: role in the development of cancer and various chronic conditions. Journal of carcinogenesis 5: 14.

Weinberg, R.A. 2013. The biology of cancer, 2nd editio. ed. Garland Science.

Weinstein, I.B., Joe, A.K. 2006. Mechanisms of disease: Oncogene addiction--a rationale for molecular targeting in cancer therapy. Nature clinical practice. Oncology 3: 448–57.

Wong, R.S.Y. 2011. Apoptosis in cancer: from pathogenesis to treatment. Journal of experimental & clinical cancer research : CR 30: 1–14.

World cancer factsheet 2014. . World Health Organization 2012: 2012–2015.

World Cancer Report 2008.

Wright, J. 2014. Deliver on a promise. Nature 311: 1–2.

Wyllie, A.H. 2010. "Where, O death, is thy sting?" A brief review of apoptosis biology. Molecular neurobiology 42: 4–9.

Xue, Q., Lv, L., Wan, C., Chen, B., Li, M., Ni, T., Liu, Y., Liu, Y., Cong, X., Zhou, Y., Ni, R., Mao, G. 2013. Expression and clinical role of small glutamine-rich tetratricopeptide repeat (TPR)-containing protein alpha (SGTA) as a novel cell cycle protein in NSCLC. Journal of cancer research and clinical oncology 139: 1539–1549.

Yardley, D. a 2013. Drug resistance and the role of combination chemotherapy in improving patient outcomes. International journal of breast cancer 2013: 1–16.

Yousuf, S., Muthu, I. V, Enoch, V. 2014. Binding of the Bi (III) Complex of Naringin with B-Cyclodextrin / Calf Thymus DNA : Absorption and Fluorescence Characteristics. International Journal of Spectroscopy 2014: 1–8.

Zack, T.I., Schumacher, S.E., Carter, S.L., Cherniack, A.D., Saksena, G., Tabak, B., Lawrence, M.S., Zhang, C.-Z., Wala, J., Mermel, C.H., Sougnez, C., Gabriel, S.B., Hernandez, B., Shen, H., Laird, P.W., Getz, G., Meyerson, M., Beroukhim, R. 2013. Pan-cancer patterns of somatic copy number alteration. Nature Genetics 45: 1134–1140.

Zoli, W., Ricotti, L., Tesei, a, Barzanti, F., Amadori, D. 2001. *In vitro* preclinical models for a rational design of chemotherapy combinations in human tumors. Critical reviews in oncology/hematology 37: 69–82.

Appendix A

Chemical structure of the assayed chlorogold compounds and related information.

Dichloro(2-pyridinecarboxylato)gold(III)

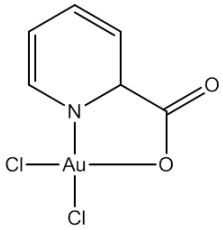

Chemical Formula: $C_6H_5AuCl_2NO_2$
Molecular Weight: 389.97
Elemental Analysis: C, 18.43; H, 1.29; Au, 50.38; Cl, 18.14; N, 3.58; O, 8.18

A

Chlorotrimethylphosphinegold(I)

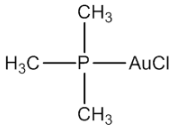

Chemical Formula: C_3H_9AuClP
Molecular Weight: 308,50
Elemental Analysis: C, 11.68; H, 2.94; Au, 63.85; Cl, 11.49; P, 10.04

B

1,3-Bis(2,6-di-isopropylphenyl)imidazol-2ylidenegold(I) chloride

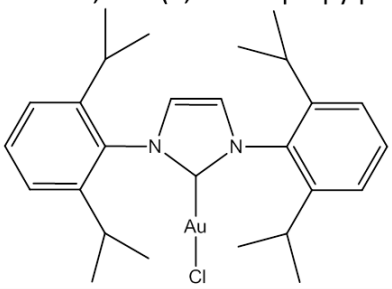

Chemical Formula: $C_{27}H_{37}AuClN_2$
Molecular Weight: 621,01
Elemental Analysis: C, 52.14; H, 6.00; Au, 31.67; Cl, 5.70; N, 4.50

C

Chlorotriphenylphosphinegold(I)

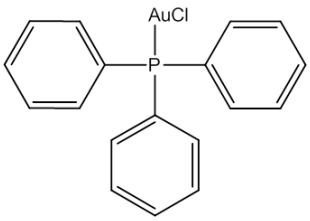

Chemical Formula: $C_{18}H_{15}AuClP$
Molecular Weight: 494.03
Elemental Analysis: C, 43.70; H, 3.06; Au, 39.81; Cl, 7.17; P, 6.26

D

Appendix B

Compound B and compound D cytotoxic evaluation across a library of tumoural and non-tumoural cell lines

* Next page

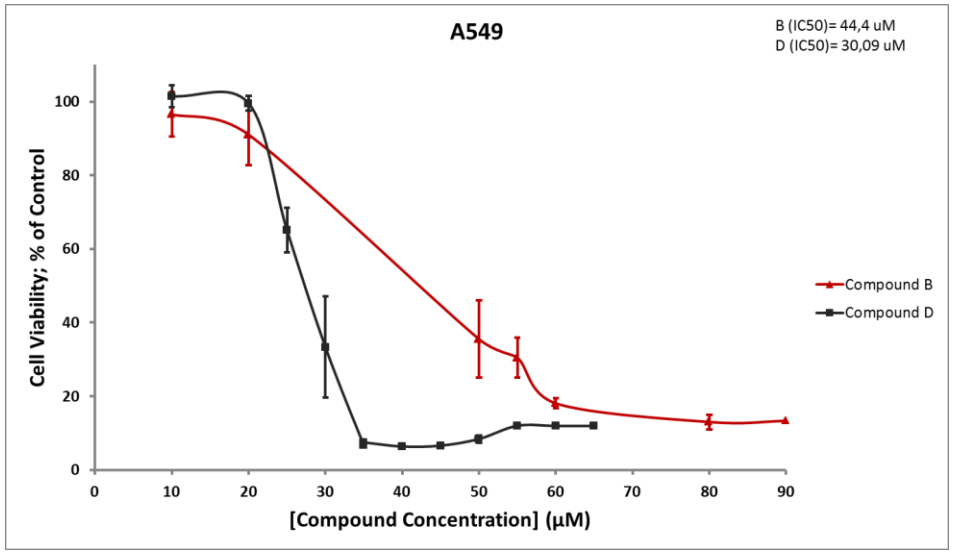
A549
B (IC50)= 44,4 uM
D (IC50)= 30,09 uM
Cell Viability; % of Control
[Compound Concentration] (µM)
Compound B
Compound D

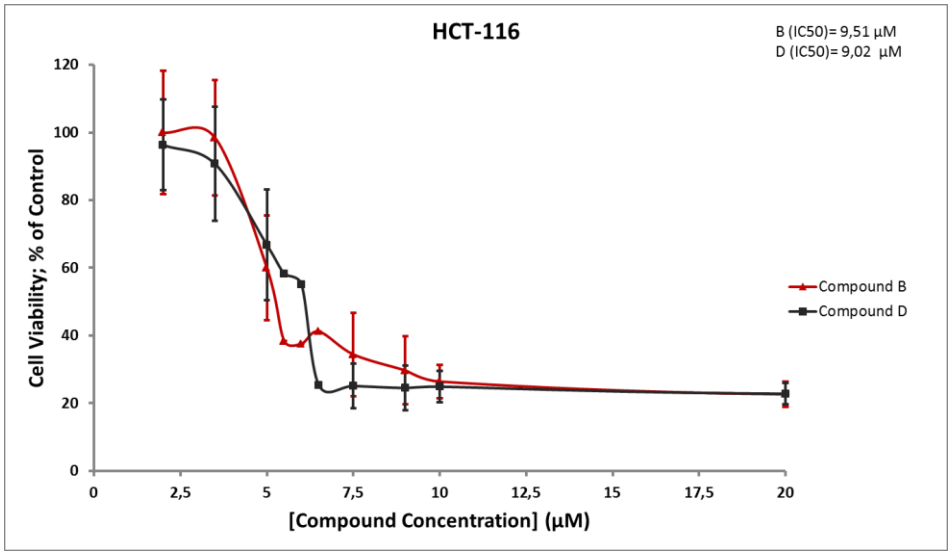
HCT-116
B (IC50)= 9,51 µM
D (IC50)= 9,02 µM
Cell Viability; % of Control
[Compound Concentration] (µM)
Compound B
Compound D

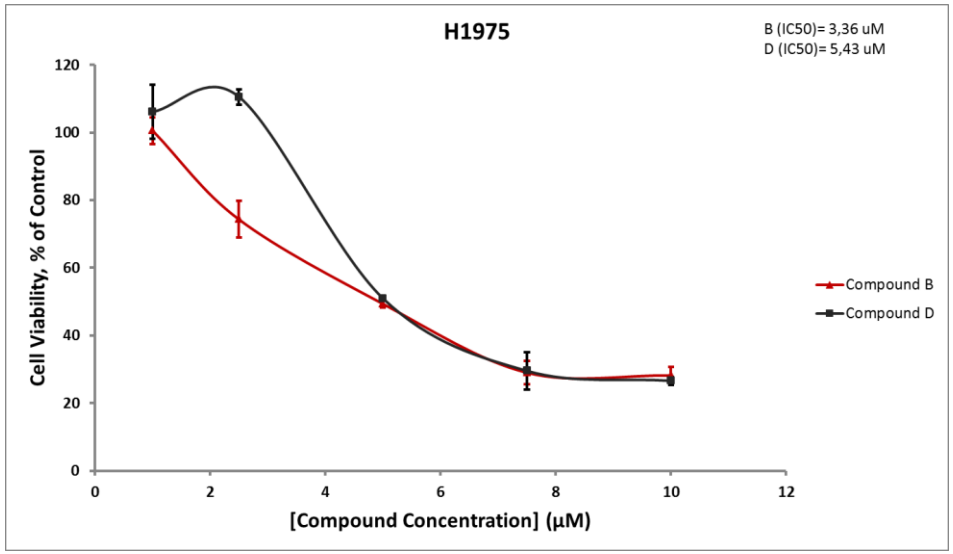
H1975
B (IC50)= 3,36 uM
D (IC50)= 5,43 uM
Cell Viability, % of Control
[Compound Concentration] (µM)
Compound B
Compound D

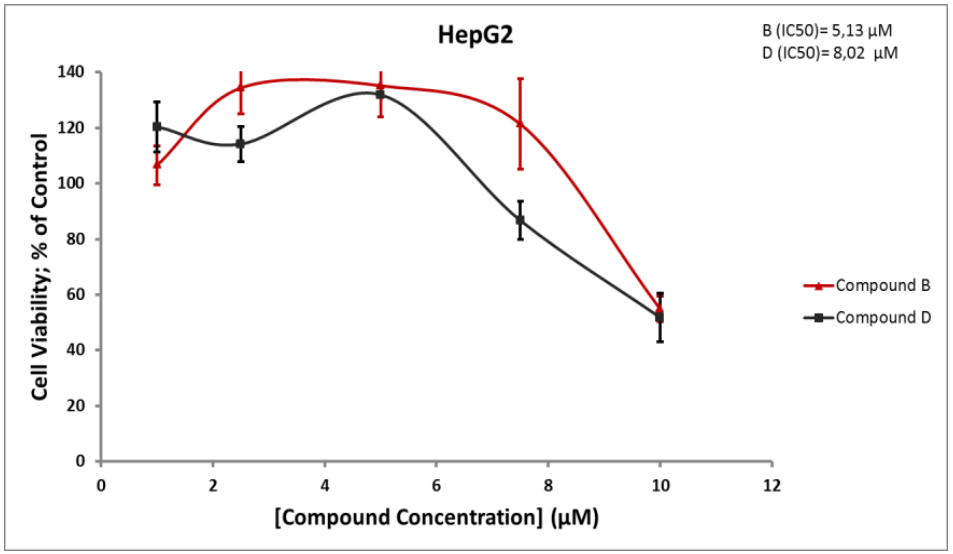
HepG2
B (IC50)= 5,13 µM
D (IC50)= 8,02 µM
Cell Viability; % of Control
[Compound Concentration] (µM)
Compound B
Compound D

C

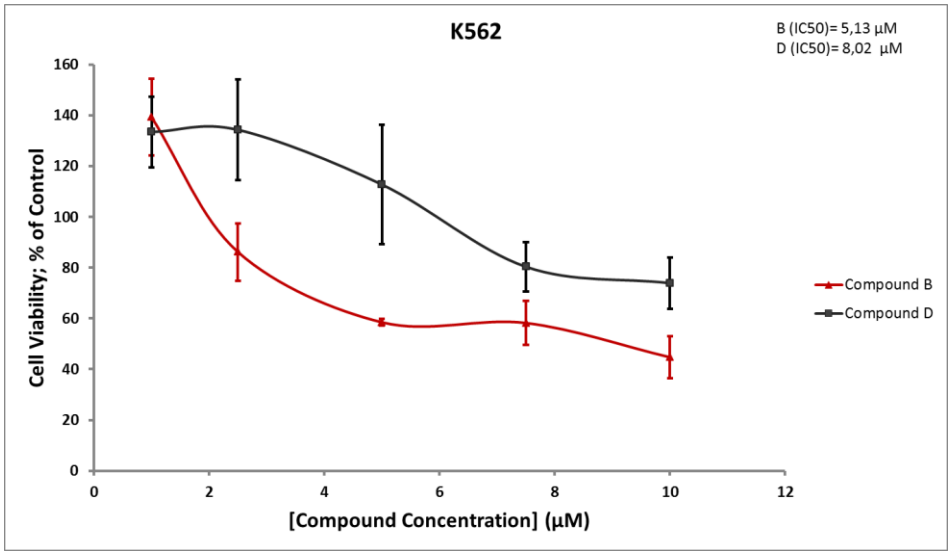
K562
B (IC50)= 5,13 µM
D (IC50)= 8,02 µM
Cell Viability; % of Control
[Compound Concentration] (µM)
Compound B
Compound D

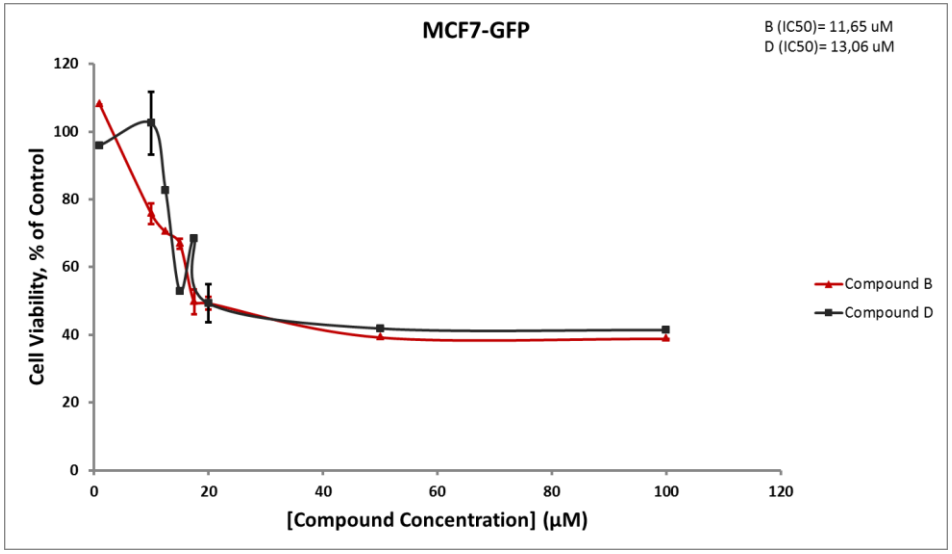
MCF7-GFP
B (IC50)= 11,65 uM
D (IC50)= 13,06 uM
Cell Viability, % of Control
[Compound Concentration] (µM)
Compound B
Compound D

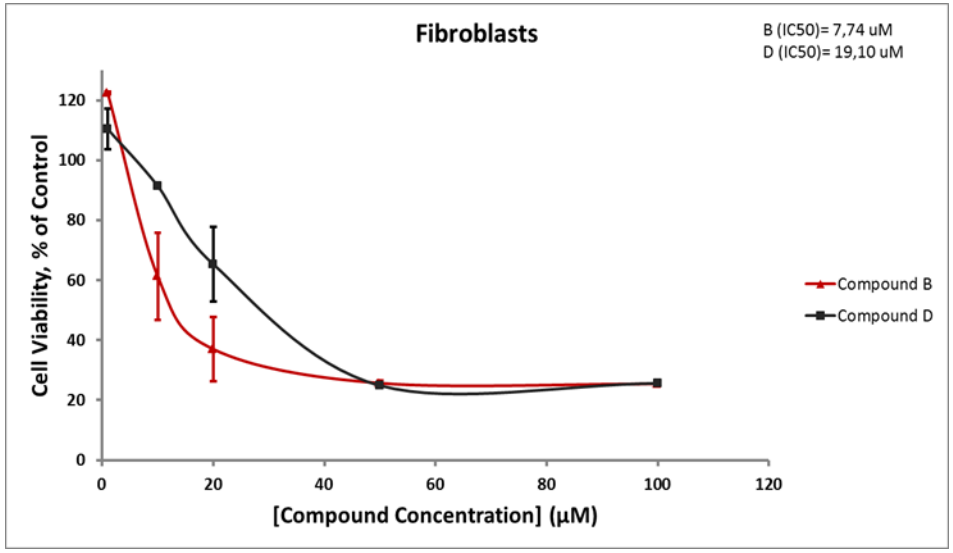
Fibroblasts
B (IC50)= 7,74 uM
D (IC50)= 19,10 uM
Cell Viability, % of Control
[Compound Concentration] (µM)
Compound B
Compound D

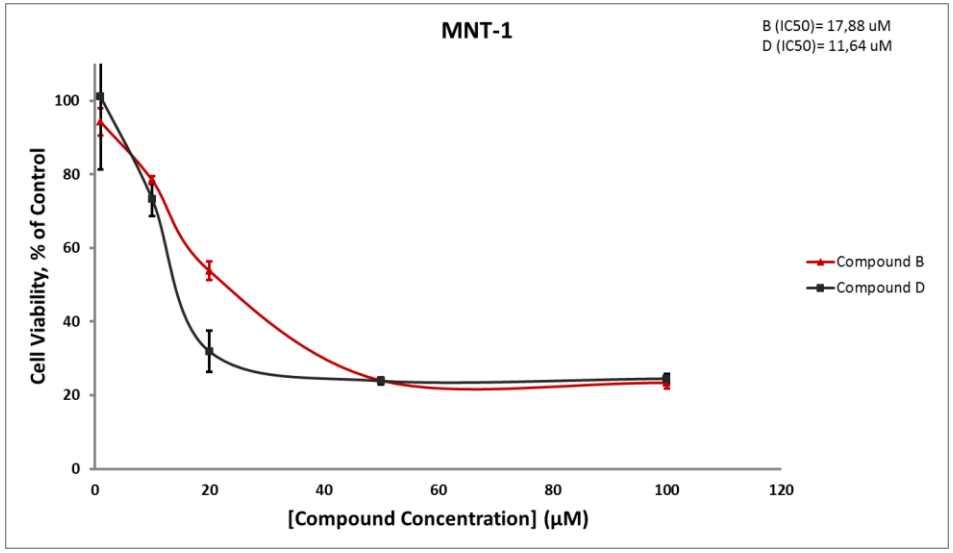
MNT-1
B (IC50)= 17,88 uM
D (IC50)= 11,64 uM
Cell Viability, % of Control
[Compound Concentration] (µM)
Compound B
Compound D

d

Appendix C

Erlotinib single drug treatment cytotoxic evaluation in A549 NSCLC cell line.

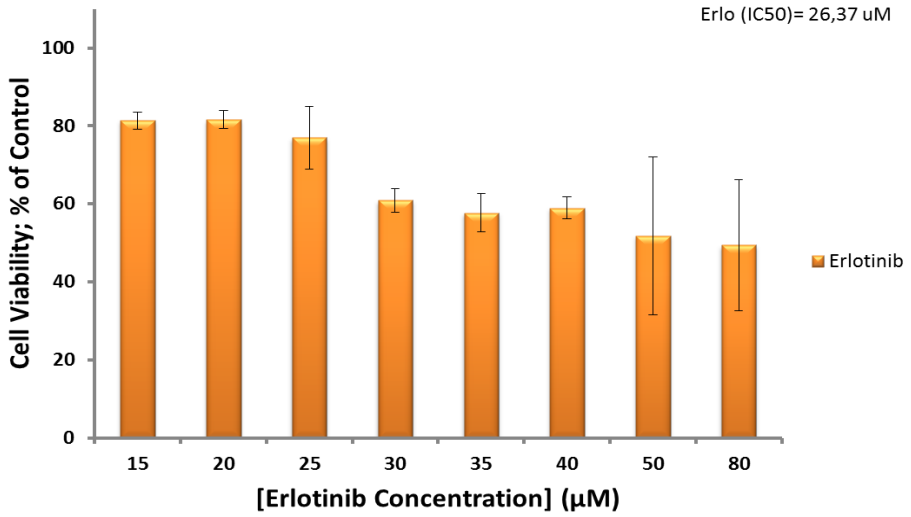

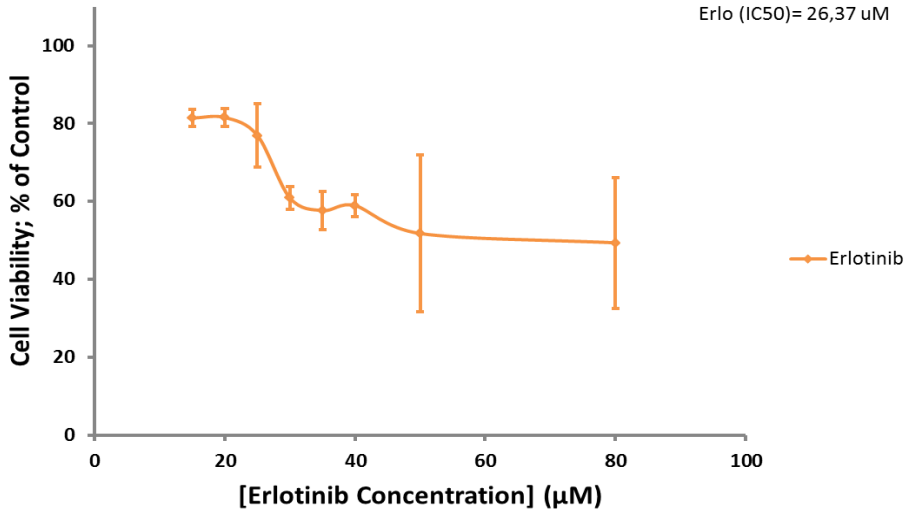

d

Appendix D

Spectroscopic analysis of chlorogold compounds B and D bound and unbound to CT-DNA: UV-visible titrations